UNIVERSITY OF AMSTERDAM

UvA-DARE (Digital Academic Repository)

Search for flavour-changing neutral tqH interactions with H → γγ in pp collisions at √s = 13 TeV using the ATLAS detector

The ATLAS Collaboration

DOI
10.1007/JHEP12(2023)195

Publication date
2023

Document Version
Final published version

Published in
Journal of High Energy Physics

License
CC BY

Link to publication

Citation for published version (APA):
The ATLAS Collaboration (2023). Search for flavour-changing neutral *tqH* interactions with *H → γγ* in *pp* collisions at *√s* = 13 TeV using the ATLAS detector. *Journal of High Energy Physics*, *2023*(12), Article 195. https://doi.org/10.1007/JHEP12(2023)195

General rights
It is not permitted to download or to forward/distribute the text or part of it without the consent of the author(s) and/or copyright holder(s), other than for strictly personal, individual use, unless the work is under an open content license (like Creative Commons).

Disclaimer/Complaints regulations
If you believe that digital publication of certain material infringes any of your rights or (privacy) interests, please let the Library know, stating your reasons. In case of a legitimate complaint, the Library will make the material inaccessible and/or remove it from the website. Please Ask the Library: https://uba.uva.nl/en/contact, or a letter to: Library of the University of Amsterdam, Secretariat, P.O. Box 19185, 1000 GD Amsterdam, The Netherlands. You will be contacted as soon as possible.

UvA-DARE is a service provided by the library of the University of Amsterdam (https://dare.uva.nl)

Download date:13 Sep 2026

Published for SISSA by Springer

Received: *September 25, 2023*
Accepted: *December 14, 2023*
Published: *December 28, 2023*

Search for flavour-changing neutral tqH interactions with $H \to \gamma\gamma$ in pp collisions at $\sqrt{s} = 13$ TeV using the ATLAS detector

The ATLAS collaboration

E-mail: atlas.publications@cern.ch

Abstract: A search for flavour-changing neutral interactions involving the top quark, the Higgs boson and an up-type quark q ($q = c, u$) is presented. The proton-proton collision data set used, with an integrated luminosity of 139 fb^{-1}, was collected at $\sqrt{s} = 13$ TeV by the ATLAS experiment at the Large Hadron Collider. Both the decay process $t \to qH$ in $t\bar{t}$ production and the production process $pp \to tH$, with the Higgs boson decaying into two photons, are investigated. No significant excess is observed and upper limits are set on the $t \to cH$ and the $t \to uH$ branching ratios of 4.3×10^{-4} and 3.8×10^{-4}, respectively, at the 95% confidence level, while the expected limits in the absence of signal are 4.7×10^{-4} and 3.9×10^{-4}. Combining this search with ATLAS searches in the $H \to \tau^+\tau^-$ and $H \to b\bar{b}$ final states yields observed (expected) upper limits on the $t \to cH$ branching ratio of 5.8×10^{-4} (3.0×10^{-4}) at the 95% confidence level. The corresponding observed (expected) upper limit on the $t \to uH$ branching ratio is 4.0×10^{-4} (2.4×10^{-4}).

Keywords: Flavour Changing Neutral Currents, Hadron-Hadron Scattering, Higgs Physics, Top Physics

ArXiv ePrint: 2309.12817

Open Access, Copyright CERN,
for the benefit of the ATLAS Collaboration.
Article funded by SCOAP^3.

https://doi.org/10.1007/JHEP12(2023)195

Contents

1 Introduction **1**

2 Detector, data set and Monte Carlo simulation **4**
2.1 ATLAS detector 4
2.2 Data set 4
2.3 Simulation samples 5

3 Event reconstruction and selection **7**
3.1 Photon reconstruction and identification 7
3.2 Reconstruction and selection of leptons, light- and heavy-flavour jets and missing transverse momentum 8
3.3 Event preselection 9
3.4 Hadronic selection 9
3.4.1 Categories 10
3.4.2 Additional BDT selection 11
3.4.3 Diphoton invariant mass distributions 13
3.5 Leptonic selection 13
3.5.1 Categories 13
3.5.2 Diphoton invariant mass distributions 17
3.6 Summary of the selections and expected number of signal events 17

4 Statistical analysis and systematic uncertainties **18**
4.1 Likelihood construction 19
4.2 Systematic uncertainties 19
4.2.1 Theoretical uncertainties 19
4.2.2 Experimental uncertainties 20

5 Results **21**
5.1 Constraints on the tqH couplings using the $H \to \gamma\gamma$ channel 21
5.2 Combination of ATLAS searches 25

6 Conclusion **26**

The ATLAS collaboration **34**

1 Introduction

Following the observation of the Higgs boson by the ATLAS [1] and the CMS [2] collaborations, a comprehensive programme of measurements of its properties is underway. The search for flavour-changing neutral current interactions (FCNC) between the Higgs boson, the top quark, and a charm or up quark is a part of the programme. Since the Higgs boson is

JHEP12(2023)195

lighter than the top quark, such tqH ($q = c, u$) interactions would manifest themselves in particular as FCNC top-quark decays, $t \to qH$.[1]

According to the Standard Model (SM), FCNC processes are forbidden at tree level and very much suppressed at the one-loop level and higher orders due to the Glashow-Iliopoulos-Maiani (GIM) mechanism [3]. Observations of FCNC decays of the top quark, which are extremely rare in the SM (with a branching ratio, $\mathcal{B}$, of about 4.2×10^{-15} for $t \to cH$ and 3.7×10^{-17} for $t \to uH$ [4]), would constitute a clear signal of new physics.

In models beyond the SM, new flavour-changing mechanisms can contribute to the tqH vertex, yielding effective couplings orders of magnitude larger than those of the SM [5]. Examples of such extensions are the quark-singlet model [6–8], the two-Higgs-doublet model (2HDM) with or without flavour violation [9–17], the Minimal Supersymmetric Standard Model [18–25], Supersymmetry with R-parity violation [26, 27], the Topcolour-assisted Technicolour model [28], models with warped extra dimensions [29, 30] and the Littlest Higgs model with T-parity conservation [31]. In composite Higgs boson models, FCNC may appear even with a single Higgs doublet [29, 32]. For a review, see ref. [33]. Among the studied potential branching ratio enhancements, the largest, $\mathcal{B}(t \to cH)$ of the order of 10^{-3}, appears in the 2HDM with the ansatz of Cheng and Sher [9] where the off-diagonal Yukawa couplings, λ_{tqH}, scale with the top- and charm- or up-quark masses, m_t and m_q, as $\lambda^{\text{CS}}_{tqH} = \sqrt{2m_q m_t}/v$ (where $v = 246$ GeV is the Higgs field vacuum expectation value). Recently, Alves et al. [34] predicted a $t \to cH$ branching ratio between 1.8×10^{-4} and 4.5×10^{-4} within the context of a 2HDM model generating CP violation in the leptonic and hadronic sectors from a common origin.

Both the ATLAS and CMS collaborations have searched for tqH couplings during Run 1 and Run 2 of the LHC [35–45]. In addition to the FCNC top-quark decay, $t \to qH$, the FCNC production process, $pp \to tH$, was for the first time taken into account by CMS using the decay mode $H \to b\bar{b}$ with a data set corresponding to an integrated luminosity of 36 fb^{-1} [43], and brought an improvement of about 20% in the sensitivity to the tuH coupling. The CMS result [44] using the decay mode $H \to \gamma\gamma$ with 137 fb^{-1} currently gives the best limits. For the tcH (tuH) couplings, 95% confidence-level (CL) upper limits of 7.3 (1.9) $\times 10^{-4}$ were observed while 5.1 (3.1) $\times 10^{-4}$ were expected. Finally, with 139 fb^{-1} of data at 13 TeV, ATLAS obtained 95% CL upper limits of 9.4 (6.9) $\times 10^{-4}$ using $H \to \tau^+\tau^-$ decays [40] and 12.0 (7.7) $\times 10^{-4}$ with $H \to b\bar{b}$ decays [41].

The tqH coupling induces both the $t \to qH$ decay and $pp \to tH$ production. Examples of Feynman diagrams for these processes are shown in figure 1. In the SM effective field theory (SMEFT), there are four FCNC operators contributing to the tqH couplings at tree level. Using the notation of ref. [46] and taking the same mass scale (Λ) for all operators, the corresponding additional contribution to the SM Lagrangian is:

$$\delta\mathcal{L} = \frac{-y_t^3}{\Lambda^2}(\varphi^\dagger\varphi - v^2/2) \sum_{i=1,2} C^{i3}_{u\varphi}\overline{q_i}\tilde{\varphi}t + C^{3i}_{u\varphi}\overline{Q}\tilde{\varphi}u_i, \tag{1.1}$$

where y_t is the top-quark Yukawa coupling, φ is the Higgs doublet ($\tilde{\varphi} = i\tau_2\varphi^*$), (Q, q_i) are the quark doublets and (t, u_i) are the quark singlets; Q and t refer to the third generation and the

[1] Throughout this paper the inclusion of charge-conjugate decay and production modes is implied.

JHEP12(2023)195

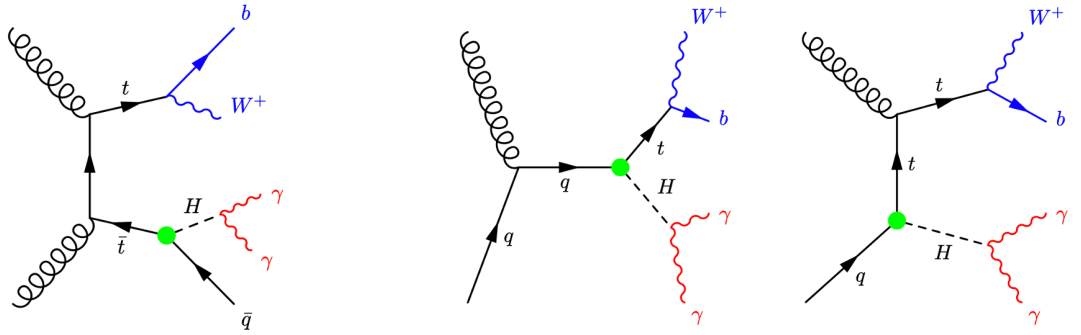

Figure 1. Examples of leading-order Feynman diagrams for FCNC processes (a) in the top-quark decay and (b, c) in the associated production of a top quark and a Higgs boson. The FCNC vertex is shown as a green filled circle.

index i runs over the first and second generations. The parameters $C^x_{u\varphi}$ ($x = i3, 3i$) are Wilson coefficients. Within SMEFT, a given branching ratio of the process $t \to qH$ can be translated to a value of $C^x_{u\varphi}/\Lambda^2$. In a simple scenario with a single operator, $\mathcal{B} = 10^{-3}$ and $\Lambda = 1$ TeV correspond to $C = 1.4$. Limits on $\mathcal{B}$ can also be translated to limits on λ_{tqH} via the relation

$$\lambda_{tqH} = (1.85 \pm 0.02) \times \sqrt{\mathcal{B}}, \tag{1.2}$$

where the mass of the light quark is neglected, the next-to-leading-order (NLO) estimations for the FCNC and SM widths are used, and the values of the Wilson coefficients for the flavour-changing chromomagnetic operators are assumed to be zero [35, 47, 48]. The uncertainty corresponds to missing higher-order corrections. The λ_{tqH} coupling corresponds to the sum in quadrature of the couplings relative to the two possible chirality combinations of the quark fields, $\lambda_{tqH} \equiv \sqrt{|\lambda_{t_\mathrm{L}q_\mathrm{R}}|^2 + |\lambda_{q_\mathrm{L}t_\mathrm{R}}|^2}$.

In the search for the tqH couplings in the decay of a top quark, only heavy-flavour tagging of reconstructed jets can be used to disentangle the c and u flavours. The associated production of a single top quark and a Higgs boson helps to lift the degeneracy between the tcH and tuH couplings from the yields of the selected events. The up quark being a valence quark in the proton and the charm quark a sea quark, the $ug \to tH$ yield is roughly seven times larger than the $cg \to tH$ one for equal couplings. Moreover, the distributions of some quantities, such as the rapidity of the Higgs boson or the charge of the W boson from the top-quark decay, show clear differences between $cg \to tH$ and $ug \to tH$. Both charm tagging and tH production are used in this analysis.

The two final states, tH and tqH, arising from the processes $pp \to tH$ and $pp \to t\bar{t} \to t\bar{q}H$, respectively, derive from the same coupling, and a single parameter of interest, namely the branching ratio for the decay $t \to qH$, is extracted or constrained from the data, assuming only one coupling, either tcH or tuH, is non-zero at a time. The analysis presented here expands on methods already used in ref. [37]. A profile likelihood fit of $\mathcal{B}$ is performed on several orthogonal regions that target events with two photons from the Higgs boson decay, zero or one charged lepton, and are further subdivided on the basis of charm tagging and top-quark reconstruction. In each category the background in the diphoton signal region

JHEP12(2023)195

is estimated in a data-driven approach by a fit to the diphoton invariant mass distribution. Given the increase in the integrated luminosity of close to a factor four, and the improved analysis, with a better categorisation and additional background rejection using multivariate discriminants, a significant gain is expected compared with ref. [37].

2 Detector, data set and Monte Carlo simulation

2.1 ATLAS detector

The ATLAS detector [49] consists of an inner detector (ID) for tracking, surrounded by a superconducting solenoid providing a 2 T magnetic field, electromagnetic and hadronic calorimeters, and a muon spectrometer. The inner detector provides tracking in the pseudorapidity[2] region $|\eta| < 2.5$ and consists of a silicon pixel detector, including the insertable B-layer [50, 51] installed before Run 2, and a microstrip detector inside a transition radiation tracker that covers $|\eta| < 2.0$. The electromagnetic calorimeter, a lead/liquid-argon sampling device with accordion geometry, is divided into one barrel ($|\eta| < 1.475$) and two endcap ($1.375 < |\eta| < 3.2$) sections. Longitudinally, it is divided into three layers. While most of the energy is deposited in the second layer, the first layer, referred to as the strip layer, has fine segmentation in the regions $|\eta| < 1.4$ and $1.5 < |\eta| < 2.4$ to help the separation of photons from neutral hadrons and to allow shower directions to be measured. In the range of $|\eta| < 1.8$, a presampler layer allows the energy to be corrected for losses upstream of the calorimeter. The barrel ($|\eta| < 1.7$) hadronic calorimeter consists of steel and scintillator tiles, while the endcap sections ($1.5 < |\eta| < 3.2$) are composed of copper and liquid argon. The forward calorimeter ($3.1 < |\eta| < 4.9$) uses copper and tungsten as absorber with liquid argon as active material. The muon spectrometer consists of precision ($|\eta| < 2.7$) and trigger ($|\eta| < 2.4$) chambers equipping a toroidal magnet system which surrounds the hadronic calorimeter. The field integral of the toroid magnets ranges between 2.0 and 6.0 Tm across most of the detector.

A two-level trigger system is used to select events. The first-level trigger is implemented in hardware and uses a subset of the detector information to accept events at a rate below 100 kHz. This is followed by a software-based trigger that reduces the accepted event rate to 1 kHz on average, depending on the data-taking conditions [52].

An extensive software suite [53] is used in the reconstruction and analysis of real and simulated data, in detector operations, and in the trigger and data acquisition systems of the experiment.

2.2 Data set

This analysis uses the full proton-proton collision data set recorded by the ATLAS detector from 2015 to 2018 (Run 2) with the LHC operating at a centre-of-mass energy of $\sqrt{s} = 13\,\text{TeV}$ and a bunch spacing of 25 ns. After application of data-quality requirements [54], the

[2]ATLAS uses a right-handed coordinate system with its origin at the nominal interaction point (IP) in the centre of the detector and the z-axis along the beam line. Observables labelled as transverse are projected onto the x–y plane. The x-axis points from the IP to the centre of the LHC ring, and the y-axis points upwards. Cylindrical coordinates (r, ϕ) are used in the transverse plane, ϕ being the azimuthal angle around the beam line. The pseudorapidity is defined in terms of the polar angle θ as $\eta = -\ln\tan(\theta/2)$. The angular distance ΔR is defined as $\Delta R \equiv \sqrt{(\Delta\eta)^2 + (\Delta\phi)^2}$. The transverse energy is $E_{\text{T}} = E/\cosh(\eta)$.

JHEP12(2023)195

integrated luminosity amounts to 139 fb^{-1}, with a relative uncertainty of 1.7% [55], obtained using the LUCID-2 detector [56] for the primary luminosity measurements. The data were recorded with instantaneous luminosities up to $1.9 \times 10^{34}\,\mathrm{cm}^{-2}\mathrm{s}^{-1}$. The mean number of interactions per bunch crossing, μ, ranged from an average of 13 in 2015 to 38 in 2017, with a global average of about 34. The inelastic collisions that occur in addition to the hard interaction produce mainly particles with low transverse momenta that form the pile-up background.

2.3 Simulation samples

Samples of simulated Monte Carlo (MC) events were produced to model the different signal and background processes.

Two sets of signal samples, corresponding to the $pp \to t\bar{t} \to bW\bar{q}H$ and $pp \to tH \to bWH$ processes, were produced at NLO in QCD. The $t\bar{t}$ production was simulated using POWHEG BOX v2 [57] and the tH production with MADGRAPH5_aMC@NLO 2.6.0 [58] and the TopFCNC Universal FeynRules Output (UFO) [59] model [60]. The top quarks are decayed by MADSPIN [61] using the TopFCNC UFO model, while the Higgs boson decay into two photons is simulated in PYTHIA 8.2 [62]. Both simulations use the NNPDF3.0NLO [63] parton distribution functions (PDF) for the matrix element and are interfaced to PYTHIA 8.2 with the A14 tune [64] for the parton shower, hadronisation and underlying event using the NNPDF2.3LO [65] PDF. The top quark mass is set to 172.5 GeV, and the Higgs boson mass, m_H, is set to 125 GeV.

For $t\bar{t}$ production, two MC samples with one top quark decaying into a charm quark and a Higgs boson were produced. The two samples correspond to the leptonic and the hadronic decays of the W boson. The leptonic decays of the W boson include all three lepton flavours ($W \to \ell\nu, \ell = e, \mu, \tau$). Equivalent samples with $t \to uH$ are also used. The nominal renormalisation and factorisation scales in the $t\bar{t}$ signal sample are chosen to be equal and given by $\mu_\mathrm{f} = \mu_\mathrm{r} = \sqrt{m_t^2 + p_\mathrm{T}^2}$, where p_T is the transverse momentum of the top quark, and the h_damp value[3] is set equal to $1.5m_t$ [66]. The cross-section for the $pp \to t\bar{t} \to bW\bar{q}H, H \to \gamma\gamma$ process is $\sigma = 2\sigma_{t\bar{t}}\mathcal{B}_{\gamma\gamma}\mathcal{B}(1-\mathcal{B})$, where $\sigma_{t\bar{t}}$ is the $t\bar{t}$ production cross-section and $\mathcal{B}_{\gamma\gamma}$ the branching ratio for the $H \to \gamma\gamma$ decay. For these two quantities, the following SM values are used: $\sigma_{t\bar{t}} = 832 \pm 51$ pb, calculated at next-to-next-to-leading order in QCD including resummation of next-to-next-to-leading logarithmic soft gluon terms with TOP++ 2.0 (see [67] and references therein), and $\mathcal{B}_{\gamma\gamma} = (2.27 \pm 0.07) \times 10^{-3}$ [68]. For a branching ratio for the FCNC top-quark decay of $\mathcal{B} = 10^{-3}$, just below the ATLAS combined limit using 36 fb^{-1} of data collected at $\sqrt{s} = 13$ TeV [39], the cross-section is 3.77 ± 0.25 fb.

For the tH signal simulation, the nominal renormalisation and factorisation scales are chosen to be equal and given by $\mu_\mathrm{f} = \mu_\mathrm{r} = m_t + m_H$. The interference between double-resonant top production and single-top production at NLO is neglected. Eight MC samples were generated, where the top quark decays into bW; for a given quark flavour (u or c) and W decay ($W \to \ell\nu$ or $q\bar{q}'$) two samples were considered according to the chirality

[3]The h_damp parameter controls the transverse momentum of the first additional emission beyond the leading-order Feynman diagram in the parton shower and therefore regulates the high-p_T emission against which the $t\bar{t}$ system recoils.

JHEP12(2023)195

Process	Generator	Showering	PDF set	Parameter tune	cross-section (fb)
ggF	Powheg Box NNLOPS [70, 71]	Pythia 8.2	PDF4LHC15	AZNLO [72]	110
VBF	Powheg Box [73]	Pythia 8.2	PDF4LHC15	AZNLO	8.6
WH	Powheg Box [74]	Pythia 8.2	PDF4LHC15	AZNLO	3.1
ZH	Powheg Box [74]	Pythia 8.2	PDF4LHC15	AZNLO	2.0
$t\bar{t}H$	Powheg Box [75]	Pythia 8.2	NNPDF3.0nlo	A14	1.2
$b\bar{b}H$	Powheg Box	Pythia 8.2	NNPDF3.0nlo	A14	1.1
$tHjb$	MadGraph5_aMC@NLO	Pythia 8.2	NNPDF3.0nlo	A14	0.17
tWH	MadGraph5_aMC@NLO	Pythia 8.2	NNPDF3.0nlo	A14	0.03
$\gamma\gamma$ + jets	Sherpa	Sherpa	NNPDF3.0nnlo	—	51.8×10^3
$t\bar{t}\gamma$	MadGraph 5	Pythia 8.2	NNPDF2.3lo	A14	4.6×10^3
$V\gamma\gamma, V = W, Z$	Sherpa	Sherpa	NNPDF3.0nnlo	—	236
$Z \to ee$	Powheg Box	Pythia 8.1	CT10	AZNLO	2×10^6
$tW\gamma$	MadGraph 5	Pythia 8.2	NNPDF3.0nlo	A14	533
$tq\gamma$	MadGraph5_aMC@NLO	Pythia 8.2	NNPDF3.0nlo	A14	1139

Table 1. Summary of the background MC samples. For Higgs boson production, the $H \to \gamma\gamma$ branching ratio is included. The non-resonant background samples are normalised according to the cross-sections provided by the generators, except the $Z \to ee$ sample, which is normalised using a control data sample.

combination of the involved quark fields. It was observed that the chirality choice has a negligible impact on the kinematic distributions. The samples are therefore combined in the following. The cross-sections for the $pp \to bWH, H \to \gamma\gamma$ process are 1.61 ± 0.13 fb and 0.24 ± 0.02 fb for $q = u$ and c, respectively, for a single FCNC operator with $C = 1.4$ and $\Lambda = 1$ TeV, see refs. [46, 60].

The contributions from the known Higgs boson production mechanisms were simulated for each of the five main SM modes: gluon-gluon fusion (ggF), vector boson fusion (VBF), associated WH, ZH and $t\bar{t}H$ production, and the rare processes $b\bar{b}H$, tHq and tWH. The cross-sections given in ref. [68] are used for normalisation, except for ggF, for which the next-to-next-to-next-to-leading-order cross-section is used. An event sample, labelled $\gamma\gamma$ + jets in the following, is used as a benchmark sample for non-resonant diphoton production with a fully hadronic final state. It was generated with Sherpa 2.2.4 [69] with up to one parton at NLO and up to three partons at LO, using the NNPDF3.0nnlo PDF and the dedicated set of tuned parton-shower parameters developed by the Sherpa authors. The (sub-)leading photon E_{T} is required to be above (18) 20 GeV and the diphoton invariant mass is required to be in the range [90, 175] GeV. Other non-resonant background processes (in particular from $t\bar{t} + \gamma$ production) have also been simulated. More details are given in table 1.

The stable particles, defined as particles with a lifetime larger than 10 ps, are passed through a full detector simulation [76] based on Geant4 [77, 78] for the resonant background and $V\gamma\gamma$ processes. For other samples, a faster version of the simulation was used, that relies on a parameterisation for the response of the calorimeters and on Geant4 for the other components of the detector [76]. The resulting "particle hits" in the active detector material are later transformed into detector signals during digitisation. Pile-up is modelled with simulated minimum-bias events generated with Pythia 8.186 [79] using the NNPDF2.3lo

JHEP12(2023)195

set of parton distribution functions and the A3 set of tuned parameters [80]. The number of events overlaid onto the hard-scattering events during digitisation is randomly chosen to reproduce the distribution of μ observed in data. The effects of pile-up events occurring in nearby bunch crossings (out-of-time pile-up) are also modelled.

3 Event reconstruction and selection

Selected events must contain two isolated, high-p_{T} photons to tag the Higgs boson decay. Additional objects, jets, leptons (electrons or muons) and missing transverse momentum, are requested as signatures of top-quark decays. The reconstruction and selection of all these objects are described below. A prerequisite is that at least one primary vertex is reconstructed in the event. In the general case of several reconstructed vertices, the $\gamma\gamma$ vertex is used [81]. It is determined taking into account the direction of each photon (determined by exploiting the longitudinal segmentation of the calorimeter), p_{T} balance using charged-particle tracks from a given vertex and the two photons, and constraints from the longitudinal size of the luminous region. This vertex is used to correct the photon's four momenta and to construct the track-based isolation, jets, flavour tagging and $E_{\mathrm{T}}^{\mathrm{miss}}$.

3.1 Photon reconstruction and identification

The photon reconstruction [82] is seeded by clusters of energy deposits in the calorimeter, formed using a dynamical, topological cell-clustering algorithm [83]. Clusters are accepted in the pseudorapidity region $|\eta| < 2.37$, with the exception of the transition region [1.37, 1.52], where dead material affects both the identification and the energy measurement. Misidentification of electrons as photon candidates is suppressed by checking if a calorimeter deposit reconstructed as a photon has a matching track compatible with the primary vertex.

Clusters without any matching track in the ID are classified as unconverted photon candidates. Clusters with a matching conversion reconstructed from one or two tracks are classified as converted photon candidates. The photon identification efficiency depends on the photon's transverse momentum, its pseudorapidity and whether it is classified as converted or unconverted [82]. First a *loose* identification criterion is required, which is based on requirements on their shower shape. The two highest-p_{T} photon candidates, which must fulfil $p_{\mathrm{T}} > 25$ GeV, are the main objects for the analysis and are used to choose the primary vertex (see above). After this preselection, the photons are further required to satisfy a *tight* identification criterion to suppress fake photon candidates.

The photon candidates are also required to satisfy *loose* isolation criteria. The track-based isolation (sum of p_{T} of tracks in a cone of $\Delta R = 0.2$ around the photon candidate) must be smaller than $0.05 \times p_{\mathrm{T}}^{\gamma}$, where p_{T}^{γ} is the photon's transverse momentum, and the calorimeter-based isolation (sum of the transverse energy of topological clusters in a cone of $\Delta R = 0.2$, corrected for pile-up and photon energy leakage) must be smaller than $0.065 \times p_{\mathrm{T}}^{\gamma}$. The dependence of the isolation efficiency on the event topology was assessed from a simulation-based study, giving an efficiency (per diphoton event) of 89.5% for the ggF production process and 82.1% for the $t\bar{t}H$ final state. The track- and calorimeter-based isolation distributions are in good agreement between data and simulation. A scale factor is used to correct for observed

JHEP12(2023)195

small differences. The results of the analysis are extracted using the sample of events where both photons satisfy the *tight* identification criterion and are isolated. An orthogonal sample, in which one of the two photons does not pass the *tight* identification or is not isolated, is used as a control sample at various stages of the analysis.

The photon energy is determined in four steps using a combination of simulation-based and data-driven calibration factors [82, 84]. The data-driven calibration factors used to set the absolute energy scale are determined from $Z \to ee$ events. The photon energy resolution in simulation is corrected to match the resolution in data. This correction is derived simultaneously with the energy calibration factors using $Z \to ee$ events by adjusting the electron energy resolution such that the width of the reconstructed Z-boson peak in simulation matches the width observed in data.

3.2 Reconstruction and selection of leptons, light- and heavy-flavour jets and missing transverse momentum

Electrons and muons are used in the leptonic selection. Electrons are reconstructed from energy clusters in the calorimeter associated with an ID track [82]. Muon candidates are built from tracks reconstructed in the muon chambers [85, 86]. A matching of these tracks to ID tracks is required in the region $|\eta| < 2.5$. Muons are required to meet the conditions $|\eta| < 2.7$ and $p_{\mathrm{T}} > 10$ GeV; for electrons the transverse momentum threshold is raised to $p_{\mathrm{T}} = 15$ GeV, to remove fake electron candidates, which are more abundant at low p_{T}. Additionally, electrons must satisfy $|\eta| < 2.47$, excluding the transition region. Both the electrons and muons must satisfy *medium* identification and *loose* isolation requirements [82, 85, 86].

Jets are reconstructed using the anti-k_t algorithm [87, 88] with the radius parameter $R = 0.4$ and are required to have a rapidity $|y| < 4.4$ and transverse momentum $p_{\mathrm{T}} > 25$ GeV. The objects used to form jets come from a particle-flow algorithm which combines information from the tracker and the calorimeters [89]. To suppress pile-up jets, the *tight* working point of the *jet vertex tagger* (JVT) [90] is used (for jets with $p_{\mathrm{T}} < 60$ GeV). Jets with $|\eta| > 2.5$ are also required to satisfy the *forward jet vertex tagger* (fJVT) [91]. To limit further pile-up effects, the jet-p_{T} threshold is set to 30 GeV.

Central jets ($|\eta| < 2.4$) that are identified as originating from a b-quark are labelled as b-jets. The DL1r tagger [92] is used, with a 77% efficiency working point, corresponding to a rejection of ~ 250 (~ 5.5) for jets with p_{T} in the range [40, 60] GeV originating from u-, d-, and s-quarks or gluons (c-quarks) in simulated $pp \to t\bar{t}$ events. The p_{T} calibration of b-jets is adjusted after they have been identified as such.[4] A dedicated charm tagger has been optimised and calibrated for this analysis. It uses the b-jet, c-jet and light-flavour jet probabilities (p_b, p_c and p_{light}) from the DL1r tagger, and combines them into a final discriminant defined as $\mathrm{DL1r}_c = \ln\left(\frac{p_c}{f_b \cdot p_b + (1-f_b)\cdot p_{\mathrm{light}}}\right)$. The b-fraction parameter, f_b, and the threshold, $\mathrm{DL1r}_c^{\mathrm{thr}}$, for a jet to be c-tagged were optimised, leading to the choices $f_b = 0.2$ and $\mathrm{DL1r}_c^{\mathrm{thr}} = 1$. The average efficiency of the charm tagging of jets originating from c-quarks in the $t\bar{t}$ signal sample is 38%. The corresponding efficiency to tag jets originating from b-quarks

[4] The four-momentum of the highest-p_{T} muon found within a cone of radius $R = \min(0.4, 0.04 + 10\ \mathrm{GeV}/p_{\mathrm{T}})$ around the jet axis is added to that of the jet, and a residual correction is applied to equalise the response to jets with leptonic or hadronic decays of heavy-flavour hadrons.

JHEP12(2023)195

(light-quarks or gluons, τ-leptons) is about 15% (3%, 31%). Efficiency measurements for this tagger are performed simultaneously for all jet flavours (b, c and light) using semileptonic and dileptonic $t\bar{t}$ events, and scale factors to be applied to jets in simulation have been derived. These scale factors are compatible with unity for jets originating from b-quarks and slightly smaller (larger) than unity for jets from c-quarks (u-, d- or s-quarks or gluons). The uncertainties in the scale factors for b-quark jets are about 5%. The uncertainties in the scale factors for the c-quark jets and jets originating from light quarks or gluons range from 5% to 15% being slightly higher for transverse momenta below 40 GeV.

In case of overlap between reconstructed particles, a removal is performed keeping, in order of priority, photons, then leptons, and finally jets. Leptons or jets within a cone of radius $\Delta R = 0.4$ around photon candidates are removed first; then jets within $\Delta R = 0.2$ of electrons are removed; at last, leptons within $\Delta R = 0.4$ of the remaining jets are removed.

The missing transverse energy, $E_{\mathrm{T}}^{\mathrm{miss}}$, is computed as the negative sum of the transverse momenta of the reconstructed photons, electrons, muons and jets, plus a "soft term" reconstructed from all tracks not associated with any of the previous objects [93]. Only tracks originating from the diphoton primary vertex are considered.

As already mentioned above, and more generally, differences between data and simulation are corrected for by using scale factors, applied as weights to MC events.

3.3 Event preselection

Events were selected with a diphoton trigger requiring at least two candidate photons with E_{T} greater than 35 GeV and 25 GeV, respectively. Both photons are required to fulfil the *loose* identification requirements for the 2015 and 2016 data sets, while *medium* criteria are required for the 2017 and 2018 ones to cope with the larger instantaneous luminosity. The requirements are based on the energy leakage in the hadronic calorimeter and on the shower shape in the second and first two layers of the electromagnetic calorimeter for the *loose* and *medium* criterion, respectively [94, 95]. The trigger selections are estimated to be fully efficient for photons satisfying the offline selection criteria discussed above and matched to the photons identified by the trigger.

The selection of candidate events starts by applying a tight diphoton selection: at least two photons satisfying the *tight* identification criteria, with *loose* calorimeter-based and track-based isolation, $p_{\mathrm{T}} > 40$ GeV (30 GeV) for the leading (sub-leading) photon candidate, and a diphoton invariant mass between 100 GeV and 160 GeV. Events without identified lepton (electron or muon) enter the hadronic selection; those with exactly one lepton enter the leptonic selection. Events with two or more identified leptons are rejected. Jets are ordered by decreasing value of p_{T}, and up to five jets are considered. The various steps of the hadronic and leptonic selections are described in sections 3.4 and 3.5, respectively, and a summary is given in diagrammatic form in section 3.6.

3.4 Hadronic selection

The hadronic selection targets the processes $t\bar{t} \to bW(q\bar{q}')\bar{q}H(\gamma\gamma)$ and $tH \to bW(q\bar{q}')H(\gamma\gamma)$, for which at least four and three jets in the final state are required, respectively. Selected

JHEP12(2023)195

events are classified in categories of decreasing purity, based on kinematic constraints and flavour tagging.

3.4.1 Categories

Addressing first the $t\bar{t}$ production, the reconstruction of the neutral current top-quark decay (called Top1 in the following) and the SM top-quark decay (called Top2) is described below. For events with four (five or more) jets, in total four (20) combinations are formed. Each combination has 1+3 jets, of which the first one is associated with the two photons in view of forming the Top1 combination, while the group of three is candidate to form Top2. All considered jets that satisfy 152 GeV $< m_{\gamma\gamma j} <$ 190 GeV are subject to c-tagging (and not to b-tagging). All other jets are subject to b-tagging. There must be exactly one b-tagged jet among them. Figure 2(a) shows the $m_{\gamma\gamma j}$ invariant mass distribution, before the selection on this variable. Figure 2(b) shows the invariant mass of the three other jets (among which one is b-tagged) for those combinations passing the Top1 condition. The Top2 condition is met if the 3-jet invariant mass satisfies 120 GeV $< m_{jjj} <$ 220 GeV. The signal distribution corresponds to the tcH coupling with an arbitrary $t \to cH$ branching ratio of $\mathcal{B} = 2\%$. The background is the sum of the $tX\gamma$ ($X = t, W, q$) and $V\gamma\gamma$ contributions as described in section 2.3, normalised to the cross-sections as given by the MC generators, together with the dominant $\gamma\gamma$ + jets contribution. An additional $Z \to ee$ contribution, relevant for the leptonic analysis, is also included.

Based on the criteria above, events accepted at this stage can fall into one or more of the following four categories:

- had-tt,c: at least one combination satisfying the Top1 and the Top2 mass requirements, for which j_0, the jet forming the Top1 combination with the diphoton system, is c-tagged;
- had-tt,$\not c$: same as tt,c except that the charm tagging condition is not met;
- had-tx,c: same as tt,c except that the Top2 mass requirement is not met. The combination which includes the b-tagged jet and whose invariant mass is closest to 170 GeV is retained;
- had-tx,$\not c$: same as tx,c except that the charm tagging condition is not met.

If an event falls into more than one of the categories, the one with the highest rank (tt,$c >$ tt,$\not c >$ tx,$c >$ tx,$\not c$) is kept.

The had-tH category, which targets the $pp \to tH$ production, is populated with events with three jets and events with four or more jets that are not retained in the above categories. All jets are subject to b-tagging and at least one 3-jet combination meeting the Top2 mass constraint is required, with the additional requirements that one of the three jets is b-tagged, and there is no additional b-tagged jet.

To improve the sensitivity of the analysis, a multivariate selection is performed, using boosted decision trees (BDT) as implemented in TMVA [96].

JHEP12(2023)195

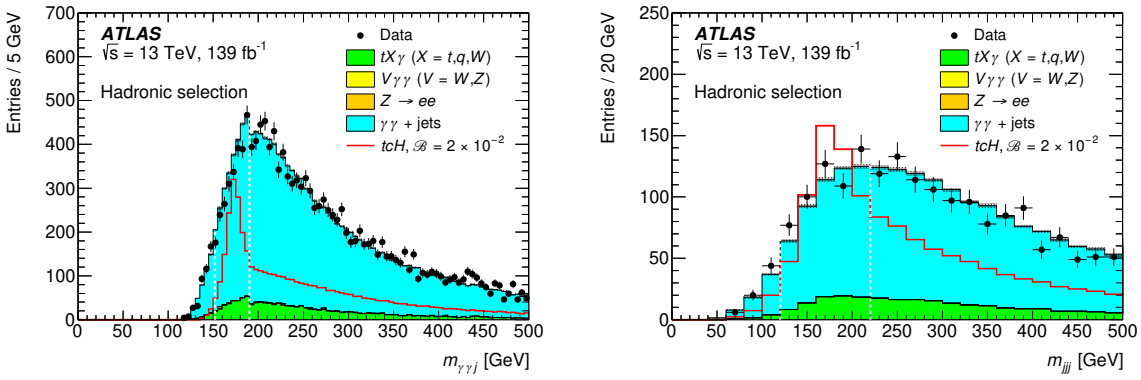

(a) (b)

Figure 2. Distributions of the invariant mass of (a) the two photons and one jet, when there is one b-tagged jet among the three other jets which will be also tested against the Top2 mass condition and (b) the three jets (among which one is b-tagged) when a combination of the two photons and another jet passes the Top1 condition (see text). To normalise the simulation to data, the $\gamma\gamma$ + jets contribution is scaled up by 3% and down by 4% in (a) and (b), respectively. The signal corresponds to the tcH coupling, with a $t \to cH$ branching ratio of 2%. The hatched bands represent the statistical uncertainty in the simulated background. The vertical dotted lines indicate the ranges of the Top1 and Top2 invariant mass selections.

3.4.2 Additional BDT selection

For the four categories addressing the $t\bar{t}$ production, the BDT is trained with events from both sub-categories c and $\not{c}$ together, as the response of the charm-tagging algorithm is largely independent of the kinematic properties of the objects entering the BDT. The BDT is trained using the tcH signal and non-resonant background processes, as described in section 2.3, with a diphoton invariant mass limited to the range [115, 135] GeV. This range is chosen to select backgrounds in the signal mass range, while keeping enough events for the BDT training.

Several combinations of jets can satisfy the selection requirements for the same analysis category. The combination for which $m_{\gamma\gamma j}$ is closest to 171 GeV, and m_{jjj} is closest to 170 GeV is used to build the BDT input variables. Starting from a large number of BDT input variables, a reduced working set is obtained by removing the least discriminating variable until a marked decrease of the significance[5] is observed. For both the $t\bar{t}$- and tH-targeted categories a set of seven variables was chosen. For the categories targeting the $t\bar{t}$ channel, the variables used as input to the BDT, ranked in decreasing order of sensitivity, are:

1. $p_{\mathrm{T}}^{\gamma\gamma}$: transverse momentum of the diphoton system;
2. m_{jj}: invariant mass of the W-boson candidate, defined as the two-jet system, that, combined with the b-jet candidate, forms the $t \to Wb$ decay candidate;
3. m_{tt}: invariant mass of the two top-quark candidates;
4. p_{T}^{b}: transverse momentum of the b-jet candidate;

[5]Here, the significance is defined as $\sqrt{2(s+b)\ln(1+s/b)-2s}$, where s is the FCNC signal yield, assuming $\mathcal{B} = 10^{-3}$, and b the non-resonant background yield in the diphoton mass range from 122 GeV to 129 GeV.

JHEP12(2023)195

5. $\max(\Delta R_{c\gamma})$: distance between the jet candidate in Top1 and the farthest photon;

6. $\min(\Delta R_{bj})$: distance between the b-jet candidate and the closest jet;

7. $H_{\mathrm{T}}^{\gamma\gamma 4j}$: scalar sum of the p_{T} of the two photons and the four jets of the retained combination.

The distributions of $p_{\mathrm{T}}^{\gamma\gamma}, m_{tt}, p_{\mathrm{T}}^{b}$ and $H_{\mathrm{T}}^{\gamma\gamma 4j}$ extend to larger values for the signal than for the dominant $\gamma\gamma$ + jets background. For signal events $\max(\Delta R_{c\gamma})$ and $\min(\Delta R_{bj})$ are on average smaller than for background, and m_{jj} peaks near m_W. The variables m_{jj} and m_{tt} are not used for the had-tx categories.

For the tH category, the BDT is trained using the tuH signal sample, which populates the tH-selected sample in similar proportions from the tH and $t\bar{t}$ production modes, as opposed to the tcH signal, where the contribution from the former is much reduced, due to a smaller $pp \to tH$ production cross-section from a charm quark. The background events used for the training are the same as the ones used for the $t\bar{t}$-targeted BDTs. The selected variables, ranked in decreasing order of sensitivity, are:

1. $p_{\mathrm{T}}^{\gamma\gamma}$;

2. m_{jj};

3. $H_{\mathrm{T}}^{\mathrm{Top2}}$: scalar sum of the p_{T} of the three jets entering the Top2 combination;

4. $H_{\mathrm{T}}^{\mathrm{jets}}$: scalar sum of the p_{T} of all selected jets;

5. $\min(\Delta R_{bj})$;

6. $(p_{\mathrm{T}}^{\gamma_1} + p_{\mathrm{T}}^{\gamma_2})/m_{\gamma\gamma}$: scalar sum of the p_{T} of the two photons normalised to the diphoton invariant mass;

7. ΔR_{bW}: distance between the b-jet candidate and the W-boson candidate.

Three of the seven variables are the same as in the $t\bar{t}$ case. Similarly to $\min(\Delta R_{bj})$, ΔR_{bW} tends to have lower values for signal than for background. The distributions of the variables $H_{\mathrm{T}}^{\mathrm{Top2}}, H_{\mathrm{T}}^{\mathrm{jets}}$ and $(p_{\mathrm{T}}^{\gamma_1} + p_{\mathrm{T}}^{\gamma_2})/m_{\gamma\gamma}$ are slightly harder for signal than for background. The normalisation to $m_{\gamma\gamma}$ for the latter variable prevents the BDT from learning that the signal is narrowly peaked in $m_{\gamma\gamma}$. For events with three selected jets, $H_{\mathrm{T}}^{\mathrm{Top2}}$ and $H_{\mathrm{T}}^{\mathrm{jets}}$ are identical.

Events with a BDT score (between -1 and 1) larger than a given threshold are retained. This threshold is determined by maximising the expected significance computed using only events satisfying 122 GeV $< m_{\gamma\gamma} <$ 129 GeV. For the tH category two thresholds are used to optimise the performance for both the tuH and the tcH signals. Events with a BDT score larger than 0.45 enter the tHT category, most relevant for tuH, while events with a score between 0.2 and 0.45 enter the tHL category, more relevant for tcH. The significance improvements are about 20% for the $t\bar{t}$-targeted categories, and 30% for the tH-targeted ones. The signal acceptances, with sub-categories c and $\not c$ grouped, are shown in table 2.

JHEP12(2023)195

Selection	Before BDT selection			After BDT selection		
Category	had-tt	had-tx	had-tH	had-tt	had-tx	had-(tHL+tHT)
tcH	2.81±0.02	2.08±0.01	3.50±0.02	2.13±0.01	1.14±0.01	1.80±0.01
tuH	2.23±0.01	1.66±0.01	3.55±0.02	1.58±0.01	0.94 ±0.01	2.01±0.02

Table 2. Acceptance, in percent, of the hadronic selection for simulated signal events. The sub-categories c and $\not c$ are grouped. The acceptances for the tH category with BDT selection are given for tHL and tHT together. The uncertainties are statistical only.

3.4.3 Diphoton invariant mass distributions

The distributions of the diphoton invariant mass, for each of the six categories, after the BDT selection, are shown in figure 3. The contribution of the $tX\gamma$ and $V\gamma\gamma$ processes are normalised to the cross-sections as predicted by the MC generators and the integrated luminosity of the sample. The $\gamma\gamma$ + jets normalisation is obtained by scaling this sample, in such a way that the total number of simulated events outside of the [120, 130] GeV $m_{\gamma\gamma}$ interval matches the number observed in data, for each channel independently. The FCNC signal contributions correspond to $\mathcal{B} = 5 \times 10^{-4}$.

3.5 Leptonic selection

The leptonic selection targets the processes $t\bar{t} \to bW(\ell\nu)\bar{q}H(\gamma\gamma)$ and $tH \to bW(\ell\nu)H(\gamma\gamma)$. Exactly one lepton and one or more jets are required, in addition to the two photons. Figure 4 shows the transverse mass, m_{T}, of the W-boson candidate, calculated from the transverse momentum of the lepton and the missing transverse momentum. An additional requirement of exactly one b-tagged jet is applied. The sum of the non-resonant backgrounds ($tX\gamma, V\gamma\gamma$ and $\gamma\gamma$ + jets) is shown together with data. A Zee component, resulting from $Z \to ee$ events, in which one of the electrons is misidentified as a photon candidate and the other photon is genuine, is also considered. Its normalisation is fixed using the electron-photon (leading and sub-leading) mass distributions, which show an enhancement at the Z-boson mass. Altogether, the different contributions provide a relatively good description of the background although in the low-m_{T} region, the simulation overestimates the data.

Using a W-boson mass constraint allows for the calculation of the longitudinal momentum of the escaping neutrino, and therefore the reconstruction of the invariant mass $m_{\ell\nu j}$ of the $\ell\nu j$ system (Top2). To ensure a reliable reconstruction of this mass and to reject background, the events are required to satisfy $m_{\mathrm{T}} > 30\,\mathrm{GeV}$, except for those collected in the very loose category lep-R, defined later. If there are two valid solutions for the longitudinal momentum of the neutrino, the solution giving a Top2 mass closer to 170 GeV is retained. In the absence of a real solution, m_W is replaced by $m_{\mathrm{T}} + 100\,\mathrm{MeV}$ in the mass constraint, which ensures two almost degenerate, real solutions.

3.5.1 Categories

Addressing first the $t\bar{t}$ production, the $m_{\gamma\gamma j}$ invariant mass distribution is formed, considering each of the up to five jets in the event. The distribution is shown in figure 5(a). All jets that satisfy 152 GeV $< m_{\gamma\gamma j} <$ 190 GeV are subject to c-tagging (and not to b-tagging).

JHEP12(2023)195

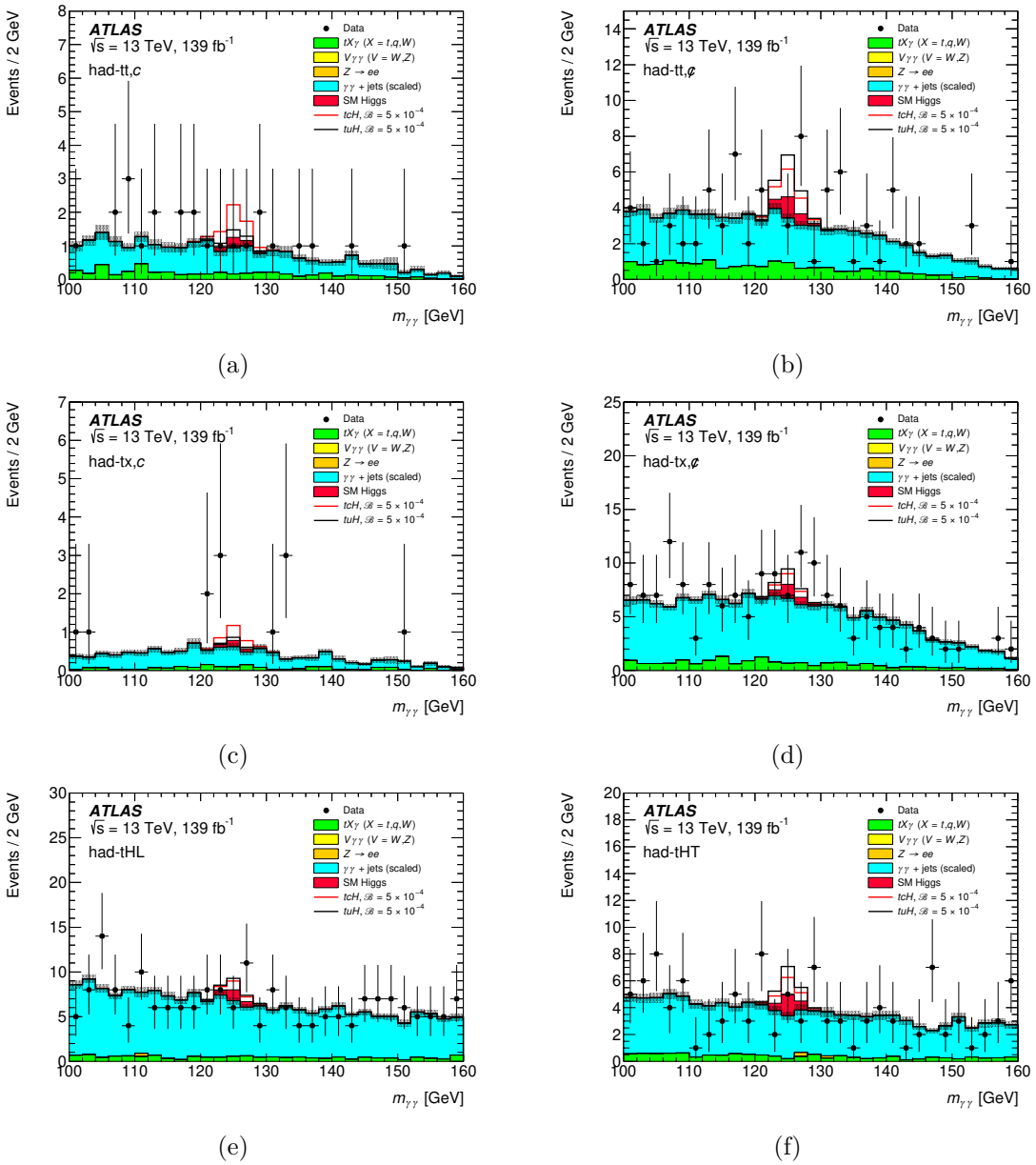

Figure 3. Distributions of the diphoton invariant mass for data, signal, Higgs boson production in the SM, and non-resonant background for the (a) had-tt,c, (b) had-tt,$\not{c}$, (c) had-tx,c, (d) had-tx,$\not{c}$ categories after the BDT selection, and (e) had-tHL and (f) had-tHT categories. The hatched bands correspond to the statistical uncertainty in the sum of the simulated non-resonant backgrounds.

JHEP12(2023)195

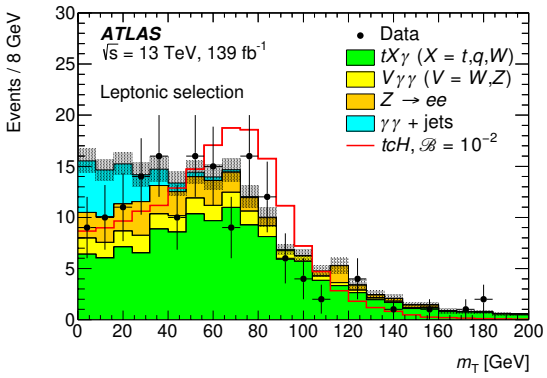

Figure 4. Distribution of the transverse mass of the lepton and $E_{\mathrm{T}}^{\mathrm{miss}}$, for events with exactly one charged lepton and one b-tagged jet. The distributions of the main backgrounds and of a tcH signal with a branching ratio of 1% are also shown. The statistical uncertainty in the sum of the non-resonant backgrounds is represented as a hatched band.

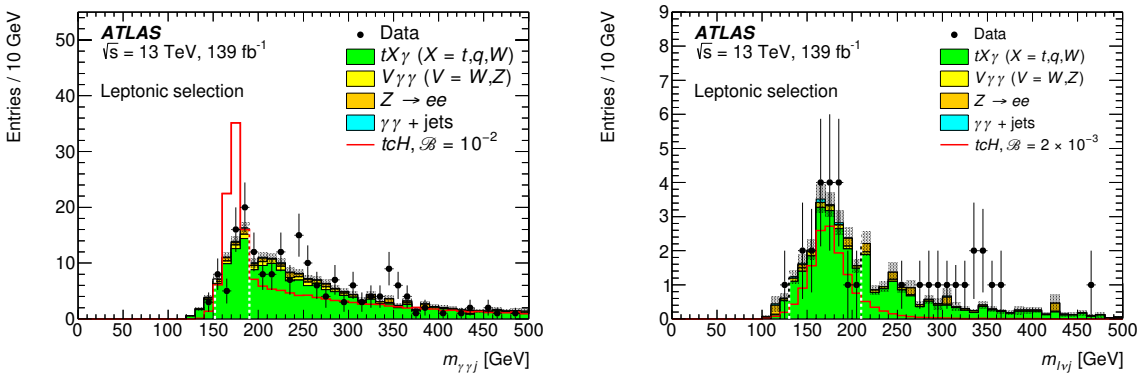

(a) (b)

Figure 5. Distributions of (a) the invariant mass of the two photons and one jet, with the additional condition that there is one b-tagged jet among the other jets that can form a Top2 candidate with the lepton and $E_{\mathrm{T}}^{\mathrm{miss}}$, and (b) $m_{\ell\nu j}$ (j is the b-tagged jet) when at least a combination of the two photons and another jet passes the Top1 condition. The signal corresponds to the tcH coupling with a 1% or 0.2% $t \to cH$ branching ratio for (a) and (b), respectively. The simulation (except for Zee) is rescaled to match the data by a factor of 0.96 and 0.83 in (a) and (b), respectively. The statistical uncertainty in the sum of the non-resonant backgrounds is represented as a hatched band.

All other jets are subject to b-tagging. There must be exactly one b-tagged jet among those eligible. After the requirement that at least one $\gamma\gamma j$ combination passes the Top1 condition, the distribution of the $m_{\ell\nu j}$ invariant mass is shown in figure 5(b). Only one entry is made if more than one jet could be associated with the two photons and satisfy the Top1 condition.

JHEP12(2023)195

Events with at least one combination fulfilling the Top1 condition, for which, in addition, the Top2 requirement 130 GeV $< m_{\ell\nu j} <$ 210 GeV is met with the b-tagged jet, are assigned to category lep-tt. If the jet in the $\gamma\gamma j$ combination meeting the Top1 condition is c-tagged, the event is assigned to the lep-tt,c category and otherwise to the lep-tt,$\not c$ category.

The lep-tH category, which targets the $pp \to tH$ production, contains events with only one jet, and events with two or more jets for which no Top1 condition is satisfied. All jets are subject to b-tagging, and there must be exactly one b-tagged jet among the (up to five) leading ones. The $m_{\ell\nu j}$ invariant mass is required to satisfy the Top2 condition, with the b-tagged jet. In the lep-tH category, the background is still reducible, and a further selection is made using a BDT. Similarly to the had-tH categories, the signal originating from the tuH coupling is used for training. The background sample is the sum of the $tX\gamma$, $V\gamma\gamma$ and $\gamma\gamma$ + jets contributions. To have enough events in the background sample, the full diphoton mass range from 100 GeV to 160 GeV is used for the training. The seven most sensitive variables used as input to the BDT, ranked in decreasing order of sensitivity, are:

1. $p_{\mathrm{T}}^{\gamma\gamma}$;
2. m_{T}: the transverse mass of the lepton+$E_{\mathrm{T}}^{\mathrm{miss}}$ system;
3. Q_{lep}: the lepton's electric charge;
4. $\mathrm{N}_{\mathrm{jets}}$: the number of jets passing the p_{T} and y requirements;
5. H_{T}: the sum of $E_{\mathrm{T}}^{\mathrm{miss}}$, lepton p_{T} and p_{T} of the all jets passing the jet selection;
6. $y_{\gamma\gamma}$: the rapidity of the diphoton system;
7. $(p_{\mathrm{T}}^{\gamma_1} + p_{\mathrm{T}}^{\gamma_2})/m_{\gamma\gamma}$.

Four of the seven retained variables are equivalent to the ones used in the hadronic tH selection. The value of $\mathrm{N}_{\mathrm{jets}}$ is significantly smaller on average for the signal than for backgrounds, and Q_{lep} has twice as many positives than negatives, while $y_{\gamma\gamma}$ extends towards larger values, altogether providing additional separation power. For a tcH-originating signal, a BDT trained with a tcH signal does not yield a better significance than the one trained with the signal originating from tuH, thus only the latter is used, with a single optimum lower threshold of 0.15. The BDT brings a significance improvement of about 25% (20%) for a signal originating from tuH (tcH).

All other events that have one lepton, two photons, and one b-tagged jet — excluding those categorised as lep-tt,c, lep-tt,$\not c$, or lep-tH after BDT selection — are assigned to an additional category named lep-R.

The signal acceptance is shown in table 3. Here, the categories c and $\not c$ are grouped, as their sum is independent of the c-tagging working point. Altogether, the total acceptance of the hadronic plus leptonic selections, adding the $t\bar{t}$ and tH production modes, is 8.3% (7.4%) for tcH (tuH).

JHEP12(2023)195

Selection	Before BDT selection			After BDT selection
Category	lep-R	lep-tt	lep-tH	lep-tH
tcH	1.42±0.01	1.09±0.01	1.11±0.01	0.69±0.01
tuH	1.27±0.01	0.87±0.01	1.15±0.01	0.77±0.01

Table 3. Acceptance, in percent, of the leptonic selection for simulated signal events. The sub-categories tt,c and tt,$\not{c}$ are grouped. The uncertainties are statistical only.

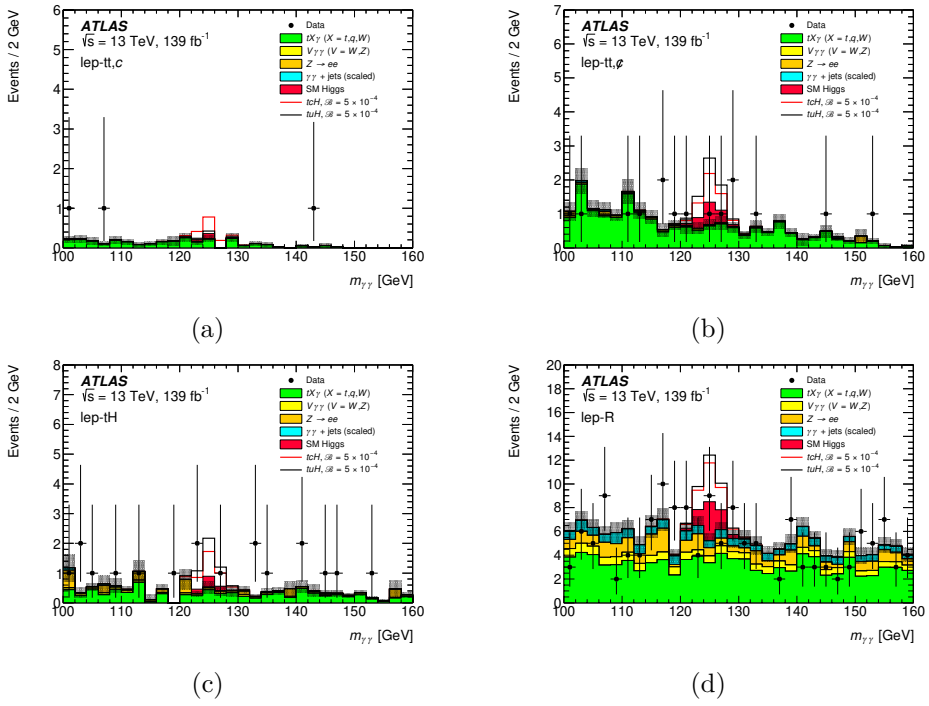

Figure 6. Distributions of the diphoton invariant mass for data, signal, Higgs boson production in the SM, and non-resonant background for events in categories (a) lep-tt,c, (b) lep-tt,$\not{c}$, (c) lep-tH after the BDT selection and (d) lep-R. The hatched bands correspond to the statistical uncertainty in the sum of the simulated non-resonant contributions.

3.5.2 Diphoton invariant mass distributions

The distributions of the diphoton invariant mass are shown in figure 6. The non-resonant background is normalised using the cross-sections as predicted by the MC generators, and the integrated luminosity. For all categories this gives an expected contribution in agreement with data within statistical uncertainty. The FCNC signal contributions are normalised to $\mathcal{B} = 5 \times 10^{-4}$.

3.6 Summary of the selections and expected number of signal events

Figure 7 summarises the selection criteria described in the previous sections, and table 4 shows the numbers of events expected in the ten analysis categories.

JHEP12(2023)195

Selection	Hadronic					Leptonic			
Category	had-tt,c	had-tt,$\not{c}$	had-tx,c	had-tx,$\not{c}$	had-(tHL+tHT)	lep-tt,c	lep-tt,$\not{c}$	lep-tH	lep-R
tcH	2.32±0.15	3.62±0.24	0.90±0.06	2.30±0.15	5.04±0.30	1.00±0.07	2.05±0.14	1.92±0.11	3.94±0.24
tuH	0.54±0.04	5.39±0.34	0.18±0.01	3.35±0.21	7.56±0.45	0.17±0.01	3.08±0.20	2.90±0.15	4.74±0.26

Table 4. Number of signal events expected after the BDT selection. A branching ratio of 5×10^{-4}, close to the 95% CL expected limit in the absence of signal, is assumed for the FCNC decay. The categories had-tHL and had-tHT are grouped in this table. The uncertainties include the statistical uncertainty from the number of selected events, the theoretical uncertainties in the $pp \to t\bar{t}$ and the $pp \to tH$ cross-sections and in the $H \to \gamma\gamma$ branching ratio.

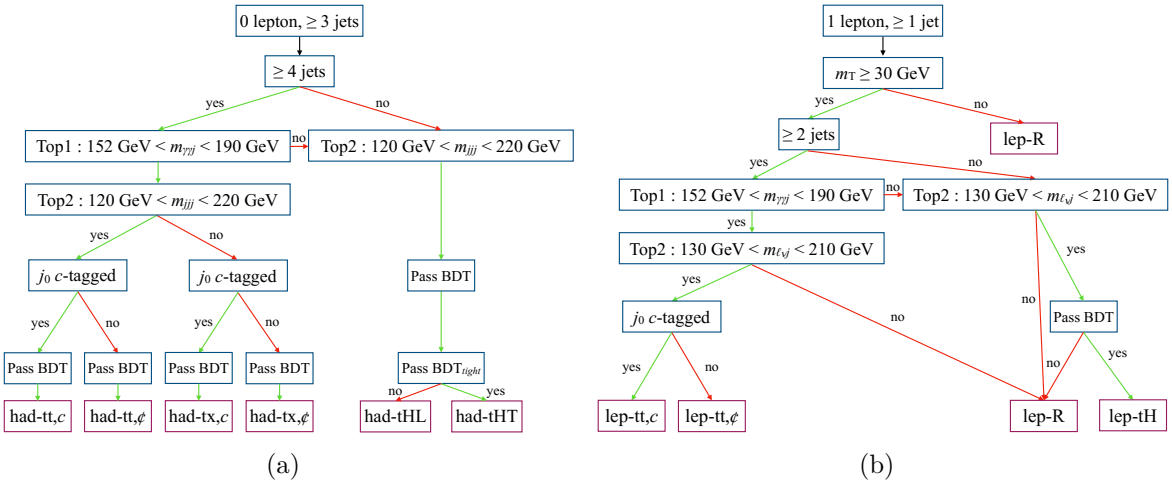

Figure 7. Summary of the categories used in the statistical analysis for the (a) hadronic and (b) leptonic channels. Green (red) arrows indicate that the criterion in the box is met (not met). Exactly one b-jet is required. The jet j_0, combined with the diphoton system, forms the $t \to qH$ decay candidate.

4 Statistical analysis and systematic uncertainties

The branching ratio $\mathcal{B}$ of the decay $t \to c(u)H$ is determined in a fit to data by using a likelihood function $L(\mathcal{B})$, defined as the product of the likelihoods for the ten categories. Hypothesised values of $\mathcal{B}$ are probed with a test statistic based on a profile likelihood ratio. The theoretical uncertainties are mainly related to the $t\bar{t}$ and tH production cross-sections, the $H \to \gamma\gamma$ branching ratio, the resonant background from SM processes and the signal generator uncertainties. The estimate of the uncertainty in the non-resonant background is explained in section 4.1. The experimental and the event generator systematic uncertainties are detailed in section 4.2. All systematic uncertainties are introduced as nuisance parameters in the likelihood.

JHEP12(2023)195

4.1 Likelihood construction

Two different likelihood constructions are used according to the number of events observed in the side band (SB) of the $m_{\gamma\gamma}$ mass distribution (defined as $m_{\gamma\gamma} \in [100, 122[\cup]129, 160]$ GeV). A too small number prevents a reliable fit of the background shape parameters. This is the case for the lep-tt,c category, for which simple event counting is used. Here, the number of non-resonant background events in the signal region (SR defined by $m_{\gamma\gamma} \in [122, 129]$ GeV) is estimated as $b^{SR} = \alpha b$, where b is the yield of the non-resonant background in the side-band region, and α is a transfer factor discussed below. For the nine other categories, the number of events in the SB is enough to determine the background shape and a standard unbinned extended likelihood is used.

The resonant diphoton invariant mass distributions, assumed to be the same for the signal and SM Higgs boson processes, are described by double-sided Crystal-Ball [97] (DSCB) functions (a Gaussian function with power-law tails on both sides), whose parameters are obtained from a fit to the mass spectrum of the simulated FCNC signal.

For all categories but lep-tt,c, the background shapes are determined using the $m_{\gamma\gamma}$ distributions built from the simulation (MC templates). A set of smooth templates is additionally built using kernel smoothing [98] applied to the background distributions. Fits of a signal + background model to the templates are performed using an analytic function for the background model. The Higgs boson mass hypothesis is scanned in the range [121, 129] GeV in steps of 0.5 GeV and a background functional form is accepted if the condition $n_{sp} < 0.2\sigma_{bkg}$ is met for all m_H, where n_{sp} is the fitted spurious signal and σ_{bkg} is the statistical uncertainty in the fitted signal yield. The preference is given to the raw templates, for which a relaxed spurious signal criterion (made to accommodate 2σ local fluctuations in the MC template, if the MC statistical uncertainty is large) must be used in some cases, resulting in larger n_{sp}. However, the chosen functional form must also satisfy the standard criterion for the smooth template. When several functions pass the spurious signal criteria, the one with the smallest number of parameters is chosen. The functions chosen for the background model are a Fermi-Dirac function for category had-tt,c, an exponential of second order polynomial for categories had-tt,$\not{c}$ and had-tx, and a decreasing exponential function for the other categories; n_{sp} ranges from 0.16 event for the had-tt,c category to 2.3 events for the lep-R category.

In the lep-tt,c category, the transfer factor α is estimated as the average obtained from two sources: a control data sample for which one of the two photons is either not isolated, or not tightly identified, and the simulation sample, normalised to match the uncertainty from the data control sample. The resulting transfer factor is $\alpha = 0.27 \pm 0.15$, where the uncertainty is dominated by the statistical uncertainty of the control sample. For a uniform $m_{\gamma\gamma}$ distribution $\alpha = 0.13$ is expected.

4.2 Systematic uncertainties

4.2.1 Theoretical uncertainties

The uncertainties in the absolute normalisation of the signal yield take into account the uncertainties in the $pp \to t\bar{t}$ (6.1%) and $pp \to tH$ cross-sections. The latter were estimated with MadGraph5_aMC@NLO and the TopFCNC UFO at NLO, and amount to 7.9%

JHEP12(2023)195

(7.5%) for the tcH (tuH) coupling. The uncertainty in the $H \to \gamma\gamma$ branching ratio[6] (2.9% [68]) is included as well.

The uncertainties related to the choice of the factorisation and renormalisation scales in the signal acceptances are estimated by varying the scales in the matrix element up and down by a factor of two relative to the nominal values, and recalculating the acceptance in each case. The largest deviation from the nominal acceptance is taken as the uncertainty. The impact of the proton PDFs+α_s choice is obtained by using the root mean square of the signal acceptance when considering the 100 MC replicas available in the NNPDF3.0NLO set. The uncertainty due to parton shower, underlying event and multiple interaction modelling is estimated as the difference between the yields predicted from alternative signal samples, produced with Herwig 7.1.6 [101], and those using the nominal samples produced with Pythia 8.2. Depending on the category, the corresponding uncertainties range from 2% to 16% for the $pp \to t\bar{t}$ process and 1% to 30% for the $pp \to tH$ process; the largest uncertainties are found in categories with a small acceptance for the considered process. This is the case, for example, for the latter number: it corresponds to the variation of the yield of the process $pp \to tH \to q\bar{q}'bH$ in the lep-tt,$\not e$ category, whose acceptance is below 2% relative to the dominant contribution. The impact of the NLO tool choice for the generation of the $t\bar{t}$ events has been studied by comparing Powheg+Pythia 8.2 (nominal) and MadGraph5_aMC@NLO+Pythia 8.2, for a subsample of events and the tcH coupling. The observed difference corresponds to an uncertainty ranging between 3% and 10%, depending on the category. The value of the top-quark mass has a small impact on the acceptance of the tight criterion used to select Top1 candidates. The corresponding uncertainty in the acceptance ranges from 0.3% to 1.0%, depending on the analysis category and on the production process.

SM cross-sections are assumed for the Higgs boson production. An uncertainty in the global normalisation is taken into account (in addition to the $H \to \gamma\gamma$ branching ratio uncertainty), which combines the QCD and PDF+α_s uncertainties as provided in ref. [68].

4.2.2 Experimental uncertainties

The uncertainty in the integrated luminosity is 1.7% [55], affecting the overall normalisation of the signal and resonant background processes.

The systematic uncertainties in the photon energy scale and energy resolution have a large impact on the signal shape. This impact is quantified from the relative variations of the mean and interquartile range of the $m_{\gamma\gamma}$ distribution between the nominal samples, and samples obtained by varying the energy scale or energy resolution of the photon candidates according to their uncertainties. They amount to approximately 0.5% for the mean and up to 15% for the width. The mean and width parameters of the DSCB functions are allowed to float within these uncertainties. The impact of the uncertainties in the photon energy scale and energy resolution on the signal yields is found to be negligible.

The uncertainties associated with the photon trigger and identification amount to about 2.8%, dominated by the identification efficiency uncertainty.

[6]The SM branching ratio, confirmed by the ATLAS and CMS collaborations at the $\mathcal{O}(10)$% level [99, 100], is used.

JHEP12(2023)195

The differences in b-tagging and c-tagging efficiencies between data and simulation are included in the event weights of the simulated samples. The uncertainties in these weights induce variations of the expected signal yield of the order of 1.5% for b-tagging and up to about 10% for c-tagging in the tt,c categories for a $t\bar{t}$ signal with a non-zero tcH coupling. The uncertainties related to the JVT and fJVT selection are estimated in the same way.

The systematic uncertainties associated with the jet energy scale and jet energy resolution [102] are determined by modifying the jet transverse momenta, re-running the analysis and estimating the yield variations in each category. The changes in jet momenta are propagated to $E_{\mathrm{T}}^{\mathrm{miss}}$ in this procedure. Adding in quadrature all effects, the variations range from about 1% to 9%, depending on the category and the process ($t\bar{t}$ or tH) for categories where the signal yield is significant.

The uncertainty associated with the lepton energy scale, identification, and reconstruction efficiency is smaller than 1%. The uncertainty associated with $E_{\mathrm{T}}^{\mathrm{miss}}$ is obtained with the same methodology as that used for the jet energy scale, applied to the soft term introduced in section 3.2.

Since many of the uncertainties have a small impact and the analysis is statistically limited, uncertainties affecting b-tagging, $E_{\mathrm{T}}^{\mathrm{miss}}$, photon identification and lepton-related reconstruction are grouped to have only one effective nuisance parameter for each of these quantities.

The same uncertainties are included for the resonant background estimate. Since this background mostly comes from the $pp \to t\bar{t}H$ process, only this production mode is considered to assess the size of the uncertainties, which are then used to scale the total yield from SM Higgs boson production.

5 Results

5.1 Constraints on the tqH couplings using the $H \to \gamma\gamma$ channel

The diphoton mass spectra in the most significant categories are shown in figure 8, together with the fitted background shapes and the resonant background and signal shapes, assuming a non-zero tcH coupling. No signal is observed, and the best fit estimate of the $t \to cH$ branching ratio, $\hat{\mathcal{B}}$, is $(-1.3 \pm 2.3) \times 10^{-4}$, assuming the tuH coupling to be zero. A summary of the fitted numbers of background events, together with the numbers of observed events in the SR, is given in table 5. The yields for the standard Higgs boson production modes are constrained to the SM prediction within theoretical and experimental uncertainties. The fitted $t \to uH$ branching ratio assuming the tcH coupling to be zero is $(-0.5 \pm 1.9) \times 10^{-4}$.

The evolution of $q_{\mathcal{B}} = -2\left(\ln L(\mathcal{B}) - \ln L(\hat{\mathcal{B}})\right)$ as a function of $\mathcal{B}$ for each category individually, and for the combined likelihood for the tcH (top) and tuH (bottom) couplings is presented in figure 9 (left), using an Asimov data set [103] assuming the background-only hypothesis. Several categories contribute in a similar way to the sensitivity to the tcH coupling (had-tt,c, had-tt,$\not{c}$, lep-tt,$\not{c}$, lep-tH), while for tuH the categories had-tt,$\not{c}$, lep-tt,$\not{c}$, had-tHT and lep-tH dominate. In figure 9 (right), the evolution of $q_{\mathcal{B}}$ for the data is compared with the one obtained with the Asimov data set.

JHEP12(2023)195

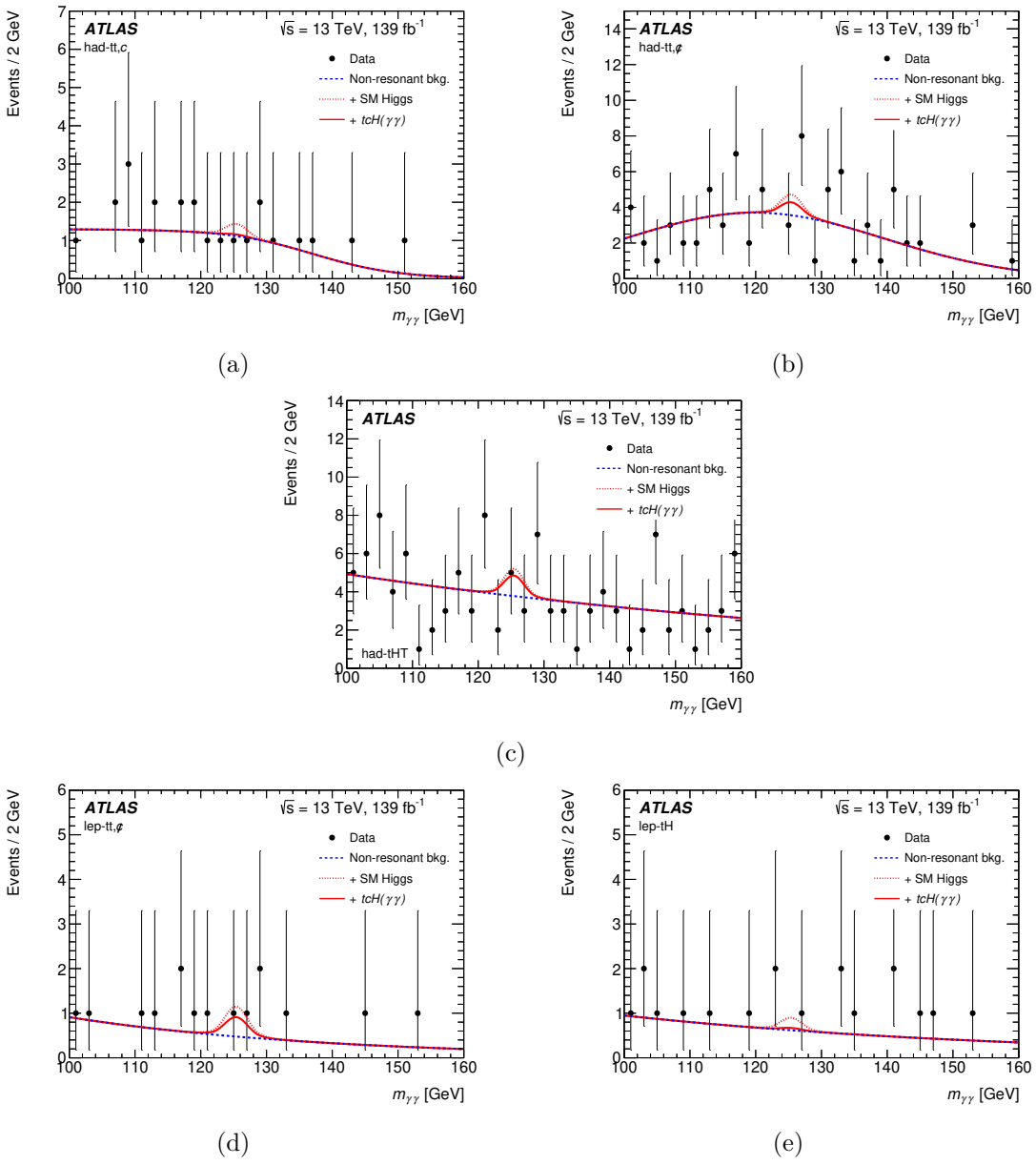

Figure 8. Distributions of the diphoton invariant mass for the most relevant categories: three in the hadronic selection ((a) had-tt,c, (b) had-tt,$\not{\ell}$, and (c) had-tHT) and two in the leptonic selection ((d) lep-tt,$\not{\ell}$ and (e) lep-tH). The result of a fit to the data of the sum (full line) of a signal component with the mass of the Higgs boson fixed to $m_H = 125$ GeV and assuming a non-zero tcH coupling, a non-resonant background component (dashed line) and the SM Higgs boson contribution (difference between the dotted and dashed lines) is superimposed.

JHEP12(2023)195

Selection	Hadronic					
Category	had-tt,c	had-tt,$\not{c}$	had-tx,c	had-tx,$\not{c}$	had-tHL	had-tHT
SM Higgs boson	0.65	2.40	0.33	2.62	2.37	2.77
Other background	3.9	12.4	2.0	24.3	23.0	13.2
Total background	4.5 ± 1.0	14.8 ± 1.6	2.3 ± 0.6	26.9 ± 2.7	25.4 ± 1.7	16.0 ± 1.3
Data	5	11	3	33	27	14

Selection	Leptonic			
Category	lep-tt,c	lep-tt,$\not{c}$	lep-tH	lep-R
SM Higgs boson	0.27	1.37	0.68	6.4
Other background	0.5	1.6	2.2	17.2
Total background	0.8 ± 0.6	3.0 ± 0.5	2.8 ± 0.5	23.6 ± 1.6
Data	0	3	3	22

Table 5. Numbers of events in the SR ($m_{\gamma\gamma} \in [122, 129]$ GeV) for the SM Higgs boson production and the fitted non-resonant background, assuming a non-zero tcH coupling, together with the number of observed events in data, in the ten categories. The uncertainty in the total background yield in each category is also shown.

The evolution of the signal confidence level, CL_s, as a function of the $t \to cH$ branching ratio is shown in figure 10. For a confidence level of 5%, the observed limit on the branching ratio is 4.3×10^{-4}. The expected exclusion limit in the absence of signal is 4.7×10^{-4}. For the tuH coupling, the observed limit at 95% CL is 3.8×10^{-4}, while 3.9×10^{-4} is expected in the absence of signal.

The sensitivity of the analysis is limited by the statistical precision. With all constrained nuisance parameters fixed at their best fit estimates, the expected 95% CL upper limit on $\mathcal{B}$ is 4.4×10^{-4} for the tcH coupling and 3.6×10^{-4} for the tuH coupling. The most relevant systematic uncertainties affecting the limit on the tqH coupling are presented in table 6, where the impact is given as the relative variation of the expected upper limit when fixing the corresponding nuisance parameters at their best-fit value. The largest contributions to the uncertainty originate from the photon energy resolution, the $t\bar{t}$ cross-section, the $H \to \gamma\gamma$ branching ratio, the parton shower description and the non-resonant background shape choices.

The relevance of the c-tagging categorisation has been appraised by studying the separation between the tcH and the tuH hypotheses. The test statistic used to quantify this separation is defined as $q_c \equiv \left(\ln L(c, \hat{\hat{\mathcal{B}}}_c) - \ln L(u, \hat{\hat{\mathcal{B}}}_u)\right)$, where $\hat{\hat{\mathcal{B}}}_{c(u)}$ is the conditional maximum-likelihood estimator of $\mathcal{B}_{c(u)}$ under the hypothesis of a non-zero tcH (tuH) coupling. Distributions of the test statistic for the tcH and tuH hypotheses, for the nominal analysis and the alternative one, where no c-tagging is used, have been built for a $t \to qH$ branching ratio of 10^{-3}, using 3500 pseudo-experiments.[7] The fractions of experiments from the tuH hypothesis above the median q_c of the distribution for the tcH hypothesis are about 8% and 40% for the nominal and alternative analyses, respectively. Even though the c-tagging categorisation has a small impact on the expected upper limit on the $t \to qH$ branching ratio, it thus has a significant power for the characterisation of a potential signal.

[7]This value of the branching ratio has been chosen as it is slightly below the ATLAS combined limit obtained with 36 fb^{-1} [39], and would have resulted in a sufficient sensitivity for an observation.

JHEP12(2023)195

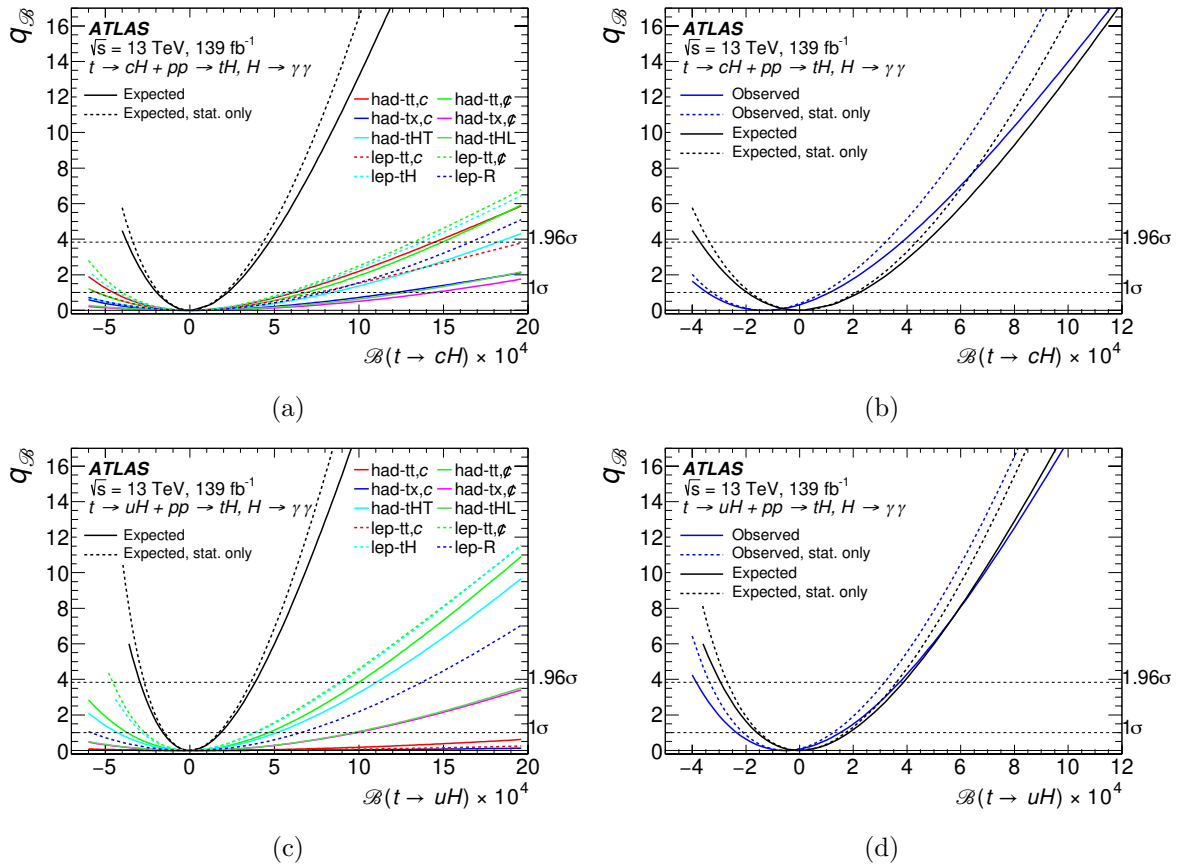

Figure 9. Evolution of $q_{\mathcal{B}}$, the negative log-profile-likelihood ratio (times 2), as a function of the $t \to cH$ (top) and $t \to uH$ (bottom) branching ratios. In (a) and (c) the evolutions for each category and the combined sample are shown for the expected result in the absence of signal, while (b) and (d) show a comparison between the observed result and the expectation in the absence of signal. The likelihood functions are only defined for a positive expected number of events, hence some categories and combined curves do not cover the full scanned range.

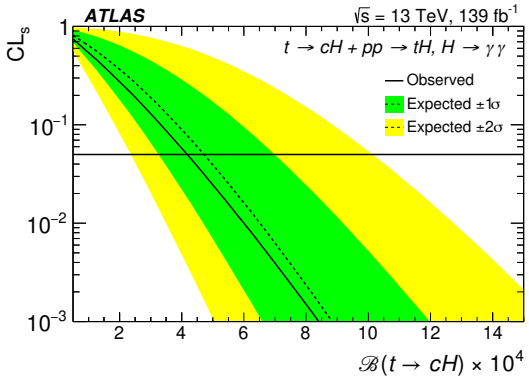

Figure 10. Evolution of the signal confidence level, $\mathrm{CL_s}$, as a function of the $t \to cH$ branching ratio $\mathcal{B}$ for the observation (full line) and the expectation in the absence of signal (dashed line). The bands at $\pm 1\sigma$ and $\pm 2\sigma$ around the expected curve are also shown.

JHEP12(2023)195

Source	relative impact (%)
Experimental	
Photon energy resolution	1.5
Photon identification	0.4
Luminosity, pile-up modelling	0.3
Jet energy scale and resolution, flavour tagging	< 0.2
Theoretical	
Normalisation $(\sigma(pp \to t\bar{t}, tH), \mathcal{B}(H \to \gamma\gamma))$	1.1
Parton showering model	0.8
m_t value, NLO generator for $pp \to tH$	0.5
Resonant background	0.5
Non-resonant background	2.3

Table 6. Most relevant systematic uncertainties and their relative impact (in percent) on the expected upper limit on the $t \to qH$ branching ratio.

5.2 Combination of ATLAS searches

The analysis described above has been combined with the corresponding ATLAS searches using the $H \to \tau^+\tau^-$ [40] and $H \to b\bar{b}$ [41] decays. The correlations between the uncertainties in the different channels have been assessed. The luminosity uncertainty, the uncertainty in the pile-up modelling and the uncertainties related to the jet energy scale and energy resolution are correlated among the three channels. The uncertainties pertaining to b-tagging are correlated between the $H \to \tau^+\tau^-$ and $H \to b\bar{b}$ analyses. The remaining uncertainties (mostly from experimental sources, and signal and background modelling) are taken as uncorrelated. Although some of the sources of systematic uncertainties (especially related to b-tagging, electron and muon identification and signal modelling) are common to the three search channels, they have not been correlated for simplicity. In each search, the dominant systematic uncertainties are different. In addition, the $H \to \tau^+\tau^-$ and $H \to \gamma\gamma$ channels are dominated by the data's statistical uncertainty. Therefore, the combined result has a very low sensitivity to the assumed correlations of uncertainties across channels.

The observed (expected) 95% CL combined upper limits on the branching ratios are 5.8×10^{-4} (3.0×10^{-4}) and 4.0×10^{-4} (2.4×10^{-4}) for the decays $t \to cH$ and $t \to uH$, respectively. A summary of the upper limits on the branching ratios obtained by the individual searches, and their combination, is given in figure 11. Using eq. (1.2), the observed upper limit in the tcH combined analysis corresponds to $\lambda_{tqH} < 0.045$ at 95% CL, slightly smaller than the value $\lambda_{tqH}^{\mathrm{CS}} = 0.057$ obtained by applying the Cheng and Sher ansatz [9], using running charm-quark and top-quark masses at the top-quark mass of 0.61 GeV and 163 GeV, respectively. In the SMEFT framework, the limit observed for the $t \to cH$ $(t \to uH)$ branching ratio translates to a limit on the corresponding Wilson coefficient of $C_{u\varphi}^{23,32} = 1.07$ $(C_{u\varphi}^{13,31} = 0.88)$ at 95% CL, assuming $C_{u\varphi}^{32,23} = 0$ $(C_{u\varphi}^{31,13} = 0)$, and for a mass scale $\Lambda = 1$ TeV.

JHEP12(2023)195

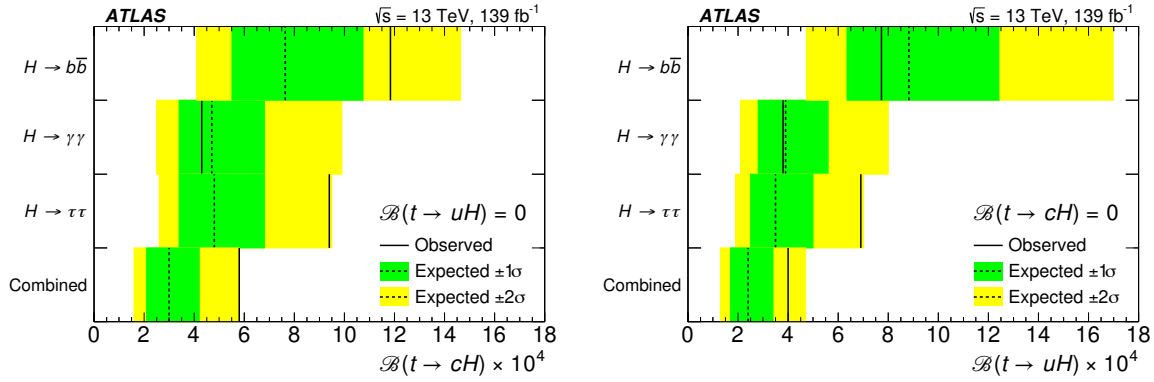

(a) (b)

Figure 11. 95% CL upper limits on (a) $\mathcal{B}(t \to cH)$ assuming $\mathcal{B}(t \to uH) = 0$ and (b) $\mathcal{B}(t \to uH)$ assuming $\mathcal{B}(t \to cH) = 0$ for the individual searches and their combination. The observed limits (solid lines) are compared with the expected (median) limits under the background-only hypothesis (dotted lines). The surrounding shaded bands correspond to the 68% and 95% CL intervals around the expected limits, denoted by $\pm 1\sigma$ and $\pm 2\sigma$, respectively.

6 Conclusion

The FCNC coupling of a top quark with a lighter up-type quark q ($q = c, u$) and a Higgs boson has been searched for in a data set of 139 fb^{-1} of 13 TeV proton-proton collisions recorded by the ATLAS experiment at the LHC, using the Higgs boson decay mode $H \to \gamma\gamma$. Both the $pp \to t\bar{t}$ production, followed by the top-quark decay $t \to qH$, and the $pp \to tH$ production are considered in the analysis. The cross-sections of both processes are parameterized in terms of the tqH coupling strength, and results are reported as constraints on the branching ratio $\mathcal{B}$ of the $t \to qH$ decay. The analysis is split into hadronic and leptonic channels, targeting the decay of the W boson from the SM top-quark decay either in a hadronic mode or in a leptonic mode. For each channel the analysis is further split into sub-channels targeting either $pp \to tH$ or $pp \to t\bar{t}$ production. In the latter case charm tagging is used in view of further separating the tcH coupling from the tuH one.

Exploiting the diphoton invariant mass distributions, a sideband technique is used to constrain the background under the signal. Taking into account the contribution of the SM Higgs boson production, an upper limit on the $t \to cH$ ($t \to uH$) decay branching ratio in the absence of signal of $\mathcal{B} = 4.7 \times 10^{-4}$ (3.9×10^{-4}) is expected at 95% CL. For the tcH coupling, the sensitivity increase relative to the analysis described in ref. [37] is a factor of ~ 1.5 better than expected from the increase of the integrated luminosity alone, thanks to an improved event reconstruction and categorisation. No statistically significant excess is observed in the data, and a limit on $\mathcal{B}$ of 4.3×10^{-4} (3.8×10^{-4}) is set at the 95% CL for $m_H = 125$ GeV.

The combination of this search with ATLAS searches using the Higgs boson decays $H \to \tau^+\tau^-$ and $H \to b\bar{b}$ yields observed (expected) 95% CL upper limits on the $t \to cH$ branching ratio of 5.8×10^{-4} (3.0×10^{-4}) assuming $\mathcal{B}(t \to uH) = 0$, and on the $t \to uH$ branching ratio of 4.0×10^{-4} (2.4×10^{-4}) assuming $\mathcal{B}(t \to cH) = 0$. Corresponding limits on the relevant Wilson coefficients in the SMEFT framework are also derived.

JHEP12(2023)195

Acknowledgments

We thank CERN for the very successful operation of the LHC, as well as the support staff from our institutions without whom ATLAS could not be operated efficiently.

We acknowledge the support of ANPCyT, Argentina; YerPhI, Armenia; ARC, Australia; BMWFW and FWF, Austria; ANAS, Azerbaijan; CNPq and FAPESP, Brazil; NSERC, NRC and CFI, Canada; CERN; ANID, Chile; CAS, MOST and NSFC, China; Minciencias, Colombia; MEYS CR, Czech Republic; DNRF and DNSRC, Denmark; IN2P3-CNRS and CEA-DRF/IRFU, France; SRNSFG, Georgia; BMBF, HGF and MPG, Germany; GSRI, Greece; RGC and Hong Kong SAR, China; ISF and Benoziyo Center, Israel; INFN, Italy; MEXT and JSPS, Japan; CNRST, Morocco; NWO, Netherlands; RCN, Norway; MEiN, Poland; FCT, Portugal; MNE/IFA, Romania; MESTD, Serbia; MSSR, Slovakia; ARRS and MIZŠ, Slovenia; DSI/NRF, South Africa; MICINN, Spain; SRC and Wallenberg Foundation, Sweden; SERI, SNSF and Cantons of Bern and Geneva, Switzerland; MOST, Taiwan; TENMAK, Türkiye; STFC, United Kingdom; DOE and NSF, United States of America. In addition, individual groups and members have received support from BCKDF, CANARIE, Compute Canada and CRC, Canada; PRIMUS 21/SCI/017 and UNCE SCI/013, Czech Republic; COST, ERC, ERDF, Horizon 2020, ICSC-NextGenerationEU and Marie Skłodowska-Curie Actions, European Union; Investissements d'Avenir Labex, Investissements d'Avenir Idex and ANR, France; DFG and AvH Foundation, Germany; Herakleitos, Thales and Aristeia programmes co-financed by EU-ESF and the Greek NSRF, Greece; BSF-NSF and MINERVA, Israel; Norwegian Financial Mechanism 2014-2021, Norway; NCN and NAWA, Poland; La Caixa Banking Foundation, CERCA Programme Generalitat de Catalunya and PROMETEO and GenT Programmes Generalitat Valenciana, Spain; Göran Gustafssons Stiftelse, Sweden; The Royal Society and Leverhulme Trust, United Kingdom.

The crucial computing support from all WLCG partners is acknowledged gratefully, in particular from CERN, the ATLAS Tier-1 facilities at TRIUMF (Canada), NDGF (Denmark, Norway, Sweden), CC-IN2P3 (France), KIT/GridKA (Germany), INFN-CNAF (Italy), NL-T1 (Netherlands), PIC (Spain), ASGC (Taiwan), RAL (U.K.) and BNL (U.S.A.), the Tier-2 facilities worldwide and large non-WLCG resource providers. Major contributors of computing resources are listed in ref. [104].

Open Access. This article is distributed under the terms of the Creative Commons Attribution License (CC-BY4.0), which permits any use, distribution and reproduction in any medium, provided the original author(s) and source are credited.

References

[1] ATLAS collaboration, *Observation of a new particle in the search for the Standard Model Higgs boson with the ATLAS detector at the LHC*, *Phys. Lett. B* **716** (2012) 1 [arXiv:1207.7214] [INSPIRE].

[2] CMS collaboration, *Observation of a new boson at a mass of* 125 *GeV with the CMS experiment at the LHC*, *Phys. Lett. B* **716** (2012) 30 [arXiv:1207.7235] [INSPIRE].

[3] S.L. Glashow, J. Iliopoulos and L. Maiani, *Weak interactions with lepton-hadron symmetry*, *Phys. Rev. D* **2** (1970) 1285 [INSPIRE].

JHEP12(2023)195

[4] W. Altmannshofer, B. Maddock and D. Tuckler, *Rare top decays as probes of flavorful Higgs bosons*, *Phys. Rev. D* **100** (2019) 015003 [arXiv:1904.10956] [INSPIRE].

[5] J.A. Aguilar-Saavedra, *Top flavor-changing neutral interactions: theoretical expectations and experimental detection*, *Acta Phys. Polon. B* **35** (2004) 2695 [hep-ph/0409342] [INSPIRE].

[6] J.A. Aguilar-Saavedra and B.M. Nobre, *Rare top decays $t \to c\gamma$, $t \to cg$ and CKM unitarity*, *Phys. Lett. B* **553** (2003) 251 [hep-ph/0210360] [INSPIRE].

[7] F. del Aguila, J.A. Aguilar-Saavedra and R. Miquel, *Constraints on top couplings in models with exotic quarks*, *Phys. Rev. Lett.* **82** (1999) 1628 [hep-ph/9808400] [INSPIRE].

[8] J.A. Aguilar-Saavedra, *Effects of mixing with quark singlets*, *Phys. Rev. D* **67** (2003) 035003 [*Erratum ibid.* **69** (2004) 099901] [hep-ph/0210112] [INSPIRE].

[9] T.P. Cheng and M. Sher, *Mass matrix ansatz and flavor nonconservation in models with multiple Higgs doublets*, *Phys. Rev. D* **35** (1987) 3484 [INSPIRE].

[10] B. Grzadkowski, J.F. Gunion and P. Krawczyk, *Neutral current flavor changing decays for the Z boson and the top quark in two Higgs doublet models*, *Phys. Lett. B* **268** (1991) 106 [INSPIRE].

[11] M.E. Luke and M.J. Savage, *Flavor changing neutral currents in the Higgs sector and rare top decays*, *Phys. Lett. B* **307** (1993) 387 [hep-ph/9303249] [INSPIRE].

[12] D. Atwood, L. Reina and A. Soni, *Phenomenology of two Higgs doublet models with flavor changing neutral currents*, *Phys. Rev. D* **55** (1997) 3156 [hep-ph/9609279] [INSPIRE].

[13] S. Bejar, J. Guasch and J. Sola, *Loop induced flavor changing neutral decays of the top quark in a general two Higgs doublet model*, *Nucl. Phys. B* **600** (2001) 21 [hep-ph/0011091] [INSPIRE].

[14] I. Baum, G. Eilam and S. Bar-Shalom, *Scalar flavor changing neutral currents and rare top quark decays in a two Higgs doublet model 'for the top quark'*, *Phys. Rev. D* **77** (2008) 113008 [arXiv:0802.2622] [INSPIRE].

[15] G.C. Branco et al., *Theory and phenomenology of two-Higgs-doublet models*, *Phys. Rept.* **516** (2012) 1 [arXiv:1106.0034] [INSPIRE].

[16] K.-F. Chen, W.-S. Hou, C. Kao and M. Kohda, *When the Higgs meets the top: search for $t \to ch^0$ at the LHC*, *Phys. Lett. B* **725** (2013) 378 [arXiv:1304.8037] [INSPIRE].

[17] D. Atwood, S.K. Gupta and A. Soni, *Constraining the flavor changing Higgs couplings to the top-quark at the LHC*, *JHEP* **10** (2014) 057 [arXiv:1305.2427] [INSPIRE].

[18] C.S. Li, R.J. Oakes and J.M. Yang, *Rare decay of the top quark in the minimal supersymmetric model*, *Phys. Rev. D* **49** (1994) 293 [*Erratum ibid.* **56** (1997) 3156] [INSPIRE].

[19] G.M. de Divitiis, R. Petronzio and L. Silvestrini, *Flavor changing top decays in supersymmetric extensions of the standard model*, *Nucl. Phys. B* **504** (1997) 45 [hep-ph/9704244] [INSPIRE].

[20] J.L. Lopez, D.V. Nanopoulos and R. Rangarajan, *New supersymmetric contributions to $t \to cV$*, *Phys. Rev. D* **56** (1997) 3100 [hep-ph/9702350] [INSPIRE].

[21] J. Guasch and J. Sola, *FCNC top quark decays: a door to SUSY physics in high luminosity colliders?*, *Nucl. Phys. B* **562** (1999) 3 [hep-ph/9906268] [INSPIRE].

[22] D. Delepine and S. Khalil, *Top flavor violating decays in general supersymmetric models*, *Phys. Lett. B* **599** (2004) 62 [hep-ph/0406264] [INSPIRE].

[23] J.J. Liu, C.S. Li, L.L. Yang and L.G. Jin, *$t \to cV$ via SUSY FCNC couplings in the unconstrained MSSM*, *Phys. Lett. B* **599** (2004) 92 [hep-ph/0406155] [INSPIRE].

JHEP12(2023)195

[24] J.J. Cao et al., *SUSY-induced FCNC top-quark processes at the Large Hadron Collider*, *Phys. Rev. D* **75** (2007) 075021 [hep-ph/0702264] [INSPIRE].

[25] J. Cao et al., *SUSY induced top quark FCNC decay $t \to ch$ after run I of LHC*, *Eur. Phys. J. C* **74** (2014) 3058 [arXiv:1404.1241] [INSPIRE].

[26] J.M. Yang, B.-L. Young and X. Zhang, *Flavor changing top quark decays in R parity violating SUSY*, *Phys. Rev. D* **58** (1998) 055001 [hep-ph/9705341] [INSPIRE].

[27] G. Eilam et al., *Top quark rare decay $t \to ch$ in R-parity violating SUSY*, *Phys. Lett. B* **510** (2001) 227 [hep-ph/0102037] [INSPIRE].

[28] G.-R. Lu, F.-R. Yin, X.-L. Wang and L.-D. Wan, *The rare top quark decays $t \to cV$ in the topcolor assisted technicolor model*, *Phys. Rev. D* **68** (2003) 015002 [hep-ph/0303122] [INSPIRE].

[29] K. Agashe and R. Contino, *Composite Higgs-mediated FCNC*, *Phys. Rev. D* **80** (2009) 075016 [arXiv:0906.1542] [INSPIRE].

[30] A. Azatov, M. Toharia and L. Zhu, *Higgs mediated FCNC's in warped extra dimensions*, *Phys. Rev. D* **80** (2009) 035016 [arXiv:0906.1990] [INSPIRE].

[31] B. Yang, N. Liu and J. Han, *Top quark flavor-changing neutral-current decay to a 125 GeV Higgs boson in the littlest Higgs model with T parity*, *Phys. Rev. D* **89** (2014) 034020 [arXiv:1308.4852] [INSPIRE].

[32] A. Azatov, G. Panico, G. Perez and Y. Soreq, *On the flavor structure of natural composite Higgs models & top flavor violation*, *JHEP* **12** (2014) 082 [arXiv:1408.4525] [INSPIRE].

[33] Top Quark Working Group collaboration, *Working group report: top quark*, in the proceedings of the *Snowmass* 2013*: Snowmass on the Mississippi*, (2013) [arXiv:1311.2028] [INSPIRE].

[34] J.M. Alves et al., *The framework for a common origin of $\delta_{\rm CKM}$ and $\delta_{\rm PMNS}$*, *Eur. Phys. J. C* **81** (2021) 727 [arXiv:2105.14054] [INSPIRE].

[35] ATLAS collaboration, *Search for top quark decays $t \to qH$ with $H \to \gamma\gamma$ using the ATLAS detector*, *JHEP* **06** (2014) 008 [arXiv:1403.6293] [INSPIRE].

[36] ATLAS collaboration, *Search for flavour-changing neutral current top quark decays $t \to Hq$ in pp collisions at $\sqrt{s} = 8$ TeV with the ATLAS detector*, *JHEP* **12** (2015) 061 [arXiv:1509.06047] [INSPIRE].

[37] ATLAS collaboration, *Search for top quark decays $t \to qH$, with $H \to \gamma\gamma$, in $\sqrt{s} = 13$ TeV pp collisions using the ATLAS detector*, *JHEP* **10** (2017) 129 [arXiv:1707.01404] [INSPIRE].

[38] ATLAS collaboration, *Search for flavor-changing neutral currents in top quark decays $t \to Hc$ and $t \to Hu$ in multilepton final states in proton-proton collisions at $\sqrt{s} = 13$ TeV with the ATLAS detector*, *Phys. Rev. D* **98** (2018) 032002 [arXiv:1805.03483] [INSPIRE].

[39] ATLAS collaboration, *Search for top-quark decays $t \to Hq$ with 36 fb^{-1} of pp collision data at $\sqrt{s} = 13$ TeV with the ATLAS detector*, *JHEP* **05** (2019) 123 [arXiv:1812.11568] [INSPIRE].

[40] ATLAS collaboration, *Search for flavour-changing neutral current interactions of the top quark and the Higgs boson in events with a pair of τ-leptons in pp collisions at $\sqrt{s} = 13$ TeV with the ATLAS detector*, *JHEP* **06** (2023) 155 [arXiv:2208.11415] [INSPIRE].

[41] ATLAS collaboration, *Search for a new scalar resonance in flavour-changing neutral-current top-quark decays $t \to qX$ $(q = u, c)$, with $X \to b\bar{b}$, in proton-proton collisions at $\sqrt{s} = 13$ TeV with the ATLAS detector*, *JHEP* **07** (2023) 199 [arXiv:2301.03902] [INSPIRE].

JHEP12(2023)195

[42] CMS collaboration, *Search for top quark decays via Higgs-boson-mediated flavor-changing neutral currents in pp collisions at* $\sqrt{s} = 8$ *TeV*, *JHEP* **02** (2017) 079 [arXiv:1610.04857] [INSPIRE].

[43] CMS collaboration, *Search for the flavor-changing neutral current interactions of the top quark and the Higgs boson which decays into a pair of b quarks at* $\sqrt{s} = 13$ *TeV*, *JHEP* **06** (2018) 102 [arXiv:1712.02399] [INSPIRE].

[44] CMS collaboration, *Search for flavor-changing neutral current interactions of the top quark and Higgs boson in final states with two photons in proton-proton collisions at* $\sqrt{s} = 13$ *TeV*, *Phys. Rev. Lett.* **129** (2022) 032001 [arXiv:2111.02219] [INSPIRE].

[45] CMS collaboration, *Search for flavor-changing neutral current interactions of the top quark and the Higgs boson decaying to a bottom quark-antiquark pair at* $\sqrt{s} = 13$ *TeV*, *JHEP* **02** (2022) 169 [arXiv:2112.09734] [INSPIRE].

[46] G. Durieux, F. Maltoni and C. Zhang, *Global approach to top-quark flavor-changing interactions*, *Phys. Rev. D* **91** (2015) 074017 [arXiv:1412.7166] [INSPIRE].

[47] C. Zhang and F. Maltoni, *Top-quark decay into Higgs boson and a light quark at next-to-leading order in QCD*, *Phys. Rev. D* **88** (2013) 054005 [arXiv:1305.7386] [INSPIRE].

[48] A. Greljo, J.F. Kamenik and J. Kopp, *Disentangling flavor violation in the top-Higgs sector at the LHC*, *JHEP* **07** (2014) 046 [arXiv:1404.1278] [INSPIRE].

[49] ATLAS collaboration, *The ATLAS experiment at the CERN Large Hadron Collider*, 2008 *JINST* **3** S08003 [INSPIRE].

[50] ATLAS collaboration, *ATLAS Insertable B-Layer: technical design report*, ATLAS-TDR-19, CERN, Geneva, Switzerland (2010).

[51] ATLAS IBL collaboration, *Production and integration of the ATLAS Insertable B-Layer*, 2018 *JINST* **13** T05008 [arXiv:1803.00844] [INSPIRE].

[52] ATLAS collaboration, *Performance of the ATLAS trigger system in* 2015, *Eur. Phys. J. C* **77** (2017) 317 [arXiv:1611.09661] [INSPIRE].

[53] ATLAS collaboration, *The ATLAS collaboration software and firmware*, ATL-SOFT-PUB-2021-001, CERN, Geneva, Switzerland (2021).

[54] ATLAS collaboration, *ATLAS data quality operations and performance for* 2015–2018 *data-taking*, 2020 *JINST* **15** P04003 [arXiv:1911.04632] [INSPIRE].

[55] ATLAS collaboration, *Luminosity determination in pp collisions at* $\sqrt{s} = 13$ *TeV using the ATLAS detector at the LHC*, ATLAS-CONF-2019-021, CERN, Geneva, Switzerland (2019).

[56] G. Avoni et al., *The new LUCID-2 detector for luminosity measurement and monitoring in ATLAS*, 2018 *JINST* **13** P07017 [INSPIRE].

[57] S. Frixione, P. Nason and G. Ridolfi, *A positive-weight next-to-leading-order Monte Carlo for heavy flavour hadroproduction*, *JHEP* **09** (2007) 126 [arXiv:0707.3088] [INSPIRE].

[58] J. Alwall et al., *The automated computation of tree-level and next-to-leading order differential cross sections, and their matching to parton shower simulations*, *JHEP* **07** (2014) 079 [arXiv:1405.0301] [INSPIRE].

[59] C. Degrande et al., *UFO — the Universal FeynRules Output*, *Comput. Phys. Commun.* **183** (2012) 1201 [arXiv:1108.2040] [INSPIRE].

JHEP12(2023)195

[60] C. Degrande, F. Maltoni, J. Wang and C. Zhang, *Automatic computations at next-to-leading order in QCD for top-quark flavor-changing neutral processes*, *Phys. Rev. D* **91** (2015) 034024 [arXiv:1412.5594] [INSPIRE].

[61] P. Artoisenet, R. Frederix, O. Mattelaer and R. Rietkerk, *Automatic spin-entangled decays of heavy resonances in Monte Carlo simulations*, *JHEP* **03** (2013) 015 [arXiv:1212.3460] [INSPIRE].

[62] T. Sjöstrand et al., *An introduction to PYTHIA* 8.2, *Comput. Phys. Commun.* **191** (2015) 159 [arXiv:1410.3012] [INSPIRE].

[63] NNPDF collaboration, *Parton distributions for the LHC run II*, *JHEP* **04** (2015) 040 [arXiv:1410.8849] [INSPIRE].

[64] ATLAS collaboration, *ATLAS Pythia* 8 *tunes to* 7 *TeV data*, ATL-PHYS-PUB-2014-021, CERN, Geneva, Switzerland (2014).

[65] R.D. Ball et al., *Parton distributions with LHC data*, *Nucl. Phys. B* **867** (2013) 244 [arXiv:1207.1303] [INSPIRE].

[66] ATLAS collaboration, *Improvements in $t\bar{t}$ modelling using NLO+PS Monte Carlo generators for run* 2, ATL-PHYS-PUB-2018-009, CERN, Geneva, Switzerland (2018).

[67] M. Czakon and A. Mitov, *Top++: a program for the calculation of the top-pair cross-section at hadron colliders*, *Comput. Phys. Commun.* **185** (2014) 2930 [arXiv:1112.5675] [INSPIRE].

[68] LHC Higgs Cross Section Working Group collaboration, *Handbook of LHC Higgs cross sections: 4. Deciphering the nature of the Higgs sector*, arXiv:1610.07922 [DOI:10.23731/CYRM-2017-002] [INSPIRE].

[69] Sherpa collaboration, *Event generation with Sherpa* 2.2, *SciPost Phys.* **7** (2019) 034 [arXiv:1905.09127] [INSPIRE].

[70] S. Alioli, P. Nason, C. Oleari and E. Re, *NLO Higgs boson production via gluon fusion matched with shower in POWHEG*, *JHEP* **04** (2009) 002 [arXiv:0812.0578] [INSPIRE].

[71] K. Hamilton, P. Nason, E. Re and G. Zanderighi, *NNLOPS simulation of Higgs boson production*, *JHEP* **10** (2013) 222 [arXiv:1309.0017] [INSPIRE].

[72] ATLAS collaboration, *Measurement of the Z/γ^* boson transverse momentum distribution in pp collisions at $\sqrt{s} = 7$ TeV with the ATLAS detector*, *JHEP* **09** (2014) 145 [arXiv:1406.3660] [INSPIRE].

[73] P. Nason and C. Oleari, *NLO Higgs boson production via vector-boson fusion matched with shower in POWHEG*, *JHEP* **02** (2010) 037 [arXiv:0911.5299] [INSPIRE].

[74] G. Luisoni, P. Nason, C. Oleari and F. Tramontano, *$HW^{\pm}/HZ + 0$ and* 1 *jet at NLO with the POWHEG BOX interfaced to GoSam and their merging within MiNLO*, *JHEP* **10** (2013) 083 [arXiv:1306.2542] [INSPIRE].

[75] H.B. Hartanto, B. Jäger, L. Reina and D. Wackeroth, *Higgs boson production in association with top quarks in the POWHEG BOX*, *Phys. Rev. D* **91** (2015) 094003 [arXiv:1501.04498] [INSPIRE].

[76] ATLAS collaboration, *The ATLAS simulation infrastructure*, *Eur. Phys. J. C* **70** (2010) 823 [arXiv:1005.4568] [INSPIRE].

[77] GEANT4 collaboration, *GEANT4 — a simulation toolkit*, *Nucl. Instrum. Meth. A* **506** (2003) 250 [INSPIRE].

JHEP12(2023)195

[78] A. Ribon et al., *Status of GEANT4 hadronic physics for the simulation of LHC experiments at the start of the LHC physics program*, CERN-LCGAPP-2010-02, CERN, Geneva, Switzerland (2010).

[79] T. Sjöstrand, S. Mrenna and P.Z. Skands, *A brief introduction to PYTHIA* 8.1, *Comput. Phys. Commun.* **178** (2008) 852 [arXiv:0710.3820] [INSPIRE].

[80] ATLAS collaboration, *The Pythia* 8 *A*3 *tune description of ATLAS minimum bias and inelastic measurements incorporating the Donnachie-Landshoff diffractive model*, ATL-PHYS-PUB-2016-017, CERN, Geneva, Switzerland (2016).

[81] ATLAS collaboration, *Measurement of Higgs boson production in the diphoton decay channel in pp collisions at center-of-mass energies of* 7 *and* 8 *TeV with the ATLAS detector*, *Phys. Rev. D* **90** (2014) 112015 [arXiv:1408.7084] [INSPIRE].

[82] ATLAS collaboration, *Electron and photon performance measurements with the ATLAS detector using the* 2015–2017 *LHC proton-proton collision data*, 2019 *JINST* **14** P12006 [arXiv:1908.00005] [INSPIRE].

[83] ATLAS collaboration, *Topological cell clustering in the ATLAS calorimeters and its performance in LHC run* 1, *Eur. Phys. J. C* **77** (2017) 490 [arXiv:1603.02934] [INSPIRE].

[84] ATLAS collaboration, *Electron and photon energy calibration with the ATLAS detector using* 2015–2016 *LHC proton-proton collision data*, 2019 *JINST* **14** P03017 [arXiv:1812.03848] [INSPIRE].

[85] ATLAS collaboration, *Muon reconstruction performance of the ATLAS detector in proton-proton collision data at* $\sqrt{s} = 13$ *TeV*, *Eur. Phys. J. C* **76** (2016) 292 [arXiv:1603.05598] [INSPIRE].

[86] ATLAS collaboration, *Muon reconstruction and identification efficiency in ATLAS using the full run* 2 *pp collision data set at* $\sqrt{s} = 13$ *TeV*, *Eur. Phys. J. C* **81** (2021) 578 [arXiv:2012.00578] [INSPIRE].

[87] M. Cacciari, G.P. Salam and G. Soyez, *The anti-*k_t *jet clustering algorithm*, *JHEP* **04** (2008) 063 [arXiv:0802.1189] [INSPIRE].

[88] M. Cacciari, G.P. Salam and G. Soyez, *FastJet user manual*, *Eur. Phys. J. C* **72** (2012) 1896 [arXiv:1111.6097] [INSPIRE].

[89] ATLAS collaboration, *Jet reconstruction and performance using particle flow with the ATLAS detector*, *Eur. Phys. J. C* **77** (2017) 466 [arXiv:1703.10485] [INSPIRE].

[90] ATLAS collaboration, *Tagging and suppression of pileup jets with the ATLAS detector*, ATLAS-CONF-2014-018, CERN, Geneva, Switzerland (2014).

[91] ATLAS collaboration, *Identification and rejection of pile-up jets at high pseudorapidity with the ATLAS detector*, *Eur. Phys. J. C* **77** (2017) 580 [*Erratum ibid.* **77** (2017) 712] [arXiv:1705.02211] [INSPIRE].

[92] ATLAS collaboration, *ATLAS flavour-tagging algorithms for the LHC run* 2 *pp collision dataset*, *Eur. Phys. J. C* **83** (2023) 681 [arXiv:2211.16345] [INSPIRE].

[93] ATLAS collaboration, *Performance of missing transverse momentum reconstruction with the ATLAS detector using proton-proton collisions at* $\sqrt{s} = 13$ *TeV*, *Eur. Phys. J. C* **78** (2018) 903 [arXiv:1802.08168] [INSPIRE].

[94] ATLAS collaboration, *Performance of electron and photon triggers in ATLAS during LHC run* 2, *Eur. Phys. J. C* **80** (2020) 47 [arXiv:1909.00761] [INSPIRE].

JHEP12(2023)195

[95] ATLAS collaboration, *Performance of the upgraded preprocessor of the ATLAS level-1 calorimeter trigger*, 2020 *JINST* **15** P11016 [arXiv:2005.04179] [INSPIRE].

[96] A. Hoecker et al., *TMVA — toolkit for multivariate data analysis*, physics/0703039.

[97] M. Oreglia, *A study of the reactions* $\psi' \to \gamma\gamma\psi$, Ph.D. thesis, Stanford University, Stanford, CA, U.S.A. (1980) [INSPIRE].

[98] K.S. Cranmer, *Kernel estimation in high-energy physics*, *Comput. Phys. Commun.* **136** (2001) 198 [hep-ex/0011057] [INSPIRE].

[99] ATLAS collaboration, *A detailed map of Higgs boson interactions by the ATLAS experiment ten years after the discovery*, *Nature* **607** (2022) 52 [*Erratum ibid.* **612** (2022) E24] [arXiv:2207.00092] [INSPIRE].

[100] CMS collaboration, *A portrait of the Higgs boson by the CMS experiment ten years after the discovery*, *Nature* **607** (2022) 60 [arXiv:2207.00043] [INSPIRE].

[101] J. Bellm et al., *Herwig* 7.1 *release note*, arXiv:1705.06919 [INSPIRE].

[102] ATLAS collaboration, *Jet energy scale and resolution measured in proton-proton collisions at* $\sqrt{s} = 13$ *TeV with the ATLAS detector*, *Eur. Phys. J. C* **81** (2021) 689 [arXiv:2007.02645] [INSPIRE].

[103] G. Cowan, K. Cranmer, E. Gross and O. Vitells, *Asymptotic formulae for likelihood-based tests of new physics*, *Eur. Phys. J. C* **71** (2011) 1554 [*Erratum ibid.* **73** (2013) 2501] [arXiv:1007.1727] [INSPIRE].

[104] ATLAS collaboration, *ATLAS computing acknowledgements*, ATL-SOFT-PUB-2023-001, CERN, Geneva, Switzerland (2023).

JHEP12(2023)195

The ATLAS collaboration

G. Aad[102], B. Abbott[120], K. Abeling[55], N.J. Abicht[49], S.H. Abidi[29], A. Aboulhorma[35e], H. Abramowicz[151], H. Abreu[150], Y. Abulaiti[117], B.S. Acharya[69a,69b,m], C. Adam Bourdarios[4], L. Adamczyk[86a], S.V. Addepalli[26], M.J. Addison[101], J. Adelman[115], A. Adiguzel[21c], T. Adye[134], A.A. Affolder[136], Y. Afik[36], M.N. Agaras[13], J. Agarwala[73a,73b], A. Aggarwal[100], C. Agheorghiesei[27c], A. Ahmad[36], F. Ahmadov[38,y], W.S. Ahmed[104], S. Ahuja[95], X. Ai[62a], G. Aielli[76a,76b], A. Aikot[163], M. Ait Tamlihat[35e], B. Aitbenchikh[35a], I. Aizenberg[169], M. Akbiyik[100], T.P.A. Åkesson[98], A.V. Akimov[37], D. Akiyama[168], N.N. Akolkar[24], K. Al Khoury[41], G.L. Alberghi[23b], J. Albert[165], P. Albicocco[53], G.L. Albouy[60], S. Alderweireldt[52], M. Aleksa[36], I.N. Aleksandrov[38], C. Alexa[27b], T. Alexopoulos[10], F. Alfonsi[23b], M. Algren[56], M. Alhroob[120], B. Ali[132], H.M.J. Ali[91], S. Ali[148], S.W. Alibocus[92], M. Aliev[145], G. Alimonti[71a], W. Alkakhi[55], C. Allaire[66], B.M.M. Allbrooke[146], J.F. Allen[52], C.A. Allendes Flores[137f], P.P. Allport[20], A. Aloisio[72a,72b], F. Alonso[90], C. Alpigiani[138], M. Alvarez Estevez[99], A. Alvarez Fernandez[100], M. Alves Cardoso[56], M.G. Alviggi[72a,72b], M. Aly[101], Y. Amaral Coutinho[83b], A. Ambler[104], C. Amelung[36], M. Amerl[101], C.G. Ames[109], D. Amidei[106], S.P. Amor Dos Santos[130a], K.R. Amos[163], V. Ananiev[125], C. Anastopoulos[139], T. Andeen[11], J.K. Anders[36], S.Y. Andrean[47a,47b], A. Andreazza[71a,71b], S. Angelidakis[9], A. Angerami[41,ab], A.V. Anisenkov[37], A. Annovi[74a], C. Antel[56], M.T. Anthony[139], E. Antipov[145], M. Antonelli[53], F. Anulli[75a], M. Aoki[84], T. Aoki[153], J.A. Aparisi Pozo[163], M.A. Aparo[146], L. Aperio Bella[48], C. Appelt[18], A. Apyan[26], N. Aranzabal[36], S.J. Arbiol Val[87], C. Arcangeletti[53], A.T.H. Arce[51], E. Arena[92], J-F. Arguin[108], S. Argyropoulos[54], J.-H. Arling[48], O. Arnaez[4], H. Arnold[114], G. Artoni[75a,75b], H. Asada[111], K. Asai[118], S. Asai[153], N.A. Asbah[61], J. Assahsah[35d], K. Assamagan[29], R. Astalos[28a], S. Atashi[160], R.J. Atkin[33a], M. Atkinson[162], H. Atmani[35f], P.A. Atmasiddha[106], K. Augsten[132], S. Auricchio[72a,72b], A.D. Auriol[20], V.A. Austrup[101], G. Avolio[36], K. Axiotis[56], G. Azuelos[108,ag], D. Babal[28b], H. Bachacou[135], K. Bachas[152,p], A. Bachiu[34], F. Backman[47a,47b], A. Badea[61], T.M. Baer[106], P. Bagnaia[75a,75b], M. Bahmani[18], A.J. Bailey[163], V.R. Bailey[162], J.T. Baines[134], L. Baines[94], O.K. Baker[172], E. Bakos[15], D. Bakshi Gupta[8], V. Balakrishnan[120], R. Balasubramanian[114], E.M. Baldin[37], P. Balek[86a], E. Ballabene[23b,23a], F. Balli[135], L.M. Baltes[63a], W.K. Balunas[32], J. Balz[100], E. Banas[87], M. Bandieramonte[129], A. Bandyopadhyay[24], S. Bansal[24], L. Barak[151], M. Barakat[48], E.L. Barberio[105], D. Barberis[57b,57a], M. Barbero[102], M.Z. Barel[114], K.N. Barends[33a], T. Barillari[110], M-S. Barisits[36], T. Barklow[143], P. Baron[122], D.A. Baron Moreno[101], A. Baroncelli[62a], G. Barone[29], A.J. Barr[126], J.D. Barr[96], L. Barranco Navarro[47a,47b], F. Barreiro[99], J. Barreiro Guimarães da Costa[14a], U. Barron[151], M.G. Barros Teixeira[130a], S. Barsov[37], F. Bartels[63a], R. Bartoldus[143], A.E. Barton[91], P. Bartos[28a], A. Basan[100], M. Baselga[49], A. Bassalat[66,b], M.J. Basso[156a], C.R. Basson[101], R.L. Bates[59], S. Batlamous[35e], J.R. Batley[32], B. Batool[141], M. Battaglia[136], D. Battulga[18], M. Bauce[75a,75b], M. Bauer[36], P. Bauer[24], L.T. Bazzano Hurrell[30], J.B. Beacham[51], T. Beau[127], J.Y. Beaucamp[90], P.H. Beauchemin[158], F. Becherer[54], P. Bechtle[24], H.P. Beck[19,o], K. Becker[167], A.J. Beddall[82], V.A. Bednyakov[38], C.P. Bee[145], L.J. Beemster[15],

JHEP12(2023)195

T.A. Beermann[36], M. Begalli[83d], M. Begel[29], A. Behera[145], J.K. Behr[48], J.F. Beirer[55], F. Beisiegel[24], M. Belfkir[159], G. Bella[151], L. Bellagamba[23b], A. Bellerive[34], P. Bellos[20], K. Beloborodov[37], D. Benchekroun[35a], F. Bendebba[35a], Y. Benhammou[151], M. Benoit[29], J.R. Bensinger[26], S. Bentvelsen[114], L. Beresford[48], M. Beretta[53], E. Bergeaas Kuutmann[161], N. Berger[4], B. Bergmann[132], J. Beringer[17a], G. Bernardi[5], C. Bernius[143], F.U. Bernlochner[24], F. Bernon[36,102], A. Berrocal Guardia[13], T. Berry[95], P. Berta[133], A. Berthold[50], I.A. Bertram[91], S. Bethke[110], A. Betti[75a,75b], A.J. Bevan[94], N.K. Bhalla[54], M. Bhamjee[33c], S. Bhatta[145], D.S. Bhattacharya[166], P. Bhattarai[143], V.S. Bhopatkar[121], R. Bi[29,aj], R.M. Bianchi[129], G. Bianco[23b,23a], O. Biebel[109], R. Bielski[123], M. Biglietti[77a], M. Bindi[55], A. Bingul[21b], C. Bini[75a,75b], A. Biondini[92], C.J. Birch-sykes[101], G.A. Bird[20,134], M. Birman[169], M. Biros[133], S. Biryukov[146], T. Bisanz[49], E. Bisceglie[43b,43a], J.P. Biswal[134], D. Biswas[141], A. Bitadze[101], K. Bjørke[125], I. Bloch[48], C. Blocker[26], A. Blue[59], U. Blumenschein[94], J. Blumenthal[100], G.J. Bobbink[114], V.S. Bobrovnikov[37], M. Boehler[54], B. Boehm[166], D. Bogavac[36], A.G. Bogdanchikov[37], C. Bohm[47a], V. Boisvert[95], P. Bokan[48], T. Bold[86a], M. Bomben[5], M. Bona[94], M. Boonekamp[135], C.D. Booth[95], A.G. Borbély[59], I.S. Bordulev[37], H.M. Borecka-Bielska[108], G. Borissov[91], D. Bortoletto[126], D. Boscherini[23b], M. Bosman[13], J.D. Bossio Sola[36], K. Bouaouda[35a], N. Bouchhar[163], J. Boudreau[129], E.V. Bouhova-Thacker[91], D. Boumediene[40], R. Bouquet[165], A. Boveia[119], J. Boyd[36], D. Boye[29], I.R. Boyko[38], J. Bracinik[20], N. Brahimi[62d], G. Brandt[171], O. Brandt[32], F. Braren[48], B. Brau[103], J.E. Brau[123], R. Brener[169], L. Brenner[114], R. Brenner[161], S. Bressler[169], D. Britton[59], D. Britzger[110], I. Brock[24], G. Brooijmans[41], W.K. Brooks[137f], E. Brost[29], L.M. Brown[165], L.E. Bruce[61], T.L. Bruckler[126], P.A. Bruckman de Renstrom[87], B. Brüers[48], A. Bruni[23b], G. Bruni[23b], M. Bruschi[23b], N. Bruscino[75a,75b], T. Buanes[16], Q. Buat[138], D. Buchin[110], A.G. Buckley[59], O. Bulekov[37], B.A. Bullard[143], S. Burdin[92], C.D. Burgard[49], A.M. Burger[40], B. Burghgrave[8], O. Burlayenko[54], J.T.P. Burr[32], C.D. Burton[11], J.C. Burzynski[142], E.L. Busch[41], V. Büscher[100], P.J. Bussey[59], J.M. Butler[25], C.M. Buttar[59], J.M. Butterworth[96], W. Buttinger[134], C.J. Buxo Vazquez[107], A.R. Buzykaev[37], S. Cabrera Urbán[163], L. Cadamuro[66], D. Caforio[58], H. Cai[129], Y. Cai[14a,14e], Y. Cai[14c], V.M.M. Cairo[36], O. Cakir[3a], N. Calace[36], P. Calafiura[17a], G. Calderini[127], P. Calfayan[68], G. Callea[59], L.P. Caloba[83b], D. Calvet[40], S. Calvet[40], T.P. Calvet[102], M. Calvetti[74a,74b], R. Camacho Toro[127], S. Camarda[36], D. Camarero Munoz[26], P. Camarri[76a,76b], M.T. Camerlingo[72a,72b], D. Cameron[36], C. Camincher[165], M. Campanelli[96], A. Camplani[42], V. Canale[72a,72b], A. Canesse[104], J. Cantero[163], Y. Cao[162], F. Capocasa[26], M. Capua[43b,43a], A. Carbone[71a,71b], R. Cardarelli[76a], J.C.J. Cardenas[8], F. Cardillo[163], G. Carducci[43b,43a], T. Carli[36], G. Carlino[72a], J.I. Carlotto[13], B.T. Carlson[129,q], E.M. Carlson[165,156a], L. Carminati[71a,71b], A. Carnelli[135], M. Carnesale[75a,75b], S. Caron[113], E. Carquin[137f], S. Carrá[71a], G. Carratta[23b,23a], F. Carrio Argos[33g], J.W.S. Carter[155], T.M. Carter[52], M.P. Casado[13,i], M. Caspar[48], F.L. Castillo[4], L. Castillo Garcia[13], V. Castillo Gimenez[163], N.F. Castro[130a,130e], A. Catinaccio[36], J.R. Catmore[125], V. Cavaliere[29], N. Cavalli[23b,23a], V. Cavasinni[74a,74b], Y.C. Cekmecelioglu[48], E. Celebi[21a], F. Celli[126], M.S. Centonze[70a,70b], V. Cepaitis[56], K. Cerny[122], A.S. Cerqueira[83a],

JHEP12(2023)195

A. Cerri[146], L. Cerrito[76a,76b], F. Cerutti[17a], B. Cervato[141], A. Cervelli[23b], G. Cesarini[53], S.A. Cetin[82], Z. Chadi[35a], D. Chakraborty[115], J. Chan[170], W.Y. Chan[153], J.D. Chapman[32], E. Chapon[135], B. Chargeishvili[149b], D.G. Charlton[20], T.P. Charman[94], M. Chatterjee[19], C. Chauhan[133], S. Chekanov[6], S.V. Chekulaev[156a], G.A. Chelkov[38,a], A. Chen[106], B. Chen[151], B. Chen[165], H. Chen[14c], H. Chen[29], J. Chen[62c], J. Chen[142], M. Chen[126], S. Chen[153], S.J. Chen[14c], X. Chen[62c,135], X. Chen[14b,af], Y. Chen[62a], C.L. Cheng[170], H.C. Cheng[64a], S. Cheong[143], A. Cheplakov[38], E. Cheremushkina[48], E. Cherepanova[114], R. Cherkaoui El Moursli[35e], E. Cheu[7], K. Cheung[65], L. Chevalier[135], V. Chiarella[53], G. Chiarelli[74a], N. Chiedde[102], G. Chiodini[70a], A.S. Chisholm[20], A. Chitan[27b], M. Chitishvili[163], M.V. Chizhov[38], K. Choi[11], A.R. Chomont[75a,75b], Y. Chou[103], E.Y.S. Chow[113], T. Chowdhury[33g], K.L. Chu[169], M.C. Chu[64a], X. Chu[14a,14e], J. Chudoba[131], J.J. Chwastowski[87], D. Cieri[110], K.M. Ciesla[86a], V. Cindro[93], A. Ciocio[17a], F. Cirotto[72a,72b], Z.H. Citron[169,k], M. Citterio[71a], D.A. Ciubotaru[27b], B.M. Ciungu[155], A. Clark[56], P.J. Clark[52], C. Clarry[155], J.M. Clavijo Columbie[48], S.E. Clawson[48], C. Clement[47a,47b], J. Clercx[48], L. Clissa[23b,23a], Y. Coadou[102], M. Cobal[69a,69c], A. Coccaro[57b], R.F. Coelho Barrue[130a], R. Coelho Lopes De Sa[103], S. Coelli[71a], H. Cohen[151], A.E.C. Coimbra[71a,71b], B. Cole[41], J. Collot[60], P. Conde Muiño[130a,130g], M.P. Connell[33c], S.H. Connell[33c], I.A. Connelly[59], E.I. Conroy[126], F. Conventi[72a,ah], H.G. Cooke[20], A.M. Cooper-Sarkar[126], A. Cordeiro Oudot Choi[127], L.D. Corpe[40], M. Corradi[75a,75b], F. Corriveau[104,w], A. Cortes-Gonzalez[18], M.J. Costa[163], F. Costanza[4], D. Costanzo[139], B.M. Cote[119], G. Cowan[95], K. Cranmer[170], D. Cremonini[23b,23a], S. Crépé-Renaudin[60], F. Crescioli[127], M. Cristinziani[141], M. Cristoforetti[78a,78b], V. Croft[114], J.E. Crosby[121], G. Crosetti[43b,43a], A. Cueto[99], T. Cuhadar Donszelmann[160], H. Cui[14a,14e], Z. Cui[7], W.R. Cunningham[59], F. Curcio[43b,43a], P. Czodrowski[36], M.M. Czurylo[63b], M.J. Da Cunha Sargedas De Sousa[57b,57a], J.V. Da Fonseca Pinto[83b], C. Da Via[101], W. Dabrowski[86a], T. Dado[49], S. Dahbi[33g], T. Dai[106], D. Dal Santo[19], C. Dallapiccola[103], M. Dam[42], G. D'amen[29], V. D'Amico[109], J. Damp[100], J.R. Dandoy[128], M.F. Daneri[30], M. Danninger[142], V. Dao[36], G. Darbo[57b], S. Darmora[6], S.J. Das[29,aj], S. D'Auria[71a,71b], C. David[156b], T. Davidek[133], B. Davis-Purcell[34], I. Dawson[94], H.A. Day-hall[132], K. De[8], R. De Asmundis[72a], N. De Biase[48], S. De Castro[23b,23a], N. De Groot[113], P. de Jong[114], H. De la Torre[115], A. De Maria[14c], A. De Salvo[75a], U. De Sanctis[76a,76b], A. De Santo[146], J.B. De Vivie De Regie[60], D.V. Dedovich[38], J. Degens[114], A.M. Deiana[44], F. Del Corso[23b,23a], J. Del Peso[99], F. Del Rio[63a], F. Deliot[135], C.M. Delitzsch[49], M. Della Pietra[72a,72b], D. Della Volpe[56], A. Dell'Acqua[36], L. Dell'Asta[71a,71b], M. Delmastro[4], P.A. Delsart[60], S. Demers[172], M. Demichev[38], S.P. Denisov[37], L. D'Eramo[40], D. Derendarz[87], F. Derue[127], P. Dervan[92], K. Desch[24], C. Deutsch[24], F.A. Di Bello[57b,57a], A. Di Ciaccio[76a,76b], L. Di Ciaccio[4], A. Di Domenico[75a,75b], C. Di Donato[72a,72b], A. Di Girolamo[36], G. Di Gregorio[36], A. Di Luca[78a,78b], B. Di Micco[77a,77b], R. Di Nardo[77a,77b], C. Diaconu[102], M. Diamantopoulou[34], F.A. Dias[114], T. Dias Do Vale[142], M.A. Diaz[137a,137b], F.G. Diaz Capriles[24], M. Didenko[163], E.B. Diehl[106], L. Diehl[54], S. Díez Cornell[48], C. Diez Pardos[141], C. Dimitriadi[161,24,161], A. Dimitrievska[17a], J. Dingfelder[24], I-M. Dinu[27b], S.J. Dittmeier[63b], F. Dittus[36],

JHEP12(2023)195

F. Djama[102], T. Djobava[149b], J.I. Djuvsland[16], C. Doglioni[101,98], A. Dohnalova[28a], J. Dolejsi[133], Z. Dolezal[133], K.M. Dona[39], M. Donadelli[83c], B. Dong[107], J. Donini[40], A. D'Onofrio[77a,77b], M. D'Onofrio[92], J. Dopke[134], A. Doria[72a], N. Dos Santos Fernandes[130a], P. Dougan[101], M.T. Dova[90], A.T. Doyle[59], M.A. Draguet[126], E. Dreyer[169], I. Drivas-koulouris[10], M. Drnevich[117], A.S. Drobac[158], M. Drozdova[56], D. Du[62a], T.A. du Pree[114], F. Dubinin[37], M. Dubovsky[28a], E. Duchovni[169], G. Duckeck[109], O.A. Ducu[27b], D. Duda[52], A. Dudarev[36], E.R. Duden[26], M. D'uffizi[101], L. Duflot[66], M. Dührssen[36], C. Dülsen[171], A.E. Dumitriu[27b], M. Dunford[63a], S. Dungs[49], K. Dunne[47a,47b], A. Duperrin[102], H. Duran Yildiz[3a], M. Düren[58], A. Durglishvili[149b], B.L. Dwyer[115], G.I. Dyckes[17a], M. Dyndal[86a], B.S. Dziedzic[87], Z.O. Earnshaw[146], G.H. Eberwein[126], B. Eckerova[28a], S. Eggebrecht[55], E. Egidio Purcino De Souza[127], L.F. Ehrke[56], G. Eigen[16], K. Einsweiler[17a], T. Ekelof[161], P.A. Ekman[98], S. El Farkh[35b], Y. El Ghazali[35b], H. El Jarrari[35e,148], A. El Moussaouy[108], V. Ellajosyula[161], M. Ellert[161], F. Ellinghaus[171], N. Ellis[36], J. Elmsheuser[29], M. Elsing[36], D. Emeliyanov[134], Y. Enari[153], I. Ene[17a], S. Epari[13], J. Erdmann[49], P.A. Erland[87], M. Errenst[171], M. Escalier[66], C. Escobar[163], E. Etzion[151], G. Evans[130a], H. Evans[68], L.S. Evans[95], M.O. Evans[146], A. Ezhilov[37], S. Ezzarqtouni[35a], F. Fabbri[59], L. Fabbri[23b,23a], G. Facini[96], V. Fadeyev[136], R.M. Fakhrutdinov[37], S. Falciano[75a], L.F. Falda Ulhoa Coelho[36], P.J. Falke[24], J. Faltova[133], C. Fan[162], Y. Fan[14a], Y. Fang[14a,14e], M. Fanti[71a,71b], M. Faraj[69a,69b], Z. Farazpay[97], A. Farbin[8], A. Farilla[77a], T. Farooque[107], S.M. Farrington[52], F. Fassi[35e], D. Fassouliotis[9], M. Faucci Giannelli[76a,76b], W.J. Fawcett[32], L. Fayard[66], P. Federic[133], P. Federicova[131], O.L. Fedin[37,a], G. Fedotov[37], M. Feickert[170], L. Feligioni[102], D.E. Fellers[123], C. Feng[62b], M. Feng[14b], Z. Feng[114], M.J. Fenton[160], A.B. Fenyuk[37], L. Ferencz[48], R.A.M. Ferguson[91], S.I. Fernandez Luengo[137f], P. Fernandez Martinez[13], M.J.V. Fernoux[102], J. Ferrando[48], A. Ferrari[161], P. Ferrari[114,113], R. Ferrari[73a], D. Ferrere[56], C. Ferretti[106], F. Fiedler[100], P. Fiedler[132], A. Filipčič[93], E.K. Filmer[1], F. Filthaut[113], M.C.N. Fiolhais[130a,130c,c], L. Fiorini[163], W.C. Fisher[107], T. Fitschen[101], P.M. Fitzhugh[135], I. Fleck[141], P. Fleischmann[106], T. Flick[171], M. Flores[33d,ac], L.R. Flores Castillo[64a], L. Flores Sanz De Acedo[36], F.M. Follega[78a,78b], N. Fomin[16], J.H. Foo[155], B.C. Forland[68], A. Formica[135], A.C. Forti[101], E. Fortin[36], A.W. Fortman[61], M.G. Foti[17a], L. Fountas[9,j], D. Fournier[66], H. Fox[91], P. Francavilla[74a,74b], S. Francescato[61], S. Franchellucci[56], M. Franchini[23b,23a], S. Franchino[63a], D. Francis[36], L. Franco[113], V. Franco Lima[36], L. Franconi[48], M. Franklin[61], G. Frattari[26], A.C. Freegard[94], W.S. Freund[83b], Y.Y. Frid[151], J. Friend[59], N. Fritzsche[50], A. Froch[54], D. Froidevaux[36], J.A. Frost[126], Y. Fu[62a], S. Fuenzalida Garrido[137f], M. Fujimoto[118,ad], E. Fullana Torregrosa[163,*], K.Y. Fung[64a], E. Furtado De Simas Filho[83b], M. Furukawa[153], J. Fuster[163], A. Gabrielli[23b,23a], A. Gabrielli[155], P. Gadow[36], G. Gagliardi[57b,57a], L.G. Gagnon[17a], E.J. Gallas[126], B.J. Gallop[134], K.K. Gan[119], S. Ganguly[153], Y. Gao[52], F.M. Garay Walls[137a,137b], B. Garcia[29], C. García[163], A. Garcia Alonso[114], A.G. Garcia Caffaro[172], J.E. García Navarro[163], M. Garcia-Sciveres[17a], G.L. Gardner[128], R.W. Gardner[39], N. Garelli[158], D. Garg[80], R.B. Garg[143,n], J.M. Gargan[52], C.A. Garner[155], C.M. Garvey[33a], P. Gaspar[83b], V.K. Gassmann[158], G. Gaudio[73a], V. Gautam[13],

JHEP12(2023)195

P. Gauzzi[75a,75b], I.L. Gavrilenko[37], A. Gavrilyuk[37], C. Gay[164], G. Gaycken[48], E.N. Gazis[10], A.A. Geanta[27b], C.M. Gee[136], C. Gemme[57b], M.H. Genest[60], S. Gentile[75a,75b], A.D. Gentry[112], S. George[95], W.F. George[20], T. Geralis[46], P. Gessinger-Befurt[36], M.E. Geyik[171], M. Ghani[167], M. Ghneimat[141], K. Ghorbanian[94], A. Ghosal[141], A. Ghosh[160], A. Ghosh[7], B. Giacobbe[23b], S. Giagu[75a,75b], T. Giani[114], P. Giannetti[74a], A. Giannini[62a], S.M. Gibson[95], M. Gignac[136], D.T. Gil[86b], A.K. Gilbert[86a], B.J. Gilbert[41], D. Gillberg[34], G. Gilles[114], N.E.K. Gillwald[48], L. Ginabat[127], D.M. Gingrich[2,ag], M.P. Giordani[69a,69c], P.F. Giraud[135], G. Giugliarelli[69a,69c], D. Giugni[71a], F. Giuli[36], I. Gkialas[9,j], L.K. Gladilin[37], C. Glasman[99], G.R. Gledhill[123], G. Glemža[48], M. Glisic[123], I. Gnesi[43b,f], Y. Go[29,aj], M. Goblirsch-Kolb[36], B. Gocke[49], D. Godin[108], B. Gokturk[21a], S. Goldfarb[105], T. Golling[56], M.G.D. Gololo[33g], D. Golubkov[37], J.P. Gombas[107], A. Gomes[130a,130b], G. Gomes Da Silva[141], A.J. Gomez Delegido[163], R. Gonçalo[130a,130c], G. Gonella[123], L. Gonella[20], A. Gongadze[149c], F. Gonnella[20], J.L. Gonski[41], R.Y. González Andana[52], S. González de la Hoz[163], S. Gonzalez Fernandez[13], R. Gonzalez Lopez[92], C. Gonzalez Renteria[17a], M.V. Gonzalez Rodrigues[48], R. Gonzalez Suarez[161], S. Gonzalez-Sevilla[56], G.R. Gonzalvo Rodriguez[163], L. Goossens[36], B. Gorini[36], E. Gorini[70a,70b], A. Gorišek[93], T.C. Gosart[128], A.T. Goshaw[51], M.I. Gostkin[38], S. Goswami[121], C.A. Gottardo[36], S.A. Gotz[109], M. Gouighri[35b], V. Goumarre[48], A.G. Goussiou[138], N. Govender[33c], I. Grabowska-Bold[86a], K. Graham[34], E. Gramstad[125], S. Grancagnolo[70a,70b], M. Grandi[146], C.M. Grant[1,135], P.M. Gravila[27f], F.G. Gravili[70a,70b], H.M. Gray[17a], M. Greco[70a,70b], C. Grefe[24], I.M. Gregor[48], P. Grenier[143], S.G. Grewe[110], C. Grieco[13], A.A. Grillo[136], K. Grimm[31], S. Grinstein[13,s], J.-F. Grivaz[66], E. Gross[169], J. Grosse-Knetter[55], C. Grud[106], J.C. Grundy[126], L. Guan[106], W. Guan[29], C. Gubbels[164], J.G.R. Guerrero Rojas[163], G. Guerrieri[69a,69c], F. Guescini[110], R. Gugel[100], J.A.M. Guhit[106], A. Guida[18], T. Guillemin[4], E. Guilloton[167,134], S. Guindon[36], F. Guo[14a,14e], J. Guo[62c], L. Guo[48], Y. Guo[106], R. Gupta[48], R. Gupta[129], S. Gurbuz[24], S.S. Gurdasani[54], G. Gustavino[36], M. Guth[56], P. Gutierrez[120], L.F. Gutierrez Zagazeta[128], M. Gutsche[50], C. Gutschow[96], C. Gwenlan[126], C.B. Gwilliam[92], E.S. Haaland[125], A. Haas[117], M. Habedank[48], C. Haber[17a], H.K. Hadavand[8], A. Hadef[100], S. Hadzic[110], A.I. Hagan[91], J.J. Hahn[141], E.H. Haines[96], M. Haleem[166], J. Haley[121], J.J. Hall[139], G.D. Hallewell[102], L. Halser[19], K. Hamano[165], M. Hamer[24], G.N. Hamity[52], E.J. Hampshire[95], J. Han[62b], K. Han[62a], L. Han[14c], L. Han[62a], S. Han[17a], Y.F. Han[155], K. Hanagaki[84], M. Hance[136], D.A. Hangal[41,ab], H. Hanif[142], M.D. Hank[128], R. Hankache[101], J.B. Hansen[42], J.D. Hansen[42], P.H. Hansen[42], K. Hara[157], D. Harada[56], T. Harenberg[171], S. Harkusha[37], M.L. Harris[103], Y.T. Harris[126], J. Harrison[13], N.M. Harrison[119], P.F. Harrison[167], N.M. Hartman[110], N.M. Hartmann[109], Y. Hasegawa[140], R. Hauser[107], C.M. Hawkes[20], R.J. Hawkings[36], Y. Hayashi[153], S. Hayashida[111], D. Hayden[107], C. Hayes[106], R.L. Hayes[114], C.P. Hays[126], J.M. Hays[94], H.S. Hayward[92], F. He[62a], M. He[14a,14e], Y. He[154], Y. He[48], N.B. Heatley[94], V. Hedberg[98], A.L. Heggelund[125], N.D. Hehir[94], C. Heidegger[54], K.K. Heidegger[54], W.D. Heidorn[81], J. Heilman[34], S. Heim[48], T. Heim[17a], J.G. Heinlein[128], J.J. Heinrich[123], L. Heinrich[110,ae], J. Hejbal[131], L. Helary[48], A. Held[170], S. Hellesund[16], C.M. Helling[164],

JHEP12(2023)195

S. Hellman[47a,47b], R.C.W. Henderson[91], L. Henkelmann[32], A.M. Henriques Correia[36], H. Herde[98], Y. Hernández Jiménez[145], L.M. Herrmann[24], T. Herrmann[50], G. Herten[54], R. Hertenberger[109], L. Hervas[36], M.E. Hesping[100], N.P. Hessey[156a], H. Hibi[85], E. Hill[155], S.J. Hillier[20], J.R. Hinds[107], F. Hinterkeuser[24], M. Hirose[124], S. Hirose[157], D. Hirschbuehl[171], T.G. Hitchings[101], B. Hiti[93], J. Hobbs[145], R. Hobincu[27e], N. Hod[169], M.C. Hodgkinson[139], B.H. Hodkinson[32], A. Hoecker[36], D.D. Hofer[106], J. Hofer[48], T. Holm[24], M. Holzbock[110], L.B.A.H. Hommels[32], B.P. Honan[101], J. Hong[62c], T.M. Hong[129], B.H. Hooberman[162], W.H. Hopkins[6], Y. Horii[111], S. Hou[148], A.S. Howard[93], J. Howarth[59], J. Hoya[6], M. Hrabovsky[122], A. Hrynevich[48], T. Hryn'ova[4], P.J. Hsu[65], S.-C. Hsu[138], Q. Hu[62a], Y.F. Hu[14a,14e], S. Huang[64b], X. Huang[14c], X. Huang[14a,14e], Y. Huang[139], Y. Huang[14a], Z. Huang[101], Z. Hubacek[132], M. Huebner[24], F. Huegging[24], T.B. Huffman[126], C.A. Hugli[48], M. Huhtinen[36], S.K. Huiberts[16], R. Hulsken[104], N. Huseynov[12], J. Huston[107], J. Huth[61], R. Hyneman[143], G. Iacobucci[56], G. Iakovidis[29], I. Ibragimov[141], L. Iconomidou-Fayard[66], P. Iengo[72a,72b], R. Iguchi[153], T. Iizawa[126], Y. Ikegami[84], N. Ilic[155], H. Imam[35a], M. Ince Lezki[56], T. Ingebretsen Carlson[47a,47b], G. Introzzi[73a,73b], M. Iodice[77a], V. Ippolito[75a,75b], R.K. Irwin[92], M. Ishino[153], W. Islam[170], C. Issever[18,48], S. Istin[21a,al], H. Ito[168], J.M. Iturbe Ponce[64a], R. Iuppa[78a,78b], A. Ivina[169], J.M. Izen[45], V. Izzo[72a], P. Jacka[131,132], P. Jackson[1], R.M. Jacobs[48], B.P. Jaeger[142], C.S. Jagfeld[109], G. Jain[156a], P. Jain[54], K. Jakobs[54], T. Jakoubek[169], J. Jamieson[59], K.W. Janas[86a], M. Javurkova[103], F. Jeanneau[135], L. Jeanty[123], J. Jejelava[149a,z], P. Jenni[54,g], C.E. Jessiman[34], S. Jézéquel[4], C. Jia[62b], J. Jia[145], X. Jia[61], X. Jia[14a,14e], Z. Jia[14c], S. Jiggins[48], J. Jimenez Pena[13], S. Jin[14c], A. Jinaru[27b], O. Jinnouchi[154], P. Johansson[139], K.A. Johns[7], J.W. Johnson[136], D.M. Jones[32], E. Jones[48], P. Jones[32], R.W.L. Jones[91], T.J. Jones[92], H.L. Joos[55,36], R. Joshi[119], J. Jovicevic[15], X. Ju[17a], J.J. Junggeburth[103], T. Junkermann[63a], A. Juste Rozas[13,s], M.K. Juzek[87], S. Kabana[137e], A. Kaczmarska[87], M. Kado[110], H. Kagan[119], M. Kagan[143], A. Kahn[41], A. Kahn[128], C. Kahra[100], T. Kaji[153], E. Kajomovitz[150], N. Kakati[169], I. Kalaitzidou[54], C.W. Kalderon[29], A. Kamenshchikov[155], N.J. Kang[136], D. Kar[33g], K. Karava[126], M.J. Kareem[156b], E. Karentzos[54], I. Karkanias[152], O. Karkout[114], S.N. Karpov[38], Z.M. Karpova[38], V. Kartvelishvili[91], A.N. Karyukhin[37], E. Kasimi[152], J. Katzy[48], S. Kaur[34], K. Kawade[140], M.P. Kawale[120], C. Kawamoto[88], T. Kawamoto[135], E.F. Kay[36], F.I. Kaya[158], S. Kazakos[107], V.F. Kazanin[37], Y. Ke[145], J.M. Keaveney[33a], R. Keeler[165], G.V. Kehris[61], J.S. Keller[34], A.S. Kelly[96], J.J. Kempster[146], K.E. Kennedy[41], P.D. Kennedy[100], O. Kepka[131], B.P. Kerridge[167], S. Kersten[171], B.P. Kerševan[93], S. Keshri[66], L. Keszeghova[28a], S. Ketabchi Haghighat[155], R.A. Khan[129], M. Khandoga[127], A. Khanov[121], A.G. Kharlamov[37], T. Kharlamova[37], E.E. Khoda[138], M. Kholodenko[37], T.J. Khoo[18], G. Khoriauli[166], J. Khubua[149b], Y.A.R. Khwaira[66], A. Kilgallon[123], D.W. Kim[47a,47b], Y.K. Kim[39], N. Kimura[96], M.K. Kingston[55], A. Kirchhoff[55], C. Kirfel[24], F. Kirfel[24], J. Kirk[134], A.E. Kiryunin[110], C. Kitsaki[10], O. Kivernyk[24], M. Klassen[63a], C. Klein[34], L. Klein[166], M.H. Klein[106], M. Klein[92], S.B. Klein[56], U. Klein[92], P. Klimek[36], A. Klimentov[29], T. Klioutchnikova[36], P. Kluit[114], S. Kluth[110], E. Kneringer[79], T.M. Knight[155], A. Knue[49], R. Kobayashi[88], D. Kobylianskii[169],

JHEP12(2023)195

S.F. Koch[126], M. Kocian[143], P. Kodyš[133], D.M. Koeck[123], P.T. Koenig[24], T. Koffas[34], O. Kolay[50], M. Kolb[135], I. Koletsou[4], T. Komarek[122], K. Köneke[54], A.X.Y. Kong[1], T. Kono[118], N. Konstantinidis[96], P. Kontaxakis[56], B. Konya[98], R. Kopeliansky[68], S. Koperny[86a], K. Korcyl[87], K. Kordas[152,e], G. Koren[151], A. Korn[96], S. Korn[55], I. Korolkov[13], N. Korotkova[37], B. Kortman[114], O. Kortner[110], S. Kortner[110], W.H. Kostecka[115], V.V. Kostyukhin[141], A. Kotsokechagia[135], A. Kotwal[51], A. Koulouris[36], A. Kourkoumeli-Charalampidi[73a,73b], C. Kourkoumelis[9], E. Kourlitis[110,ae], O. Kovanda[146], R. Kowalewski[165], W. Kozanecki[135], A.S. Kozhin[37], V.A. Kramarenko[37], G. Kramberger[93], P. Kramer[100], M.W. Krasny[127], A. Krasznahorkay[36], J.W. Kraus[171], J.A. Kremer[48], T. Kresse[50], J. Kretzschmar[92], K. Kreul[18], P. Krieger[155], S. Krishnamurthy[103], M. Krivos[133], K. Krizka[20], K. Kroeninger[49], H. Kroha[110], J. Kroll[131], J. Kroll[128], K.S. Krowpman[107], U. Kruchonak[38], H. Krüger[24], N. Krumnack[81], M.C. Kruse[51], J.A. Krzysiak[87], O. Kuchinskaia[37], S. Kuday[3a], S. Kuehn[36], R. Kuesters[54], T. Kuhl[48], V. Kukhtin[38], Y. Kulchitsky[37,a], S. Kuleshov[137d,137b], M. Kumar[33g], N. Kumari[48], A. Kupco[131], T. Kupfer[49], A. Kupich[37], O. Kuprash[54], H. Kurashige[85], L.L. Kurchaninov[156a], O. Kurdysh[66], Y.A. Kurochkin[37], A. Kurova[37], M. Kuze[154], A.K. Kvam[103], J. Kvita[122], T. Kwan[104], N.G. Kyriacou[106], L.A.O. Laatu[102], C. Lacasta[163], F. Lacava[75a,75b], H. Lacker[18], D. Lacour[127], N.N. Lad[96], E. Ladygin[38], B. Laforge[127], T. Lagouri[137e], F.Z. Lahbabi[35a], S. Lai[55], I.K. Lakomiec[86a], N. Lalloue[60], J.E. Lambert[165], S. Lammers[68], W. Lampl[7], C. Lampoudis[152,e], A.N. Lancaster[115], E. Lançon[29], U. Landgraf[54], M.P.J. Landon[94], V.S. Lang[54], R.J. Langenberg[103], O.K.B. Langrekken[125], A.J. Lankford[160], F. Lanni[36], K. Lantzsch[24], A. Lanza[73a], A. Lapertosa[57b,57a], J.F. Laporte[135], T. Lari[71a], F. Lasagni Manghi[23b], M. Lassnig[36], V. Latonova[131], A. Laudrain[100], A. Laurier[150], S.D. Lawlor[139], Z. Lawrence[101], M. Lazzaroni[71a,71b], B. Le[101], E.M. Le Boulicaut[51], B. Leban[93], A. Lebedev[81], M. LeBlanc[101], F. Ledroit-Guillon[60], A.C.A. Lee[96], S.C. Lee[148], S. Lee[47a,47b], T.F. Lee[92], L.L. Leeuw[33c], H.P. Lefebvre[95], M. Lefebvre[165], C. Leggett[17a], G. Lehmann Miotto[36], M. Leigh[56], W.A. Leight[103], W. Leinonen[113], A. Leisos[152,r], M.A.L. Leite[83c], C.E. Leitgeb[48], R. Leitner[133], K.J.C. Leney[44], T. Lenz[24], S. Leone[74a], C. Leonidopoulos[52], A. Leopold[144], C. Leroy[108], R. Les[107], C.G. Lester[32], M. Levchenko[37], J. Levêque[4], D. Levin[106], L.J. Levinson[169], M.P. Lewicki[87], D.J. Lewis[4], A. Li[5], B. Li[62b], C. Li[62a], C-Q. Li[62c], H. Li[62a], H. Li[62b], H. Li[14c], H. Li[14b], H. Li[62b], J. Li[62c], K. Li[138], L. Li[62c], M. Li[14a,14e], Q.Y. Li[62a], S. Li[14a,14e], S. Li[62d,62c,d], T. Li[5], X. Li[104], Z. Li[126], Z. Li[104], Z. Li[92], Z. Li[14a,14e], S. Liang[14a,14e], Z. Liang[14a], M. Liberatore[135], B. Liberti[76a], K. Lie[64c], J. Lieber Marin[83b], H. Lien[68], K. Lin[107], R.E. Lindley[7], J.H. Lindon[2], E. Lipeles[128], A. Lipniacka[16], A. Lister[164], J.D. Little[4], B. Liu[14a], B.X. Liu[142], D. Liu[62d,62c], J.B. Liu[62a], J.K.K. Liu[32], K. Liu[62d,62c], M. Liu[62a], M.Y. Liu[62a], P. Liu[14a], Q. Liu[62d,138,62c], X. Liu[62a], Y. Liu[14d,14e], Y.L. Liu[62b], Y.W. Liu[62a], J. Llorente Merino[142], S.L. Lloyd[94], E.M. Lobodzinska[48], P. Loch[7], T. Lohse[18], K. Lohwasser[139], E. Loiacono[48], M. Lokajicek[131,*], J.D. Lomas[20], J.D. Long[162], I. Longarini[160], L. Longo[70a,70b], R. Longo[162], I. Lopez Paz[67], A. Lopez Solis[48], J. Lorenz[109], N. Lorenzo Martinez[4], A.M. Lory[109], G. Löschcke Centeno[146], O. Loseva[37], X. Lou[47a,47b], X. Lou[14a,14e],

JHEP12(2023)195

A. Lounis[66], J. Love[6], P.A. Love[91], G. Lu[14a,14e], M. Lu[80], S. Lu[128], Y.J. Lu[65], H.J. Lubatti[138], C. Luci[75a,75b], F.L. Lucio Alves[14c], A. Lucotte[60], F. Luehring[68], I. Luise[145], O. Lukianchuk[66], O. Lundberg[144], B. Lund-Jensen[144], N.A. Luongo[123], M.S. Lutz[151], A.B. Lux[25], D. Lynn[29], H. Lyons[92], R. Lysak[131], E. Lytken[98], V. Lyubushkin[38], T. Lyubushkina[38], M.M. Lyukova[145], H. Ma[29], K. Ma[62a], L.L. Ma[62b], W. Ma[62a], Y. Ma[121], D.M. Mac Donell[165], G. Maccarrone[53], J.C. MacDonald[100], P.C. Machado De Abreu Farias[83b], R. Madar[40], W.F. Mader[50], T. Madula[96], J. Maeda[85], T. Maeno[29], H. Maguire[139], V. Maiboroda[135], A. Maio[130a,130b,130d], K. Maj[86a], O. Majersky[48], S. Majewski[123], N. Makovec[66], V. Maksimovic[15], B. Malaescu[127], Pa. Malecki[87], V.P. Maleev[37], F. Malek[60], M. Mali[93], D. Malito[95], U. Mallik[80], S. Maltezos[10], S. Malyukov[38], J. Mamuzic[13], G. Mancini[53], G. Manco[73a,73b], J.P. Mandalia[94], I. Mandić[93], L. Manhaes de Andrade Filho[83a], I.M. Maniatis[169], J. Manjarres Ramos[102,aa], D.C. Mankad[169], A. Mann[109], B. Mansoulie[135], S. Manzoni[36], X. Mapekula[33c], A. Marantis[152,r], G. Marchiori[5], M. Marcisovsky[131], C. Marcon[71a], M. Marinescu[20], M. Marjanovic[120], E.J. Marshall[91], Z. Marshall[17a], S. Marti-Garcia[163], T.A. Martin[167], V.J. Martin[52], B. Martin dit Latour[16], L. Martinelli[75a,75b], M. Martinez[13,s], P. Martinez Agullo[163], V.I. Martinez Outschoorn[103], P. Martinez Suarez[13], S. Martin-Haugh[134], V.S. Martoiu[27b], A.C. Martyniuk[96], A. Marzin[36], D. Mascione[78a,78b], L. Masetti[100], T. Mashimo[153], J. Masik[101], A.L. Maslennikov[37], L. Massa[23b], P. Massarotti[72a,72b], P. Mastrandrea[74a,74b], A. Mastroberardino[43b,43a], T. Masubuchi[153], T. Mathisen[161], J. Matousek[133], N. Matsuzawa[153], J. Maurer[27b], B. Maček[93], D.A. Maximov[37], R. Mazini[148], I. Maznas[152], M. Mazza[107], S.M. Mazza[136], E. Mazzeo[71a,71b], C. Mc Ginn[29], J.P. Mc Gowan[104], S.P. Mc Kee[106], E.F. McDonald[105], A.E. McDougall[114], J.A. Mcfayden[146], R.P. McGovern[128], G. Mchedlidze[149b], R.P. Mckenzie[33g], T.C. Mclachlan[48], D.J. Mclaughlin[96], S.J. McMahon[134], C.M. Mcpartland[92], R.A. McPherson[165,w], S. Mehlhase[109], A. Mehta[92], D. Melini[150], B.R. Mellado Garcia[33g], A.H. Melo[55], F. Meloni[48], A.M. Mendes Jacques Da Costa[101], H.Y. Meng[155], L. Meng[91], S. Menke[110], M. Mentink[36], E. Meoni[43b,43a], C. Merlassino[126], L. Merola[72a,72b], C. Meroni[71a,71b], G. Merz[106], O. Meshkov[37], J. Metcalfe[6], A.S. Mete[6], C. Meyer[68], J-P. Meyer[135], R.P. Middleton[134], L. Mijović[52], G. Mikenberg[169], M. Mikestikova[131], M. Mikuž[93], H. Mildner[100], A. Milic[36], C.D. Milke[44], D.W. Miller[39], L.S. Miller[34], A. Milov[169], D.A. Milstead[47a,47b], T. Min[14c], A.A. Minaenko[37], I.A. Minashvili[149b], L. Mince[59], A.I. Mincer[117], B. Mindur[86a], M. Mineev[38], Y. Mino[88], L.M. Mir[13], M. Miralles Lopez[163], M. Mironova[17a], A. Mishima[153], M.C. Missio[113], A. Mitra[167], V.A. Mitsou[163], Y. Mitsumori[111], O. Miu[155], P.S. Miyagawa[94], T. Mkrtchyan[63a], M. Mlinarevic[96], T. Mlinarevic[96], M. Mlynarikova[36], S. Mobius[19], P. Moder[48], P. Mogg[109], A.F. Mohammed[14a,14e], S. Mohapatra[41], G. Mokgatitswane[33g], L. Moleri[169], B. Mondal[141], S. Mondal[132], K. Mönig[48], E. Monnier[102], L. Monsonis Romero[163], J. Montejo Berlingen[13], M. Montella[119], F. Montereali[77a,77b], F. Monticelli[90], S. Monzani[69a,69c], N. Morange[66], A.L. Moreira De Carvalho[130a], M. Moreno Llácer[163], C. Moreno Martinez[56], P. Morettini[57b], S. Morgenstern[36], M. Morii[61], M. Morinaga[153], A.K. Morley[36], F. Morodei[75a,75b], L. Morvaj[36], P. Moschovakos[36], B. Moser[36], M. Mosidze[149b], T. Moskalets[54],

JHEP12(2023)195

P. Moskvitina[113], J. Moss[31,l], E.J.W. Moyse[103], O. Mtintsilana[33g], S. Muanza[102], J. Mueller[129], D. Muenstermann[91], R. Müller[19], G.A. Mullier[161], A.J. Mullin[32], J.J. Mullin[128], D.P. Mungo[155], D. Munoz Perez[163], F.J. Munoz Sanchez[101], M. Murin[101], W.J. Murray[167,134], A. Murrone[71a,71b], M. Muškinja[17a], C. Mwewa[29], A.G. Myagkov[37,a], A.J. Myers[8], G. Myers[68], M. Myska[132], B.P. Nachman[17a], O. Nackenhorst[49], A. Nag[50], K. Nagai[126], K. Nagano[84], J.L. Nagle[29,aj], E. Nagy[102], A.M. Nairz[36], Y. Nakahama[84], K. Nakamura[84], K. Nakkalil[5], H. Nanjo[124], R. Narayan[44], E.A. Narayanan[112], I. Naryshkin[37], M. Naseri[34], S. Nasri[159], C. Nass[24], G. Navarro[22a], J. Navarro-Gonzalez[163], R. Nayak[151], A. Nayaz[18], P.Y. Nechaeva[37], F. Nechansky[48], L. Nedic[126], T.J. Neep[20], A. Negri[73a,73b], M. Negrini[23b], C. Nellist[114], C. Nelson[104], K. Nelson[106], S. Nemecek[131], M. Nessi[36,h], M.S. Neubauer[162], F. Neuhaus[100], J. Neundorf[48], R. Newhouse[164], P.R. Newman[20], C.W. Ng[129], Y.W.Y. Ng[48], B. Ngair[35e], H.D.N. Nguyen[108], R.B. Nickerson[126], R. Nicolaidou[135], J. Nielsen[136], M. Niemeyer[55], J. Niermann[55,36], N. Nikiforou[36], V. Nikolaenko[37,a], I. Nikolic-Audit[127], K. Nikolopoulos[20], P. Nilsson[29], I. Ninca[48], H.R. Nindhito[56], G. Ninio[151], A. Nisati[75a], N. Nishu[2], R. Nisius[110], J-E. Nitschke[50], E.K. Nkadimeng[33g], T. Nobe[153], D.L. Noel[32], T. Nommensen[147], M.B. Norfolk[139], R.R.B. Norisam[96], B.J. Norman[34], J. Novak[93], T. Novak[48], L. Novotny[132], R. Novotny[112], L. Nozka[122], K. Ntekas[160], N.M.J. Nunes De Moura Junior[83b], E. Nurse[96], J. Ocariz[127], A. Ochi[85], I. Ochoa[130a], S. Oerdek[48], J.T. Offermann[39], A. Ogrodnik[133], A. Oh[101], C.C. Ohm[144], H. Oide[84], R. Oishi[153], M.L. Ojeda[48], M.W. O'Keefe[92], Y. Okumura[153], L.F. Oleiro Seabra[130a], S.A. Olivares Pino[137d], D. Oliveira Damazio[29], D. Oliveira Goncalves[83a], J.L. Oliver[160], Ö.O. Öncel[54], A.P. O'Neill[19], A. Onofre[130a,130e], P.U.E. Onyisi[11], M.J. Oreglia[39], G.E. Orellana[90], D. Orestano[77a,77b], N. Orlando[13], R.S. Orr[155], V. O'Shea[59], L.M. Osojnak[128], R. Ospanov[62a], G. Otero y Garzon[30], H. Otono[89], P.S. Ott[63a], G.J. Ottino[17a], M. Ouchrif[35d], J. Ouellette[29], F. Ould-Saada[125], M. Owen[59], R.E. Owen[134], K.Y. Oyulmaz[21a], V.E. Ozcan[21a], F. Ozturk[87], N. Ozturk[8], S. Ozturk[82], H.A. Pacey[126], A. Pacheco Pages[13], C. Padilla Aranda[13], G. Padovano[75a,75b], S. Pagan Griso[17a], G. Palacino[68], A. Palazzo[70a,70b], S. Palestini[36], J. Pan[172], T. Pan[64a], D.K. Panchal[11], C.E. Pandini[114], J.G. Panduro Vazquez[95], H.D. Pandya[1], H. Pang[14b], P. Pani[48], G. Panizzo[69a,69c], L. Paolozzi[56], C. Papadatos[108], S. Parajuli[44], A. Paramonov[6], C. Paraskevopoulos[10], D. Paredes Hernandez[64b], K.R. Park[41], T.H. Park[155], M.A. Parker[32], F. Parodi[57b,57a], E.W. Parrish[115], V.A. Parrish[52], J.A. Parsons[41], U. Parzefall[54], B. Pascual Dias[108], L. Pascual Dominguez[151], E. Pasqualucci[75a], S. Passaggio[57b], F. Pastore[95], P. Pasuwan[47a,47b], P. Patel[87], U.M. Patel[51], J.R. Pater[101], T. Pauly[36], J. Pearkes[143], M. Pedersen[125], R. Pedro[130a], S.V. Peleganchuk[37], O. Penc[36], E.A. Pender[52], K.E. Penski[109], M. Penzin[37], B.S. Peralva[83d], A.P. Pereira Peixoto[60], L. Pereira Sanchez[47a,47b], D.V. Perepelitsa[29,aj], E. Perez Codina[156a], M. Perganti[10], L. Perini[71a,71b,*], H. Pernegger[36], O. Perrin[40], K. Peters[48], R.F.Y. Peters[101], B.A. Petersen[36], T.C. Petersen[42], E. Petit[102], V. Petousis[132], C. Petridou[152,e], A. Petrukhin[141], M. Pettee[17a], N.E. Pettersson[36], A. Petukhov[37], K. Petukhova[133], R. Pezoa[137f], L. Pezzotti[36], G. Pezzullo[172], T.M. Pham[170], T. Pham[105], P.W. Phillips[134], G. Piacquadio[145], E. Pianori[17a],

JHEP12(2023)195

F. Piazza[123], R. Piegaia[30], D. Pietreanu[27b], A.D. Pilkington[101], M. Pinamonti[69a,69c], J.L. Pinfold[2], B.C. Pinheiro Pereira[130a], A.E. Pinto Pinoargote[100,135], L. Pintucci[69a,69c], K.M. Piper[146], A. Pirttikoski[56], D.A. Pizzi[34], L. Pizzimento[64b], A. Pizzini[114], M.-A. Pleier[29], V. Plesanovs[54], V. Pleskot[133], E. Plotnikova[38], G. Poddar[4], R. Poettgen[98], L. Poggioli[127], I. Pokharel[55], S. Polacek[133], G. Polesello[73a], A. Poley[142,156a], R. Polifka[132], A. Polini[23b], C.S. Pollard[167], Z.B. Pollock[119], V. Polychronakos[29], E. Pompa Pacchi[75a,75b], D. Ponomarenko[113], L. Pontecorvo[36], S. Popa[27a], G.A. Popeneciu[27d], A. Poreba[36], D.M. Portillo Quintero[156a], S. Pospisil[132], M.A. Postill[139], P. Postolache[27c], K. Potamianos[167], P.A. Potepa[86a], I.N. Potrap[38], C.J. Potter[32], H. Potti[1], T. Poulsen[48], J. Poveda[163], M.E. Pozo Astigarraga[36], A. Prades Ibanez[163], J. Pretel[54], D. Price[101], M. Primavera[70a], M.A. Principe Martin[99], R. Privara[122], T. Procter[59], M.L. Proffitt[138], N. Proklova[128], K. Prokofiev[64c], G. Proto[110], S. Protopopescu[29], J. Proudfoot[6], M. Przybycien[86a], W.W. Przygoda[86b], J.E. Puddefoot[139], D. Pudzha[37], D. Pyatiizbyantseva[37], J. Qian[106], D. Qichen[101], Y. Qin[101], T. Qiu[52], A. Quadt[55], M. Queitsch-Maitland[101], G. Quetant[56], R.P. Quinn[164], G. Rabanal Bolanos[61], D. Rafanoharana[54], F. Ragusa[71a,71b], J.L. Rainbolt[39], J.A. Raine[56], S. Rajagopalan[29], E. Ramakoti[37], I.A. Ramirez-Berend[34], K. Ran[48,14e], N.P. Rapheeha[33g], H. Rasheed[27b], V. Raskina[127], D.F. Rassloff[63a], S. Rave[100], B. Ravina[55], I. Ravinovich[169], M. Raymond[36], A.L. Read[125], N.P. Readioff[139], D.M. Rebuzzi[73a,73b], G. Redlinger[29], A.S. Reed[110], K. Reeves[26], J.A. Reidelsturz[171], D. Reikher[151], A. Rej[49], C. Rembser[36], A. Renardi[48], M. Renda[27b], M.B. Rendel[110], F. Renner[48], A.G. Rennie[160], A.L. Rescia[48], S. Resconi[71a], M. Ressegotti[57b,57a], S. Rettie[36], J.G. Reyes Rivera[107], E. Reynolds[17a], O.L. Rezanova[37], P. Reznicek[133], N. Ribaric[91], E. Ricci[78a,78b], R. Richter[110], S. Richter[47a,47b], E. Richter-Was[86b], M. Ridel[127], S. Ridouani[35d], P. Rieck[117], P. Riedler[36], E.M. Riefel[47a,47b], J.O. Rieger[114], M. Rijssenbeek[145], A. Rimoldi[73a,73b], M. Rimoldi[36], L. Rinaldi[23b,23a], T.T. Rinn[29], M.P. Rinnagel[109], G. Ripellino[161], I. Riu[13], P. Rivadeneira[48], J.C. Rivera Vergara[165], F. Rizatdinova[121], E. Rizvi[94], B.A. Roberts[167], B.R. Roberts[17a], S.H. Robertson[104,w], D. Robinson[32], C.M. Robles Gajardo[137f], M. Robles Manzano[100], A. Robson[59], A. Rocchi[76a,76b], C. Roda[74a,74b], S. Rodriguez Bosca[63a], Y. Rodriguez Garcia[22a], A. Rodriguez Rodriguez[54], A.M. Rodríguez Vera[156b], S. Roe[36], J.T. Roemer[160], A.R. Roepe-Gier[136], J. Roggel[171], O. Røhne[125], R.A. Rojas[103], C.P.A. Roland[127], J. Roloff[29], A. Romaniouk[37], E. Romano[73a,73b], M. Romano[23b], A.C. Romero Hernandez[162], N. Rompotis[92], L. Roos[127], S. Rosati[75a], B.J. Rosser[39], E. Rossi[126], E. Rossi[72a,72b], L.P. Rossi[57b], L. Rossini[54], R. Rosten[119], M. Rotaru[27b], B. Rottler[54], C. Rougier[102,aa], D. Rousseau[66], D. Rousso[32], A. Roy[162], S. Roy-Garand[155], A. Rozanov[102], Z.M.A. Rozario[59], Y. Rozen[150], X. Ruan[33g], A. Rubio Jimenez[163], A.J. Ruby[92], V.H. Ruelas Rivera[18], T.A. Ruggeri[1], A. Ruggiero[126], A. Ruiz-Martinez[163], A. Rummler[36], Z. Rurikova[54], N.A. Rusakovich[38], H.L. Russell[165], G. Russo[75a,75b], J.P. Rutherfoord[7], S. Rutherford Colmenares[32], K. Rybacki[91], M. Rybar[133], E.B. Rye[125], A. Ryzhov[44], J.A. Sabater Iglesias[56], P. Sabatini[163], L. Sabetta[75a,75b], H.F-W. Sadrozinski[136], F. Safai Tehrani[75a], B. Safarzadeh Samani[134], M. Safdari[143], S. Saha[165], M. Sahinsoy[110], M. Saimpert[135], M. Saito[153], T. Saito[153], D. Salamani[36], A. Salnikov[143], J. Salt[163], A. Salvador Salas[151],

JHEP12(2023)195

D. Salvatore[43b,43a], F. Salvatore[146], A. Salzburger[36], D. Sammel[54], D. Sampsonidis[152,e], D. Sampsonidou[123], J. Sánchez[163], A. Sanchez Pineda[4], V. Sanchez Sebastian[163], H. Sandaker[125], C.O. Sander[48], J.A. Sandesara[103], M. Sandhoff[171], C. Sandoval[22b], D.P.C. Sankey[134], T. Sano[88], A. Sansoni[53], L. Santi[75a,75b], C. Santoni[40], H. Santos[130a,130b], S.N. Santpur[17a], A. Santra[169], K.A. Saoucha[116b], J.G. Saraiva[130a,130d], J. Sardain[7], O. Sasaki[84], K. Sato[157], C. Sauer[63b], F. Sauerburger[54], E. Sauvan[4], P. Savard[155,ag], R. Sawada[153], C. Sawyer[134], L. Sawyer[97], I. Sayago Galvan[163], C. Sbarra[23b], A. Sbrizzi[23b,23a], T. Scanlon[96], J. Schaarschmidt[138], P. Schacht[110], U. Schäfer[100], A.C. Schaffer[66,44], D. Schaile[109], R.D. Schamberger[145], C. Scharf[18], M.M. Schefer[19], V.A. Schegelsky[37], D. Scheirich[133], F. Schenck[18], M. Schernau[160], C. Scheulen[55], C. Schiavi[57b,57a], E.J. Schioppa[70a,70b], M. Schioppa[43b,43a], B. Schlag[143,n], K.E. Schleicher[54], S. Schlenker[36], J. Schmeing[171], M.A. Schmidt[171], K. Schmieden[100], C. Schmitt[100], N. Schmitt[100], S. Schmitt[48], L. Schoeffel[135], A. Schoening[63b], P.G. Scholer[54], E. Schopf[126], M. Schott[100], J. Schovancova[36], S. Schramm[56], F. Schroeder[171], T. Schroer[56], H-C. Schultz-Coulon[63a], M. Schumacher[54], B.A. Schumm[136], Ph. Schune[135], A.J. Schuy[138], H.R. Schwartz[136], A. Schwartzman[143], T.A. Schwarz[106], Ph. Schwemling[135], R. Schwienhorst[107], A. Sciandra[136], G. Sciolla[26], F. Scuri[74a], C.D. Sebastiani[92], K. Sedlaczek[115], P. Seema[18], S.C. Seidel[112], A. Seiden[136], B.D. Seidlitz[41], C. Seitz[48], J.M. Seixas[83b], G. Sekhniaidze[72a], S.J. Sekula[44], L. Selem[60], N. Semprini-Cesari[23b,23a], D. Sengupta[56], V. Senthilkumar[163], L. Serin[66], L. Serkin[69a,69b], M. Sessa[76a,76b], H. Severini[120], F. Sforza[57b,57a], A. Sfyrla[56], E. Shabalina[55], R. Shaheen[144], J.D. Shahinian[128], D. Shaked Renous[169], L.Y. Shan[14a], M. Shapiro[17a], A. Sharma[36], A.S. Sharma[164], P. Sharma[80], S. Sharma[48], P.B. Shatalov[37], K. Shaw[146], S.M. Shaw[101], A. Shcherbakova[37], Q. Shen[62c,5], P. Sherwood[96], L. Shi[96], X. Shi[14a], C.O. Shimmin[172], J.D. Shinner[95], I.P.J. Shipsey[126], S. Shirabe[56,h], M. Shiyakova[38,u], J. Shlomi[169], M.J. Shochet[39], J. Shojaii[105], D.R. Shope[125], B. Shrestha[120], S. Shrestha[119,ak], E.M. Shrif[33g], M.J. Shroff[165], P. Sicho[131], A.M. Sickles[162], E. Sideras Haddad[33g], A. Sidoti[23b], F. Siegert[50], Dj. Sijacki[15], R. Sikora[86a], F. Sili[90], J.M. Silva[20], M.V. Silva Oliveira[29], S.B. Silverstein[47a], S. Simion[66], R. Simoniello[36], E.L. Simpson[59], H. Simpson[146], L.R. Simpson[106], N.D. Simpson[98], S. Simsek[82], S. Sindhu[55], P. Sinervo[155], S. Singh[155], S. Sinha[48], S. Sinha[101], M. Sioli[23b,23a], I. Siral[36], E. Sitnikova[48], S.Yu. Sivoklokov[37,*], J. Sjölin[47a,47b], A. Skaf[55], E. Skorda[20], P. Skubic[120], M. Slawinska[87], V. Smakhtin[169], B.H. Smart[134], J. Smiesko[36], S.Yu. Smirnov[37], Y. Smirnov[37], L.N. Smirnova[37,a], O. Smirnova[98], A.C. Smith[41], E.A. Smith[39], H.A. Smith[126], J.L. Smith[92], R. Smith[143], M. Smizanska[91], K. Smolek[132], A.A. Snesarev[37], S.R. Snider[155], H.L. Snoek[114], S. Snyder[29], R. Sobie[165,w], A. Soffer[151], C.A. Solans Sanchez[36], E.Yu. Soldatov[37], U. Soldevila[163], A.A. Solodkov[37], S. Solomon[26], A. Soloshenko[38], K. Solovieva[54], O.V. Solovyanov[40], V. Solovyev[37], P. Sommer[36], A. Sonay[13], W.Y. Song[156b], J.M. Sonneveld[114], A. Sopczak[132], A.L. Sopio[96], F. Sopkova[28b], I.R. Sotarriva Alvarez[154], V. Sothilingam[63a], O.J. Soto Sandoval[137c,137b], S. Sottocornola[68], R. Soualah[116b], Z. Soumaimi[35e], D. South[48], N. Soybelman[169], S. Spagnolo[70a,70b], M. Spalla[110], D. Sperlich[54], G. Spigo[36], S. Spinali[91], D.P. Spiteri[59], M. Spousta[133], E.J. Staats[34], A. Stabile[71a,71b], R. Stamen[63a], A. Stampekis[20],

JHEP12(2023)195

M. Standke[24], E. Stanecka[87], M.V. Stange[50], B. Stanislaus[17a], M.M. Stanitzki[48], B. Stapf[48], E.A. Starchenko[37], G.H. Stark[136], J. Stark[102,aa], D.M. Starko[156b], P. Staroba[131], P. Starovoitov[63a], S. Stärz[104], R. Staszewski[87], G. Stavropoulos[46], J. Steentoft[161], P. Steinberg[29], B. Stelzer[142,156a], H.J. Stelzer[129], O. Stelzer-Chilton[156a], H. Stenzel[58], T.J. Stevenson[146], G.A. Stewart[36], J.R. Stewart[121], M.C. Stockton[36], G. Stoicea[27b], M. Stolarski[130a], S. Stonjek[110], A. Straessner[50], J. Strandberg[144], S. Strandberg[47a,47b], M. Stratmann[171], M. Strauss[120], T. Strebler[102], P. Strizenec[28b], R. Ströhmer[166], D.M. Strom[123], L.R. Strom[48], R. Stroynowski[44], A. Strubig[47a,47b], S.A. Stucci[29], B. Stugu[16], J. Stupak[120], N.A. Styles[48], D. Su[143], S. Su[62a], W. Su[62d], X. Su[62a,66], K. Sugizaki[153], V.V. Sulin[37], M.J. Sullivan[92], D.M.S. Sultan[78a,78b], L. Sultanaliyeva[37], S. Sultansoy[3b], T. Sumida[88], S. Sun[106], S. Sun[170], O. Sunneborn Gudnadottir[161], N. Sur[102], M.R. Sutton[146], H. Suzuki[157], M. Svatos[131], M. Swiatlowski[156a], T. Swirski[166], I. Sykora[28a], M. Sykora[133], T. Sykora[133], D. Ta[100], K. Tackmann[48,t], A. Taffard[160], R. Tafirout[156a], J.S. Tafoya Vargas[66], E.P. Takeva[52], Y. Takubo[84], M. Talby[102], A.A. Talyshev[37], K.C. Tam[64b], N.M. Tamir[151], A. Tanaka[153], J. Tanaka[153], R. Tanaka[66], M. Tanasini[57b,57a], Z. Tao[164], S. Tapia Araya[137f], S. Tapprogge[100], A. Tarek Abouelfadl Mohamed[107], S. Tarem[150], K. Tariq[14a], G. Tarna[102,27b], G.F. Tartarelli[71a], P. Tas[133], M. Tasevsky[131], E. Tassi[43b,43a], A.C. Tate[162], G. Tateno[153], Y. Tayalati[35e,v], G.N. Taylor[105], W. Taylor[156b], A.S. Tee[170], R. Teixeira De Lima[143], P. Teixeira-Dias[95], J.J. Teoh[155], K. Terashi[153], J. Terron[99], S. Terzo[13], M. Testa[53], R.J. Teuscher[155,w], A. Thaler[79], O. Theiner[56], N. Themistokleous[52], T. Theveneaux-Pelzer[102], O. Thielmann[171], D.W. Thomas[95], J.P. Thomas[20], E.A. Thompson[17a], P.D. Thompson[20], E. Thomson[128], Y. Tian[55], V. Tikhomirov[37,a], Yu.A. Tikhonov[37], S. Timoshenko[37], D. Timoshyn[133], E.X.L. Ting[1], P. Tipton[172], S.H. Tlou[33g], A. Tnourji[40], K. Todome[154], S. Todorova-Nova[133], S. Todt[50], M. Togawa[84], J. Tojo[89], S. Tokár[28a], K. Tokushuku[84], O. Toldaiev[68], R. Tombs[32], M. Tomoto[84,111], L. Tompkins[143,n], K.W. Topolnicki[86b], E. Torrence[123], H. Torres[102,aa], E. Torró Pastor[163], M. Toscani[30], C. Tosciri[39], M. Tost[11], D.R. Tovey[139], A. Traeet[16], I.S. Trandafir[27b], T. Trefzger[166], A. Tricoli[29], I.M. Trigger[156a], S. Trincaz-Duvoid[127], D.A. Trischuk[26], B. Trocmé[60], C. Troncon[71a], L. Truong[33c], M. Trzebinski[87], A. Trzupek[87], F. Tsai[145], M. Tsai[106], A. Tsiamis[152,e], P.V. Tsiareshka[37], S. Tsigaridas[156a], A. Tsirigotis[152,r], V. Tsiskaridze[155], E.G. Tskhadadze[149a], M. Tsopoulou[152,e], Y. Tsujikawa[88], I.I. Tsukerman[37], V. Tsulaia[17a], S. Tsuno[84], O. Tsur[150], K. Tsuri[118], D. Tsybychev[145], Y. Tu[64b], A. Tudorache[27b], V. Tudorache[27b], A.N. Tuna[36], S. Turchikhin[57b,57a], I. Turk Cakir[3a], R. Turra[71a], T. Turtuvshin[38,x], P.M. Tuts[41], S. Tzamarias[152,e], P. Tzanis[10], E. Tzovara[100], F. Ukegawa[157], P.A. Ulloa Poblete[137c,137b], E.N. Umaka[29], G. Unal[36], M. Unal[11], A. Undrus[29], G. Unel[160], J. Urban[28b], P. Urquijo[105], P. Urrejola[137a], G. Usai[8], R. Ushioda[154], M. Usman[108], Z. Uysal[21b], V. Vacek[132], B. Vachon[104], K.O.H. Vadla[125], T. Vafeiadis[36], A. Vaitkus[96], C. Valderanis[109], E. Valdes Santurio[47a,47b], M. Valente[156a], S. Valentinetti[23b,23a], A. Valero[163], E. Valiente Moreno[163], A. Vallier[102,aa], J.A. Valls Ferrer[163], D.R. Van Arneman[114], T.R. Van Daalen[138], A. Van Der Graaf[49], P. Van Gemmeren[6], M. Van Rijnbach[125,36], S. Van Stroud[96], I. Van Vulpen[114], M. Vanadia[76a,76b],

JHEP12(2023)195

W. Vandelli[36], M. Vandenbroucke[135], E.R. Vandewall[121], D. Vannicola[151], L. Vannoli[57b,57a], R. Vari[75a], E.W. Varnes[7], C. Varni[17b], T. Varol[148], D. Varouchas[66], L. Varriale[163], K.E. Varvell[147], M.E. Vasile[27b], L. Vaslin[84], G.A. Vasquez[165], A. Vasyukov[38], F. Vazeille[40], T. Vazquez Schroeder[36], J. Veatch[31], V. Vecchio[101], M.J. Veen[103], I. Veliscek[126], L.M. Veloce[155], F. Veloso[130a,130c], S. Veneziano[75a], A. Ventura[70a,70b], S. Ventura Gonzalez[135], A. Verbytskyi[110], M. Verducci[74a,74b], C. Vergis[24], M. Verissimo De Araujo[83b], W. Verkerke[114], J.C. Vermeulen[114], C. Vernieri[143], M. Vessella[103], M.C. Vetterli[142,ag], A. Vgenopoulos[152,e], N. Viaux Maira[137f], T. Vickey[139], O.E. Vickey Boeriu[139], G.H.A. Viehhauser[126], L. Vigani[63b], M. Villa[23b,23a], M. Villaplana Perez[163], E.M. Villhauer[52], E. Vilucchi[53], M.G. Vincter[34], G.S. Virdee[20], A. Vishwakarma[52], A. Visibile[114], C. Vittori[36], I. Vivarelli[146], E. Voevodina[110], F. Vogel[109], J.C. Voigt[50], P. Vokac[132], Yu. Volkotrub[86a], J. Von Ahnen[48], E. Von Toerne[24], B. Vormwald[36], V. Vorobel[133], K. Vorobev[37], M. Vos[163], K. Voss[141], J.H. Vossebeld[92], M. Vozak[114], L. Vozdecky[94], N. Vranjes[15], M. Vranjes Milosavljevic[15], M. Vreeswijk[114], R. Vuillermet[36], O. Vujinovic[100], I. Vukotic[39], S. Wada[157], C. Wagner[103], J.M. Wagner[17a], W. Wagner[171], S. Wahdan[171], H. Wahlberg[90], M. Wakida[111], J. Walder[134], R. Walker[109], W. Walkowiak[141], A. Wall[128], T. Wamorkar[6], A.Z. Wang[136], C. Wang[100], C. Wang[62c], H. Wang[17a], J. Wang[64a], R.-J. Wang[100], R. Wang[61], R. Wang[6], S.M. Wang[148], S. Wang[62b], T. Wang[62a], W.T. Wang[80], W. Wang[14a], X. Wang[14c], X. Wang[162], X. Wang[62c], Y. Wang[62d], Y. Wang[14c], Z. Wang[106], Z. Wang[62d,51,62c], Z. Wang[106], A. Warburton[104], R.J. Ward[20], N. Warrack[59], A.T. Watson[20], H. Watson[59], M.F. Watson[20], E. Watton[59,134], G. Watts[138], B.M. Waugh[96], C. Weber[29], H.A. Weber[18], M.S. Weber[19], S.M. Weber[63a], C. Wei[62a], Y. Wei[126], A.R. Weidberg[126], E.J. Weik[117], J. Weingarten[49], M. Weirich[100], C. Weiser[54], C.J. Wells[48], T. Wenaus[29], B. Wendland[49], T. Wengler[36], N.S. Wenke[110], N. Wermes[24], M. Wessels[63a], A.M. Wharton[91], A.S. White[61], A. White[8], M.J. White[1], D. Whiteson[160], L. Wickremasinghe[124], W. Wiedenmann[170], C. Wiel[50], M. Wielers[134], C. Wiglesworth[42], D.J. Wilbern[120], H.G. Wilkens[36], D.M. Williams[41], H.H. Williams[128], S. Williams[32], S. Willocq[103], B.J. Wilson[101], P.J. Windischhofer[39], F.I. Winkel[30], F. Winklmeier[123], B.T. Winter[54], J.K. Winter[101], M. Wittgen[143], M. Wobisch[97], Z. Wolffs[114], J. Wollrath[160], M.W. Wolter[87], H. Wolters[130a,130c], A.F. Wongel[48], E.L. Woodward[41], S.D. Worm[48], B.K. Wosiek[87], K.W. Woźniak[87], S. Wozniewski[55], K. Wraight[59], C. Wu[20], J. Wu[14a,14e], M. Wu[64a], M. Wu[113], S.L. Wu[170], X. Wu[56], Y. Wu[62a], Z. Wu[135], J. Wuerzinger[110,ae], T.R. Wyatt[101], B.M. Wynne[52], S. Xella[42], L. Xia[14c], M. Xia[14b], J. Xiang[64c], M. Xie[62a], X. Xie[62a], S. Xin[14a,14e], A. Xiong[123], J. Xiong[17a], D. Xu[14a], H. Xu[62a], L. Xu[62a], R. Xu[128], T. Xu[106], Y. Xu[14b], Z. Xu[52], Z. Xu[14c], B. Yabsley[147], S. Yacoob[33a], Y. Yamaguchi[154], E. Yamashita[153], H. Yamauchi[157], T. Yamazaki[17a], Y. Yamazaki[85], J. Yan[62c], S. Yan[126], Z. Yan[25], H.J. Yang[62c,62d], H.T. Yang[62a], S. Yang[62a], T. Yang[64c], X. Yang[36], X. Yang[14a], Y. Yang[44], Y. Yang[62a], Z. Yang[62a], W-M. Yao[17a], Y.C. Yap[48], H. Ye[14c], H. Ye[55], J. Ye[14a], S. Ye[29], X. Ye[62a], Y. Yeh[96], I. Yeletskikh[38], B.K. Yeo[17b], M.R. Yexley[96], P. Yin[41], K. Yorita[168], S. Younas[27b], C.J.S. Young[36], C. Young[143], C. Yu[14a,14e,ai], Y. Yu[62a], M. Yuan[106], R. Yuan[62b], L. Yue[96], M. Zaazoua[62a], B. Zabinski[87], E. Zaid[52], T. Zakareishvili[149b], N. Zakharchuk[34],

JHEP12(2023)195

S. Zambito[56], J.A. Zamora Saa[137d,137b], J. Zang[153], D. Zanzi[54], O. Zaplatilek[132], C. Zeitnitz[171], H. Zeng[14a], J.C. Zeng[162], D.T. Zenger Jr[26], O. Zenin[37], T. Ženiš[28a], S. Zenz[94], S. Zerradi[35a], D. Zerwas[66], M. Zhai[14a,14e], B. Zhang[14c], D.F. Zhang[139], J. Zhang[62b], J. Zhang[6], K. Zhang[14a,14e], L. Zhang[14c], P. Zhang[14a,14e], R. Zhang[170], S. Zhang[106], S. Zhang[44], T. Zhang[153], X. Zhang[62c], X. Zhang[62b], Y. Zhang[62c,5], Y. Zhang[96], Y. Zhang[14c], Z. Zhang[17a], Z. Zhang[66], H. Zhao[138], P. Zhao[51], T. Zhao[62b], Y. Zhao[136], Z. Zhao[62a], A. Zhemchugov[38], J. Zheng[14c], K. Zheng[162], X. Zheng[62a], Z. Zheng[143], D. Zhong[162], B. Zhou[106], H. Zhou[7], N. Zhou[62c], Y. Zhou[7], C.G. Zhu[62b], J. Zhu[106], Y. Zhu[62c], Y. Zhu[62a], X. Zhuang[14a], K. Zhukov[37], V. Zhulanov[37], N.I. Zimine[38], J. Zinsser[63b], M. Ziolkowski[141], L. Živković[15], A. Zoccoli[23b,23a], K. Zoch[61], T.G. Zorbas[139], O. Zormpa[46], W. Zou[41], L. Zwalinski[36]

[1] *Department of Physics, University of Adelaide, Adelaide; Australia*
[2] *Department of Physics, University of Alberta, Edmonton AB; Canada*
[3] [(a)] *Department of Physics, Ankara University, Ankara;* [(b)] *Division of Physics, TOBB University of Economics and Technology, Ankara; Türkiye*
[4] *LAPP, Université Savoie Mont Blanc, CNRS/IN2P3, Annecy; France*
[5] *APC, Université Paris Cité, CNRS/IN2P3, Paris; France*
[6] *High Energy Physics Division, Argonne National Laboratory, Argonne IL; United States of America*
[7] *Department of Physics, University of Arizona, Tucson AZ; United States of America*
[8] *Department of Physics, University of Texas at Arlington, Arlington TX; United States of America*
[9] *Physics Department, National and Kapodistrian University of Athens, Athens; Greece*
[10] *Physics Department, National Technical University of Athens, Zografou; Greece*
[11] *Department of Physics, University of Texas at Austin, Austin TX; United States of America*
[12] *Institute of Physics, Azerbaijan Academy of Sciences, Baku; Azerbaijan*
[13] *Institut de Física d'Altes Energies (IFAE), Barcelona Institute of Science and Technology, Barcelona; Spain*
[14] [(a)] *Institute of High Energy Physics, Chinese Academy of Sciences, Beijing;* [(b)] *Physics Department, Tsinghua University, Beijing;* [(c)] *Department of Physics, Nanjing University, Nanjing;* [(d)] *School of Science, Shenzhen Campus of Sun Yat-sen University;* [(e)] *University of Chinese Academy of Science (UCAS), Beijing; China*
[15] *Institute of Physics, University of Belgrade, Belgrade; Serbia*
[16] *Department for Physics and Technology, University of Bergen, Bergen; Norway*
[17] [(a)] *Physics Division, Lawrence Berkeley National Laboratory, Berkeley CA;* [(b)] *University of California, Berkeley CA; United States of America*
[18] *Institut für Physik, Humboldt Universität zu Berlin, Berlin; Germany*
[19] *Albert Einstein Center for Fundamental Physics and Laboratory for High Energy Physics, University of Bern, Bern; Switzerland*
[20] *School of Physics and Astronomy, University of Birmingham, Birmingham; United Kingdom*
[21] [(a)] *Department of Physics, Bogazici University, Istanbul;* [(b)] *Department of Physics Engineering, Gaziantep University, Gaziantep;* [(c)] *Department of Physics, Istanbul University, Istanbul; Türkiye*
[22] [(a)] *Facultad de Ciencias y Centro de Investigaciónes, Universidad Antonio Nariño, Bogotá;* [(b)] *Departamento de Física, Universidad Nacional de Colombia, Bogotá; Colombia*
[23] [(a)] *Dipartimento di Fisica e Astronomia A. Righi, Università di Bologna, Bologna;* [(b)] *INFN Sezione di Bologna; Italy*
[24] *Physikalisches Institut, Universität Bonn, Bonn; Germany*
[25] *Department of Physics, Boston University, Boston MA; United States of America*
[26] *Department of Physics, Brandeis University, Waltham MA; United States of America*
[27] [(a)] *Transilvania University of Brasov, Brasov;* [(b)] *Horia Hulubei National Institute of Physics and Nuclear Engineering, Bucharest;* [(c)] *Department of Physics, Alexandru Ioan Cuza University of Iasi, Iasi;* [(d)] *National Institute for Research and Development of Isotopic and Molecular Technologies, Physics Department, Cluj-Napoca;* [(e)] *University Politehnica Bucharest, Bucharest;* [(f)] *West University in Timisoara, Timisoara;* [(g)] *Faculty of Physics, University of Bucharest, Bucharest; Romania*

JHEP12(2023)195

[28] [(a)] Faculty of Mathematics, Physics and Informatics, Comenius University, Bratislava;[(b)] Department of Subnuclear Physics, Institute of Experimental Physics of the Slovak Academy of Sciences, Kosice; Slovak Republic
[29] Physics Department, Brookhaven National Laboratory, Upton NY; United States of America
[30] Universidad de Buenos Aires, Facultad de Ciencias Exactas y Naturales, Departamento de Física, y CONICET, Instituto de Física de Buenos Aires (IFIBA), Buenos Aires; Argentina
[31] California State University, CA; United States of America
[32] Cavendish Laboratory, University of Cambridge, Cambridge; United Kingdom
[33] [(a)] Department of Physics, University of Cape Town, Cape Town;[(b)] iThemba Labs, Western Cape;[(c)] Department of Mechanical Engineering Science, University of Johannesburg, Johannesburg;[(d)] National Institute of Physics, University of the Philippines Diliman (Philippines);[(e)] University of South Africa, Department of Physics, Pretoria;[(f)] University of Zululand, KwaDlangezwa;[(g)] School of Physics, University of the Witwatersrand, Johannesburg; South Africa
[34] Department of Physics, Carleton University, Ottawa ON; Canada
[35] [(a)] Faculté des Sciences Ain Chock, Réseau Universitaire de Physique des Hautes Energies — Université Hassan II, Casablanca;[(b)] Faculté des Sciences, Université Ibn-Tofail, Kénitra;[(c)] Faculté des Sciences Semlalia, Université Cadi Ayyad, LPHEA-Marrakech;[(d)] LPMR, Faculté des Sciences, Université Mohamed Premier, Oujda;[(e)] Faculté des sciences, Université Mohammed V, Rabat;[(f)] Institute of Applied Physics, Mohammed VI Polytechnic University, Ben Guerir; Morocco
[36] CERN, Geneva; Switzerland
[37] Affiliated with an institute covered by a cooperation agreement with CERN
[38] Affiliated with an international laboratory covered by a cooperation agreement with CERN
[39] Enrico Fermi Institute, University of Chicago, Chicago IL; United States of America
[40] LPC, Université Clermont Auvergne, CNRS/IN2P3, Clermont-Ferrand; France
[41] Nevis Laboratory, Columbia University, Irvington NY; United States of America
[42] Niels Bohr Institute, University of Copenhagen, Copenhagen; Denmark
[43] [(a)] Dipartimento di Fisica, Università della Calabria, Rende;[(b)] INFN Gruppo Collegato di Cosenza, Laboratori Nazionali di Frascati; Italy
[44] Physics Department, Southern Methodist University, Dallas TX; United States of America
[45] Physics Department, University of Texas at Dallas, Richardson TX; United States of America
[46] National Centre for Scientific Research "Demokritos", Agia Paraskevi; Greece
[47] [(a)] Department of Physics, Stockholm University;[(b)] Oskar Klein Centre, Stockholm; Sweden
[48] Deutsches Elektronen-Synchrotron DESY, Hamburg and Zeuthen; Germany
[49] Fakultät Physik, Technische Universität Dortmund, Dortmund; Germany
[50] Institut für Kern- und Teilchenphysik, Technische Universität Dresden, Dresden; Germany
[51] Department of Physics, Duke University, Durham NC; United States of America
[52] SUPA — School of Physics and Astronomy, University of Edinburgh, Edinburgh; United Kingdom
[53] INFN e Laboratori Nazionali di Frascati, Frascati; Italy
[54] Physikalisches Institut, Albert-Ludwigs-Universität Freiburg, Freiburg; Germany
[55] II. Physikalisches Institut, Georg-August-Universität Göttingen, Göttingen; Germany
[56] Département de Physique Nucléaire et Corpusculaire, Université de Genève, Genève; Switzerland
[57] [(a)] Dipartimento di Fisica, Università di Genova, Genova;[(b)] INFN Sezione di Genova; Italy
[58] II. Physikalisches Institut, Justus-Liebig-Universität Giessen, Giessen; Germany
[59] SUPA — School of Physics and Astronomy, University of Glasgow, Glasgow; United Kingdom
[60] LPSC, Université Grenoble Alpes, CNRS/IN2P3, Grenoble INP, Grenoble; France
[61] Laboratory for Particle Physics and Cosmology, Harvard University, Cambridge MA; United States of America
[62] [(a)] Department of Modern Physics and State Key Laboratory of Particle Detection and Electronics, University of Science and Technology of China, Hefei;[(b)] Institute of Frontier and Interdisciplinary Science and Key Laboratory of Particle Physics and Particle Irradiation (MOE), Shandong University, Qingdao;[(c)] School of Physics and Astronomy, Shanghai Jiao Tong University, Key Laboratory for Particle Astrophysics and Cosmology (MOE), SKLPPC, Shanghai;[(d)] Tsung-Dao Lee Institute, Shanghai; China

JHEP12(2023)195

[63] [(a)] Kirchhoff-Institut für Physik, Ruprecht-Karls-Universität Heidelberg, Heidelberg;[(b)] Physikalisches Institut, Ruprecht-Karls-Universität Heidelberg, Heidelberg; Germany
[64] [(a)] Department of Physics, Chinese University of Hong Kong, Shatin, N.T., Hong Kong;[(b)] Department of Physics, University of Hong Kong, Hong Kong;[(c)] Department of Physics and Institute for Advanced Study, Hong Kong University of Science and Technology, Clear Water Bay, Kowloon, Hong Kong; China
[65] Department of Physics, National Tsing Hua University, Hsinchu; Taiwan
[66] IJCLab, Université Paris-Saclay, CNRS/IN2P3, 91405, Orsay; France
[67] Centro Nacional de Microelectrónica (IMB-CNM-CSIC), Barcelona; Spain
[68] Department of Physics, Indiana University, Bloomington IN; United States of America
[69] [(a)] INFN Gruppo Collegato di Udine, Sezione di Trieste, Udine;[(b)] ICTP, Trieste;[(c)] Dipartimento Politecnico di Ingegneria e Architettura, Università di Udine, Udine; Italy
[70] [(a)] INFN Sezione di Lecce;[(b)] Dipartimento di Matematica e Fisica, Università del Salento, Lecce; Italy
[71] [(a)] INFN Sezione di Milano;[(b)] Dipartimento di Fisica, Università di Milano, Milano; Italy
[72] [(a)] INFN Sezione di Napoli;[(b)] Dipartimento di Fisica, Università di Napoli, Napoli; Italy
[73] [(a)] INFN Sezione di Pavia;[(b)] Dipartimento di Fisica, Università di Pavia, Pavia; Italy
[74] [(a)] INFN Sezione di Pisa;[(b)] Dipartimento di Fisica E. Fermi, Università di Pisa, Pisa; Italy
[75] [(a)] INFN Sezione di Roma;[(b)] Dipartimento di Fisica, Sapienza Università di Roma, Roma; Italy
[76] [(a)] INFN Sezione di Roma Tor Vergata;[(b)] Dipartimento di Fisica, Università di Roma Tor Vergata, Roma; Italy
[77] [(a)] INFN Sezione di Roma Tre;[(b)] Dipartimento di Matematica e Fisica, Università Roma Tre, Roma; Italy
[78] [(a)] INFN-TIFPA;[(b)] Università degli Studi di Trento, Trento; Italy
[79] Universität Innsbruck, Department of Astro and Particle Physics, Innsbruck; Austria
[80] University of Iowa, Iowa City IA; United States of America
[81] Department of Physics and Astronomy, Iowa State University, Ames IA; United States of America
[82] Istinye University, Sariyer, Istanbul; Türkiye
[83] [(a)] Departamento de Engenharia Elétrica, Universidade Federal de Juiz de Fora (UFJF), Juiz de Fora;[(b)] Universidade Federal do Rio De Janeiro COPPE/EE/IF, Rio de Janeiro;[(c)] Instituto de Física, Universidade de São Paulo, São Paulo;[(d)] Rio de Janeiro State University, Rio de Janeiro; Brazil
[84] KEK, High Energy Accelerator Research Organization, Tsukuba; Japan
[85] Graduate School of Science, Kobe University, Kobe; Japan
[86] [(a)] AGH University of Krakow, Faculty of Physics and Applied Computer Science, Krakow;[(b)] Marian Smoluchowski Institute of Physics, Jagiellonian University, Krakow; Poland
[87] Institute of Nuclear Physics Polish Academy of Sciences, Krakow; Poland
[88] Faculty of Science, Kyoto University, Kyoto; Japan
[89] Research Center for Advanced Particle Physics and Department of Physics, Kyushu University, Fukuoka; Japan
[90] Instituto de Física La Plata, Universidad Nacional de La Plata and CONICET, La Plata; Argentina
[91] Physics Department, Lancaster University, Lancaster; United Kingdom
[92] Oliver Lodge Laboratory, University of Liverpool, Liverpool; United Kingdom
[93] Department of Experimental Particle Physics, Jožef Stefan Institute and Department of Physics, University of Ljubljana, Ljubljana; Slovenia
[94] School of Physics and Astronomy, Queen Mary University of London, London; United Kingdom
[95] Department of Physics, Royal Holloway University of London, Egham; United Kingdom
[96] Department of Physics and Astronomy, University College London, London; United Kingdom
[97] Louisiana Tech University, Ruston LA; United States of America
[98] Fysiska institutionen, Lunds universitet, Lund; Sweden
[99] Departamento de Física Teorica C-15 and CIAFF, Universidad Autónoma de Madrid, Madrid; Spain
[100] Institut für Physik, Universität Mainz, Mainz; Germany
[101] School of Physics and Astronomy, University of Manchester, Manchester; United Kingdom
[102] CPPM, Aix-Marseille Université, CNRS/IN2P3, Marseille; France
[103] Department of Physics, University of Massachusetts, Amherst MA; United States of America
[104] Department of Physics, McGill University, Montreal QC; Canada
[105] School of Physics, University of Melbourne, Victoria; Australia

JHEP12(2023)195

[106] Department of Physics, University of Michigan, Ann Arbor MI; United States of America
[107] Department of Physics and Astronomy, Michigan State University, East Lansing MI; United States of America
[108] Group of Particle Physics, University of Montreal, Montreal QC; Canada
[109] Fakultät für Physik, Ludwig-Maximilians-Universität München, München; Germany
[110] Max-Planck-Institut für Physik (Werner-Heisenberg-Institut), München; Germany
[111] Graduate School of Science and Kobayashi-Maskawa Institute, Nagoya University, Nagoya; Japan
[112] Department of Physics and Astronomy, University of New Mexico, Albuquerque NM; United States of America
[113] Institute for Mathematics, Astrophysics and Particle Physics, Radboud University/Nikhef, Nijmegen; Netherlands
[114] Nikhef National Institute for Subatomic Physics and University of Amsterdam, Amsterdam; Netherlands
[115] Department of Physics, Northern Illinois University, DeKalb IL; United States of America
[116] [(a)] New York University Abu Dhabi, Abu Dhabi;[(b)] University of Sharjah, Sharjah; United Arab Emirates
[117] Department of Physics, New York University, New York NY; United States of America
[118] Ochanomizu University, Otsuka, Bunkyo-ku, Tokyo; Japan
[119] Ohio State University, Columbus OH; United States of America
[120] Homer L. Dodge Department of Physics and Astronomy, University of Oklahoma, Norman OK; United States of America
[121] Department of Physics, Oklahoma State University, Stillwater OK; United States of America
[122] Palacký University, Joint Laboratory of Optics, Olomouc; Czech Republic
[123] Institute for Fundamental Science, University of Oregon, Eugene, OR; United States of America
[124] Graduate School of Science, Osaka University, Osaka; Japan
[125] Department of Physics, University of Oslo, Oslo; Norway
[126] Department of Physics, Oxford University, Oxford; United Kingdom
[127] LPNHE, Sorbonne Université, Université Paris Cité, CNRS/IN2P3, Paris; France
[128] Department of Physics, University of Pennsylvania, Philadelphia PA; United States of America
[129] Department of Physics and Astronomy, University of Pittsburgh, Pittsburgh PA; United States of America
[130] [(a)] Laboratório de Instrumentação e Física Experimental de Partículas — LIP, Lisboa;[(b)] Departamento de Física, Faculdade de Ciências, Universidade de Lisboa, Lisboa;[(c)] Departamento de Física, Universidade de Coimbra, Coimbra;[(d)] Centro de Física Nuclear da Universidade de Lisboa, Lisboa;[(e)] Departamento de Física, Universidade do Minho, Braga;[(f)] Departamento de Física Teórica y del Cosmos, Universidad de Granada, Granada (Spain);[(g)] Departamento de Física, Instituto Superior Técnico, Universidade de Lisboa, Lisboa; Portugal
[131] Institute of Physics of the Czech Academy of Sciences, Prague; Czech Republic
[132] Czech Technical University in Prague, Prague; Czech Republic
[133] Charles University, Faculty of Mathematics and Physics, Prague; Czech Republic
[134] Particle Physics Department, Rutherford Appleton Laboratory, Didcot; United Kingdom
[135] IRFU, CEA, Université Paris-Saclay, Gif-sur-Yvette; France
[136] Santa Cruz Institute for Particle Physics, University of California Santa Cruz, Santa Cruz CA; United States of America
[137] [(a)] Departamento de Física, Pontificia Universidad Católica de Chile, Santiago;[(b)] Millennium Institute for Subatomic physics at high energy frontier (SAPHIR), Santiago;[(c)] Instituto de Investigación Multidisciplinario en Ciencia y Tecnología, y Departamento de Física, Universidad de La Serena;[(d)] Universidad Andres Bello, Department of Physics, Santiago;[(e)] Instituto de Alta Investigación, Universidad de Tarapacá, Arica;[(f)] Departamento de Física, Universidad Técnica Federico Santa María, Valparaíso; Chile
[138] Department of Physics, University of Washington, Seattle WA; United States of America
[139] Department of Physics and Astronomy, University of Sheffield, Sheffield; United Kingdom
[140] Department of Physics, Shinshu University, Nagano; Japan
[141] Department Physik, Universität Siegen, Siegen; Germany
[142] Department of Physics, Simon Fraser University, Burnaby BC; Canada
[143] SLAC National Accelerator Laboratory, Stanford CA; United States of America

JHEP12(2023)195

[144] Department of Physics, Royal Institute of Technology, Stockholm; Sweden
[145] Departments of Physics and Astronomy, Stony Brook University, Stony Brook NY; United States of America
[146] Department of Physics and Astronomy, University of Sussex, Brighton; United Kingdom
[147] School of Physics, University of Sydney, Sydney; Australia
[148] Institute of Physics, Academia Sinica, Taipei; Taiwan
[149] [(a)] E. Andronikashvili Institute of Physics, Iv. Javakhishvili Tbilisi State University, Tbilisi;[(b)] High Energy Physics Institute, Tbilisi State University, Tbilisi;[(c)] University of Georgia, Tbilisi; Georgia
[150] Department of Physics, Technion, Israel Institute of Technology, Haifa; Israel
[151] Raymond and Beverly Sackler School of Physics and Astronomy, Tel Aviv University, Tel Aviv; Israel
[152] Department of Physics, Aristotle University of Thessaloniki, Thessaloniki; Greece
[153] International Center for Elementary Particle Physics and Department of Physics, University of Tokyo, Tokyo; Japan
[154] Department of Physics, Tokyo Institute of Technology, Tokyo; Japan
[155] Department of Physics, University of Toronto, Toronto ON; Canada
[156] [(a)] TRIUMF, Vancouver BC;[(b)] Department of Physics and Astronomy, York University, Toronto ON; Canada
[157] Division of Physics and Tomonaga Center for the History of the Universe, Faculty of Pure and Applied Sciences, University of Tsukuba, Tsukuba; Japan
[158] Department of Physics and Astronomy, Tufts University, Medford MA; United States of America
[159] United Arab Emirates University, Al Ain; United Arab Emirates
[160] Department of Physics and Astronomy, University of California Irvine, Irvine CA; United States of America
[161] Department of Physics and Astronomy, University of Uppsala, Uppsala; Sweden
[162] Department of Physics, University of Illinois, Urbana IL; United States of America
[163] Instituto de Física Corpuscular (IFIC), Centro Mixto Universidad de Valencia — CSIC, Valencia; Spain
[164] Department of Physics, University of British Columbia, Vancouver BC; Canada
[165] Department of Physics and Astronomy, University of Victoria, Victoria BC; Canada
[166] Fakultät für Physik und Astronomie, Julius-Maximilians-Universität Würzburg, Würzburg; Germany
[167] Department of Physics, University of Warwick, Coventry; United Kingdom
[168] Waseda University, Tokyo; Japan
[169] Department of Particle Physics and Astrophysics, Weizmann Institute of Science, Rehovot; Israel
[170] Department of Physics, University of Wisconsin, Madison WI; United States of America
[171] Fakultät für Mathematik und Naturwissenschaften, Fachgruppe Physik, Bergische Universität Wuppertal, Wuppertal; Germany
[172] Department of Physics, Yale University, New Haven CT; United States of America

[a] Also Affiliated with an institute covered by a cooperation agreement with CERN
[b] Also at An-Najah National University, Nablus; Palestine
[c] Also at Borough of Manhattan Community College, City University of New York, New York NY; United States of America
[d] Also at Center for High Energy Physics, Peking University; China
[e] Also at Center for Interdisciplinary Research and Innovation (CIRI-AUTH), Thessaloniki; Greece
[f] Also at Centro Studi e Ricerche Enrico Fermi; Italy
[g] Also at CERN, Geneva; Switzerland
[h] Also at Département de Physique Nucléaire et Corpusculaire, Université de Genève, Genève; Switzerland
[i] Also at Departament de Fisica de la Universitat Autonoma de Barcelona, Barcelona; Spain
[j] Also at Department of Financial and Management Engineering, University of the Aegean, Chios; Greece
[k] Also at Department of Physics, Ben Gurion University of the Negev, Beer Sheva; Israel
[l] Also at Department of Physics, California State University, Sacramento; United States of America
[m] Also at Department of Physics, King's College London, London; United Kingdom
[n] Also at Department of Physics, Stanford University, Stanford CA; United States of America
[o] Also at Department of Physics, University of Fribourg, Fribourg; Switzerland
[p] Also at Department of Physics, University of Thessaly; Greece

JHEP12(2023)195

[q] Also at Department of Physics, Westmont College, Santa Barbara; United States of America
[r] Also at Hellenic Open University, Patras; Greece
[s] Also at Institucio Catalana de Recerca i Estudis Avancats, ICREA, Barcelona; Spain
[t] Also at Institut für Experimentalphysik, Universität Hamburg, Hamburg; Germany
[u] Also at Institute for Nuclear Research and Nuclear Energy (INRNE) of the Bulgarian Academy of Sciences, Sofia; Bulgaria
[v] Also at Institute of Applied Physics, Mohammed VI Polytechnic University, Ben Guerir; Morocco
[w] Also at Institute of Particle Physics (IPP); Canada
[x] Also at Institute of Physics and Technology, Ulaanbaatar; Mongolia
[y] Also at Institute of Physics, Azerbaijan Academy of Sciences, Baku; Azerbaijan
[z] Also at Institute of Theoretical Physics, Ilia State University, Tbilisi; Georgia
[aa] Also at L2IT, Université de Toulouse, CNRS/IN2P3, UPS, Toulouse; France
[ab] Also at Lawrence Livermore National Laboratory, Livermore; United States of America
[ac] Also at National Institute of Physics, University of the Philippines Diliman (Philippines); Philippines
[ad] Also at Ochanomizu University, Otsuka, Bunkyo-ku, Tokyo; Japan
[ae] Also at Technical University of Munich, Munich; Germany
[af] Also at The Collaborative Innovation Center of Quantum Matter (CICQM), Beijing; China
[ag] Also at TRIUMF, Vancouver BC; Canada
[ah] Also at Università di Napoli Parthenope, Napoli; Italy
[ai] Also at University of Chinese Academy of Sciences (UCAS), Beijing; China
[aj] Also at University of Colorado Boulder, Department of Physics, Colorado; United States of America
[ak] Also at Washington College, Chestertown, MD; United States of America
[al] Also at Yeditepe University, Physics Department, Istanbul; Türkiye
[*] Deceased

JHEP12(2023)195